NASA Contract Report 159027

Advanced Risk Assessment of the Effects of Graphite Fibers on Electronic and Electric Equipment

Final Phase I Report

Leon S. Pocinki, Lawrence D. Kaplan
Merrill E. Cornell, Reynold Greenstone

ORI, INC.
Silver Spring, Md 20910

CONTRACT NAS1-15379
MAY 1979

National Aeronautics and
Space Administration

Langley Research Center
Hampton, Virginia 23665
AC 804 827-3966

NASA Contract Report 159027

Advanced Risk Assessment of the Effects of Graphite Fibers on Electronic and Electric Equipment

Final Phase I Report

Leon S. Pocinki, Lawrence D. Kaplan
Merrill E. Cornell, Reynold Greenstone

ORI, INC.
Silver Spring, Md 20910

CONTRACT NAS1-15379
MAY 1979

NASA
National Aeronautics and
Space Administration

Langley Research Center
Hampton, Virginia 23665
AC 804 827-3966

ADVANCED RISK ASSESSMENT OF THE EFFECTS OF GRAPHITE FIBERS ON ELECTRONIC AND ELECTRIC EQUIPMENT

FINAL PHASE I REPORT

MAY 1979

ACKNOWLEDGMENT

This report summarizes the work performed by a team of ORI scientific staff members who are recognized as authors of the report. In addition, Mr. Fred Zusman made a most significant contribution to the effort in the development of the computer model; he was ably assisted by Ms. Elisabeth Battino. Dr. Samuel Kneale also played a key role in connection with certain mathematical refinements.

The authors wish to recognize Israel Taback of Bionetics Corporation for his contributions to all aspects of the work.

We also wish to thank the Project Officers, Dr. Karen Credeur and Mr. Robert J. Huston, of the National Aeronautics and Space Administration, Langley Research Center, for their interest and suggestions during the course of this work.

Dr. Credeur's detailed review of the draft report is appreciated. The other reviews of the draft, by Professor Norman Rasmussen, MIT, and the George Washington University Research Team were also helpful in preparing this final report.

ADVANCED RISK ASSESSMENT OF THE EFFECTS OF GRAPHITE FIBERS ON ELECTRONIC AND ELECTRICAL EQUIPMENT

EXECUTIVE SUMMARY

ORI, Inc., in Phase I of its NASA Contract No. NAS1-15379, developed a model to generate quantitative estimates of the risk associated with the release of graphite fibers during fires involving commercial aircraft constructed with graphite fiber composite materials. The model was used to estimate the risk associated with accidents at several U.S. airports. These results were then combined to provide an estimate of the total risk to the nation.

Composite material formed of graphite fibers encased in epoxy resin provides a material strong and light enough to replace aluminum, steel, or titanium in many applications. Evidence exists that these fibers can cause failures of exposed electrical, electronic, and power equipment. Further, burning of the composite material can result in the release of fibers into the environment. Thus, fires involving the composite material can result in accidental release of graphite (carbon) fibers in amounts sufficient to damage electrical or electronic equipment, and pose a hazard to the population near the accident site. The probability of such accidental release and subsequent dissemination of critical amounts of carbon fiber is not known, and therefore the associated risk cannot be accurately quantified. However, the use of graphite fiber composite material is expected to increase rapidly, and the risk will undergo a corresponding increase.

The Federal Government has implemented a plan assigning specific aspects of this problem to particular agencies, in order to deal with the potential problem associated with use of the graphite fiber material. One of the responsibilities assigned to NASA is the investigation of the vulnerability of commercial aircraft equipment. The NASA Langley Research Center is undertaking this investigation as part of a major program that examines accidental carbon fiber release, dissemination and redissemination of the fibers, transfer of the fibers into buildings and other enclosures, and vulnerability of household, industrial, and aircraft equipment. The ultimate goal of the NASA Langley Research Center program is an assessment of the magnitude of the risk.

AIRPORT - URBAN AREA RISK ASSESSMENT

In order to estimate the risk associated with accidental release of carbon fibers following a commercial aircraft accident with fire, ORI developed a Monte Carlo simulation model that replicates many possible aircraft accidents with fires and estimates the costs associated with the subsequent release of the fibers, their downwind transport under different meteorological conditions, their transfer into offices, factories, and homes, and subsequent failures of vulnerable equipment.

The Method

The method employed by ORI involves the repeated calculation of possible accident effects, using a model to represent the principal events associated with each accident, and calculating statistics after the replication of many accidents. The simulation model elements and their interrelationships are illustrated in Figure 1. The events being simulated are identified by the shaded boxes. Random accidents are generated for each simulated sample year, with repeated sampling to obtain the final statistical distributions. The principal steps followed for one sample year's events at one airport are:

- Generate Accident. We first compute the number of accidents that will be simulated during the sample year at the airport for each aircraft category. This number is obtained by making a random draw from a Poisson distribution. The mean of the distribution is estimated by calculating the ratio of the number

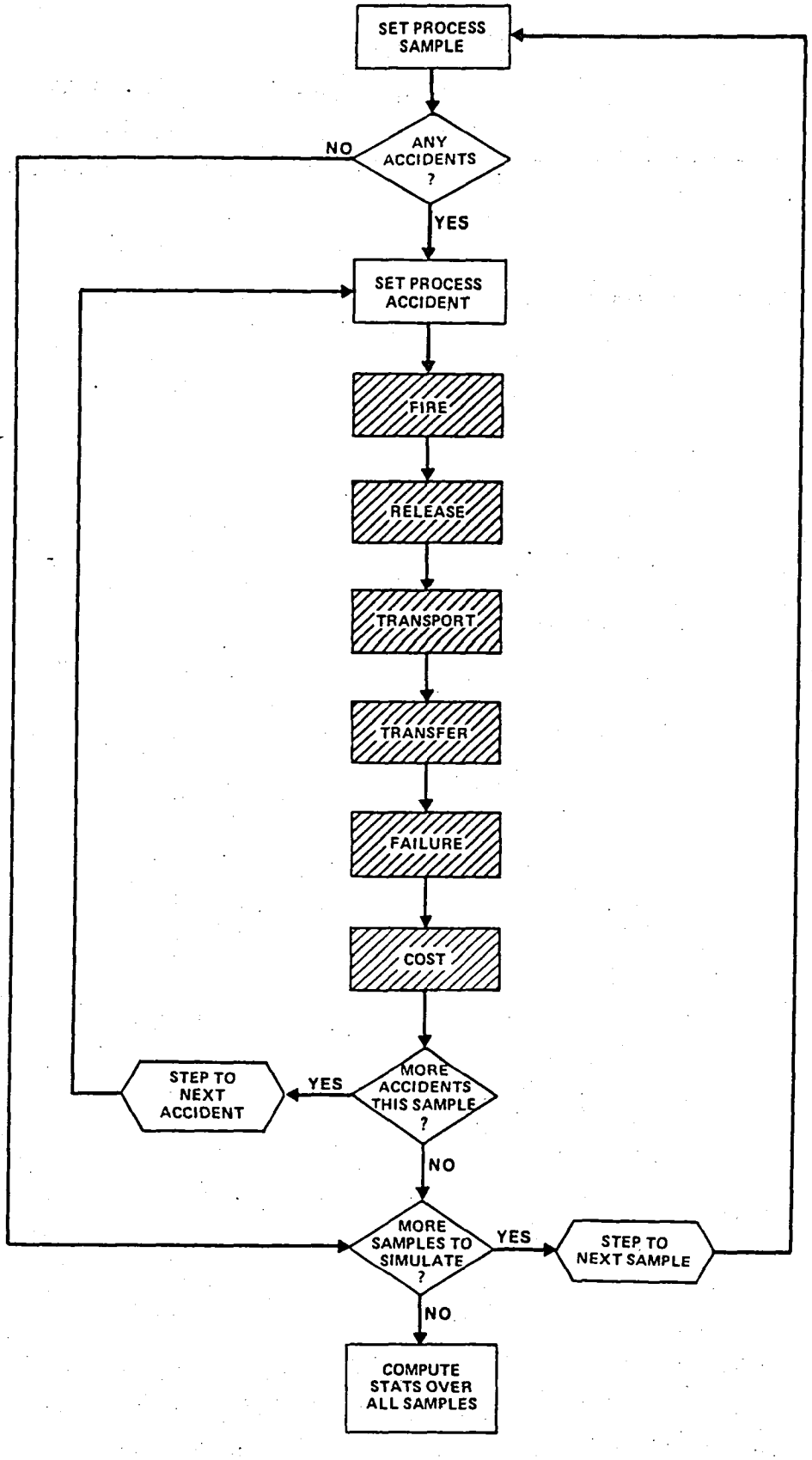

FIGURE 1. ORI RISK ASSESSMENT MODEL

Shaded blocks represent events being simulated.

of operations in the particular aircraft category to the projected total number of air carrier operations in the United States, and then multiplying by the projected national annual rate of aircraft accidents with fires. The mean is further adjusted to account for the expected fraction of aircraft in each category that will contain graphite fiber composite material. Each of the accidents will be simulated for each aircraft category processed in sequence. The model randomly assigns the operational phase and location of the accident, using probability distributions based on statistical analysis of accident data in the National Transportation Safety Board files. At the end of the generate-accident phase of the calculation, we have the aircraft category, operational phase, and location of the accident.

The techniques applied here are considered entirely appropriate. The extrapolation of accident rates into the future introduces some uncertainty, however, as does the assumption that the location and operational phase statistics generated from many accidents at different airports can be applied to one airport. There is essentially no alternative available.

- Compute Weather Details. The weather conditions which are required for subsequent calculations are the surface wind speed and direction, and the associated atmospheric stability condition. The joint distribution of these variables is available for all airports considered in a data base maintained at ORI under a joint EPA-FAA contract. One combination of wind speed and direction, and stability category is randomly selected from this historical frequency distribution. The method used here, with the meteorological data base available, introduces no approximation. At this stage in the computation we are ready to do the two calculations described next.

- Compute Plume Height. In this step the model computes the height to which the plume will grow when it is stabilized. This height is based on the aircraft class, the operational phase during

which the accident took place, and the weather conditions. The aircraft size determines the size of the fire, or rate of energy release, which, with the meteorological stability conditions, determines the behavior of the fire plume. Classical methods are used to compute the plume height, but the behavior of the fire plume at the inversion level is subject to some uncertainty. One inversion height is assigned to each stability category for each airport, and it is assumed that the plume never penetrates the inversion. This assumption is considered conservative, i.e., it overstates the risk.

- Compute Downwind Exposure. The weather details and the fire plume height are used in the downwind exposure calculation, based on a standard Gaussian plume model, modified to include fallout of the graphite fibers and partial reflection at the earth's surface. The use of a more sophisticated diffusion model did not appear warranted because of uncertainties in other phases of the computation. The amount of graphite fiber involved in the fire is also determined. The fraction of composite material in the aircraft structure that is involved in the fire is assumed to be equal to the fraction of the aircraft that is involved in the fire, which is fixed for each operational phase-aircraft type combination. This assumption was introduced because of the unavailability of detailed accident analyses, and tends to reduce the likelihood of extreme values occurring in the results.

  Exterior exposure values are computed at points within a set of representative circles covering the region around the airport out to a range of at least fifty miles. The impact calculations described below are also done for each of these points. The use of the representative circles constitutes a satisfactory approximation, since the simulation is repeated for many accident locations and wind directions, and the results are expressed probabilistically.

- Compute Interior Exposure. It was assumed that each type of residential unit, business, or industry at each of the key points for which the exposure is computed can be characterized by a typical building or type of enclosure. These characteristics determine how the exposure inside the building is related to the exposure outside; the exposure inside is calculated for each class of business and industry present. The definition of typical building types leads to results that are satisfactory in the expected-value sense, but limits the spread of the results. Increased variance in the input characteristics would, however, require additional simulation runs in order to yield stable results.

- Compute Failures. Each individual vulnerable piece of equipment obeys an exponential failure law, which is in reasonable agreement with available experimental results. For each business-industry category, as defined by the Standard Industrial Classification (SIC) two-digit code, a standard equipment configuration is defined. The model computes the overall probability of failure for each typical plant or facility from the interior exposure values and the equipment failure parameters. Similarly, household equipment failures are computed for each household class at each of the characteristic points in the geographical area. This is essentially an expected value calculation.

- Compute Costs. For each residential unit the impact is estimated on the basis of the fraction of the equipments expected to be damaged, and a standard repair cost. The business-industry impact is estimated by allocating to each local business category its share of the Gross Domestic Product, based on the ratio of its local payroll to the national payroll for the same SIC two-digit code. The impact is then obtained by multiplying each business category's overall failure probability by its allocated local daily share of the Gross Domestic Product. The calculation thus assumes that a complete closing of a business will result in a financial impact equal to the business's share of the Gross Domestic Product; this neglects the costs of effects other than a complete shutdown, but

does include some secondary effects associated with one industrial sector's effect on others.

- Compute Statistics. The computation of the interior exposure, resulting failures, and their impact is done for all industries and residential units at all of the points representing a county or a portion of a county. After the computation is done for one county, the model moves on to the next one; all industries and residential units there are processed. Damage costs for all affected geographic areas are then totalled to yield the estimate of the total impact of one accident. Any additional accidents for the same aircraft category are then treated in the same way, after which accidents in the next aircraft category are simulated. This process is repeated for all aircraft categories-- all accidents --for the sample year to obtain the total impact of graphite fiber accidents during that year. Another sample is then drawn generating the accidents to be simulated during the next replication.

The sequence of steps described above is repeated for many sample years providing the annual dollar value of the impact for each sample, after which the frequency distribution of annual costs is generated. In addition, the model prepares a risk profile, showing the probability that a given annual cost is exceeded, and details describing the ten most costly accidents.

Results

Results were obtained using input values that were the best estimates available to the NASA-ORI team for the 1985 and 1993 time periods of interest. The model computes, after many replications, a risk profile which gives the probability that the annual cost associated with equipment failures following an accident exceeds a stated amount.

The 1985 and 1993 risk profiles for Washington National Airport are shown in Figure 2. Results indicate an expected (average) annual impact of $110 for 1985 and $1,200 for 1993. For 1993, the probability that the damage in any one year would exceed $100,000 is .0025 (25 in ten thousand), while for $1,000,000 it is .0001 (1 in ten thousand).

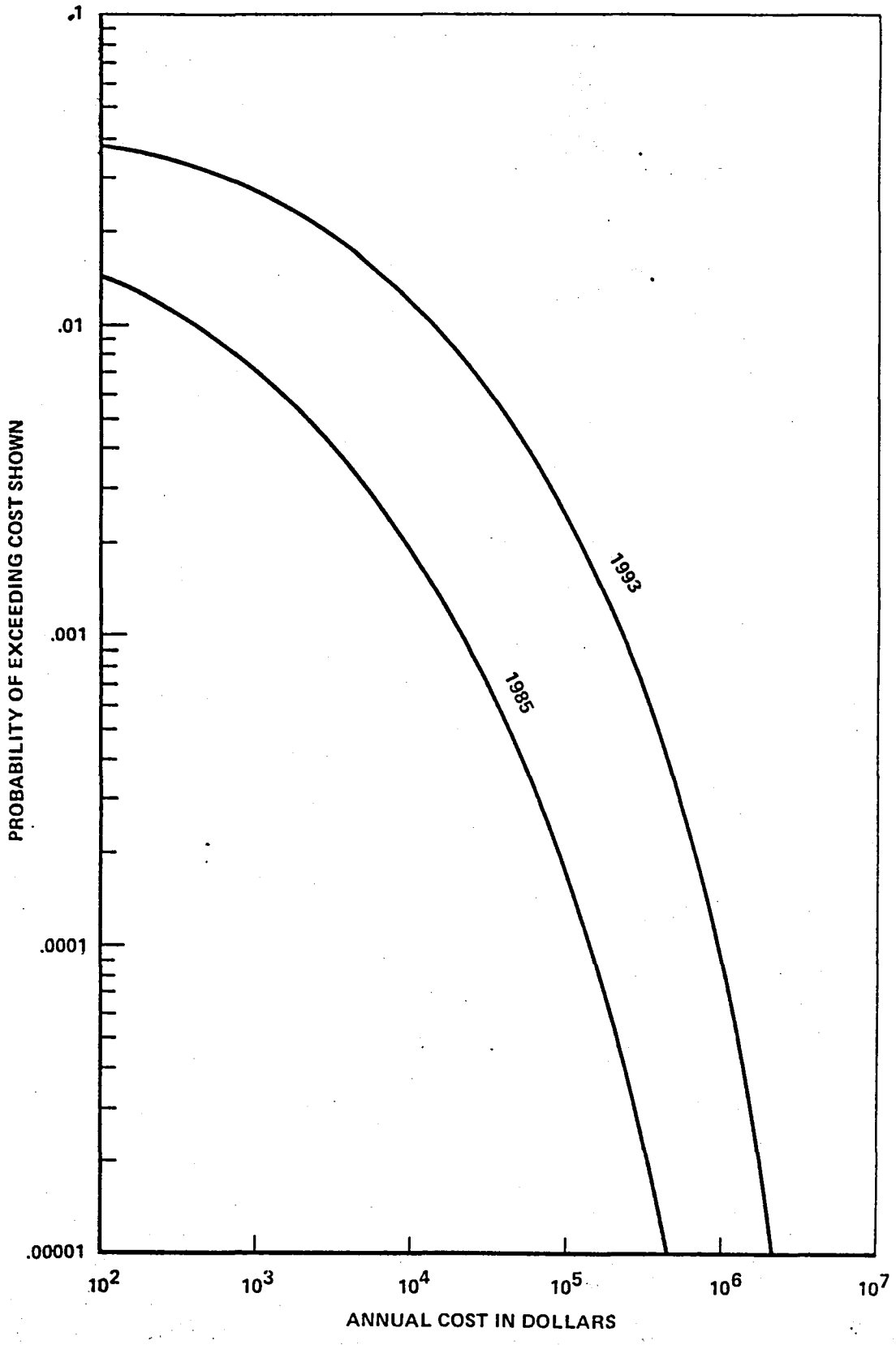

FIGURE 2. WASHINGTON NATIONAL AIRPORT RISK PROFILES for 1985 AND 1993

There is some uncertainty with regard to many of the required input parameters. If it is assumed that these uncertainties correspond to a factor of ten in the product of the amount of fiber released in the aircraft fire, the effect of downwind transport and diffusion, and the transfer into buildings, we can estimate that the risk could be as high as .01 (1 in a hundred) that the annual impact would exceed $100,000, and .002 (2 in a thousand) that it would exceed $1,000,000.

The examination of individual accidents shows that the effects of the accidental release of graphite fibers can be felt at considerable distances downwind. For example, more than half of the greater-than-$4,000,000 impact of one simulated 1993 accident at Washington National Airport was due to the calculated effect on business and industry in downtown Baltimore.

The individual airport risk is in part a function of the number of aircraft operations at an airport and the amount of business and industry at risk in the area surrounding the airport. For O'Hare Airport at Chicago, the nation's busiest, for example, the expected (average) annual risk is $300 for 1985 and $2,700 for 1993. For 1993, the probability is estimated to be .0004 (4 in ten thousand) that the annual impact will exceed $1,000,000 and .00001 (1 in a hundred thousand) that it will exceed $10,000,000. Several 1993 airport risk profiles are compared in Figure 3.

NATIONAL RISK PROFILE

The total national risk can be estimated in several ways. A national model can be exercised in the same way as the single airport model. The number of accidents in the country would be generated and accidents assigned to individual airports. Another method is to develop the risk profiles for a number of airports and then combine them to yield a national risk profile. In order to develop individual airport results which are of considerable interest in their own right, as well as the national risk estimate, the latter method was used.

The national results, illustrated by the 1985 and 1993 risk profiles in Figure 4, indicate that the expected annual national impact is approximately $3,000 for 1985 and $35,000 for 1993. For 1993, it is estimated that the probability of exceeding an annual national impact of $1,000,000 (in 1976 dollars) is approximately .005 (5 in one thousand) and decreases to .0001 (1 in ten thousand) for $10,000,000.

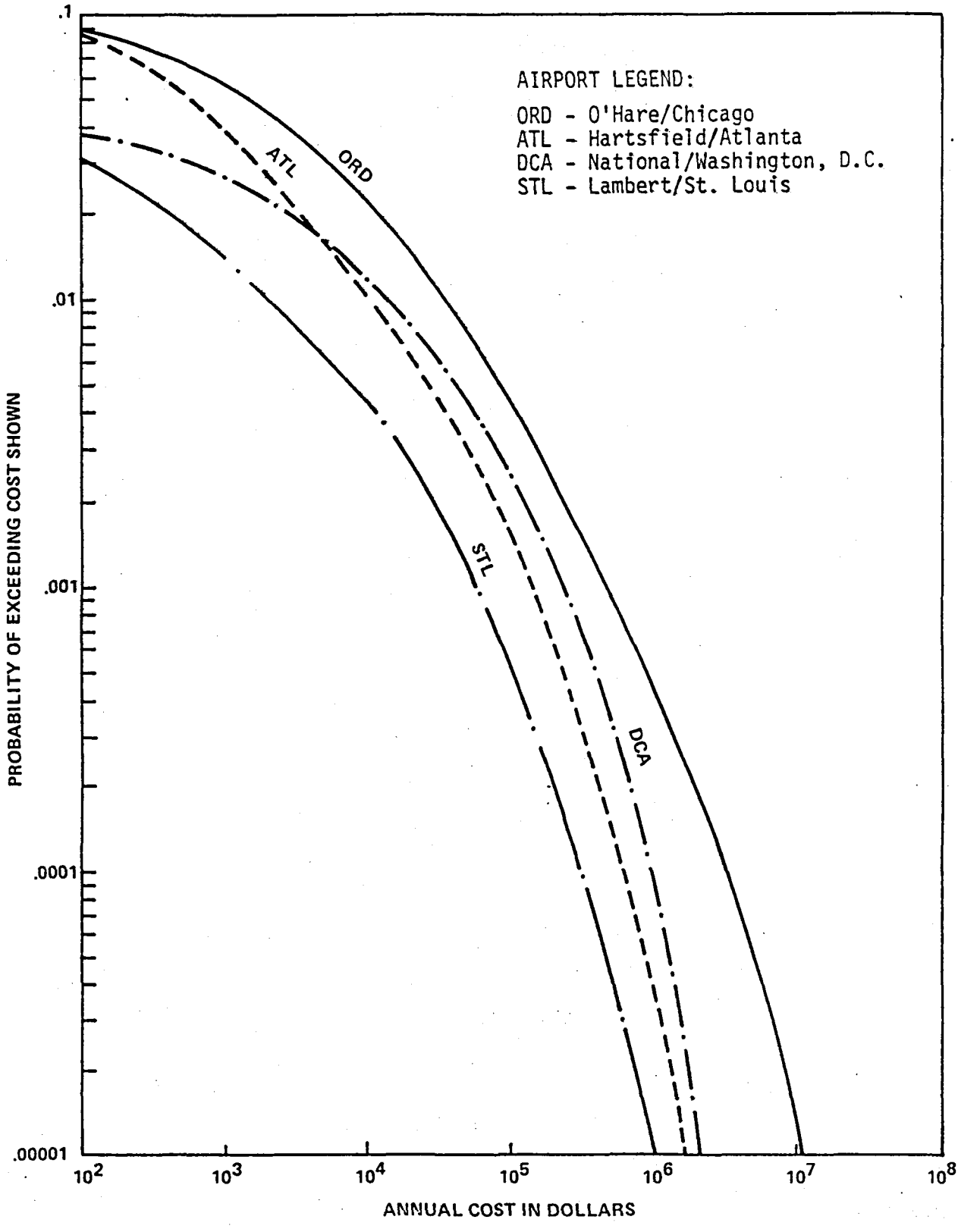

FIGURE 3. 1993 RISK PROFILES FOR SELECTED AIRPORTS

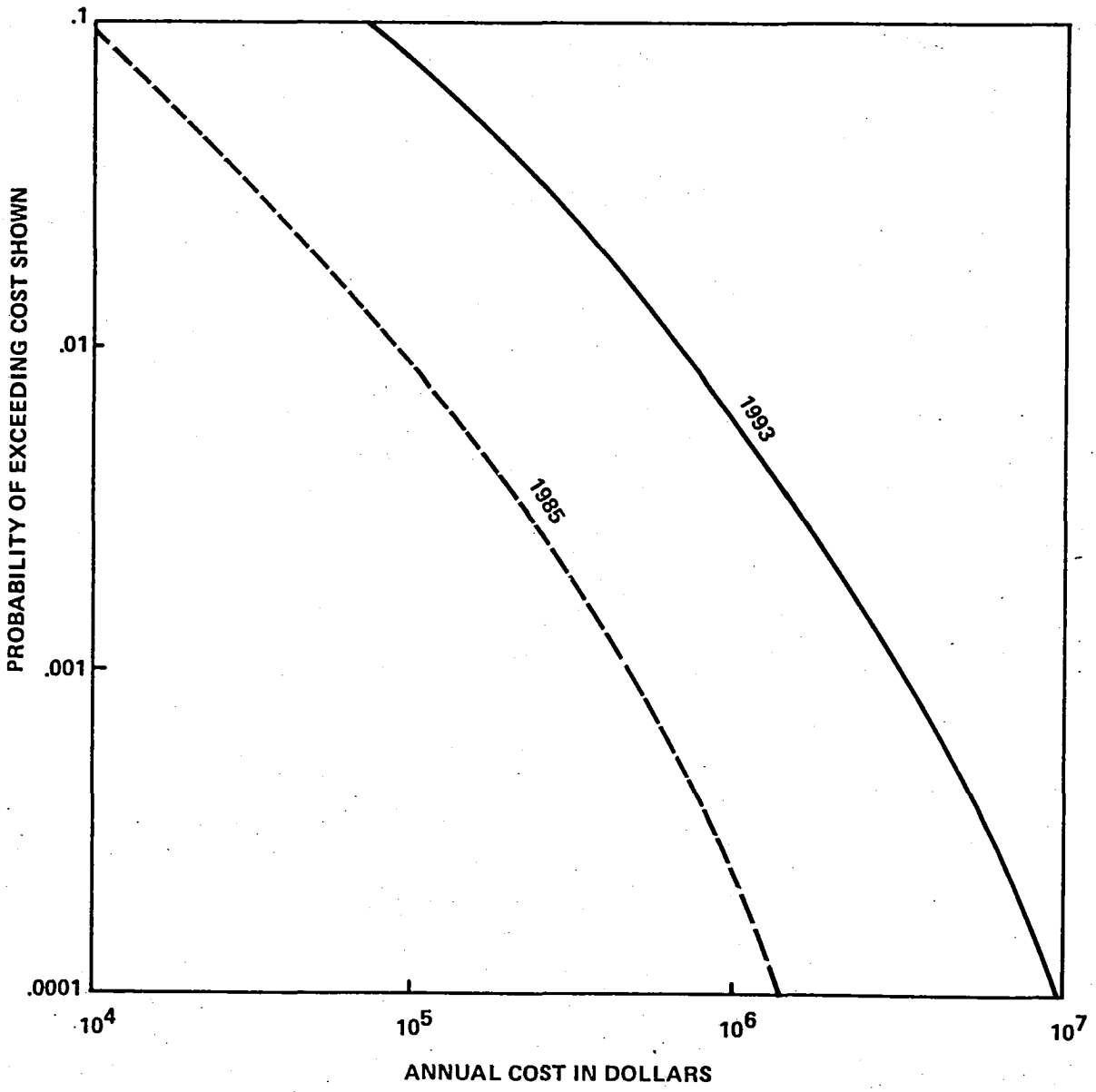

FIGURE 4. NATIONAL RISK PROFILES OBTAINED BY COMBINING NINE INDIVIDUAL AIRPORT RESULTS ADJUSTED TO ACCOUNT FOR ALL U.S. FLIGHT OPERATIONS -- 1985 AND 1993

TABLE OF CONTENTS

LIST OF FIGURES

LIST OF TABLES

I. INTRODUCTION

This is the final report of the work performed by ORI, Inc., in Phase I of the Graphite Fiber Risk Assessment Program sponsored by NASA, under Contract Number NAS1-15379. The ORI efforts were concentrated on the development of a computerized model to be used in preparing quantitative estimates of the risk associated with the release of graphite fibers during fires involving portions of commercial aircraft constructed of graphite fiber composite materials.

Composite material formed of a graphite fiber mesh encased in epoxy resin provides a material strong and light enough to replace aluminum, steel, or titanium in many applications. Graphite composite structures are under development for use in commercial transport aircraft. These developments include:

- Rudder control tab for the McDonnell Douglas DC-9 Super 80 configuration.
- Inboard ailerons for possible application on the Lockheed L-1011.
- Secondary structures on the Boeing 767.

NASA's aircraft energy efficiency (ACEE) program is supporting advanced commercial transport composite structures development. Union Carbide has announced plans to build a carbon fiber plant to begin operating in 1981

with an initial production capacity of 800,000 pounds of carbon fiber a year. They estimate the total market in 1979 to be one million pounds of carbon fiber.

In view of evidence from a variety of sources that the fiber can damage electrical equipment, and that pieces in the critical size range can be released by fires involving the composite material, NASA, as part of a national program, is investigating the potential risk that these contemplated uses of graphite/epoxy material constitute. The probability of accidental release and the dissemination of carbon fibers at critical damage levels is not known and the risk cannot be accurately quantified. However, the use of composite material is expected to increase at a rapid rate, and the risk which is related to the amount of CF in use will increase accordingly.

The Federal Government has produced a plan involving many agencies to deal with all aspects of the potential problem associated with CF. One of the responsibilities assigned to NASA is the investigation of the vulnerability of commercial aircraft equipment. NASA Langley is undertaking this investigation as part of a larger program that involves accidental fiber release, fiber dissemination and redissemination, transfer of fibers to enclosures, and equipment (household, industrial, aircraft, etc.) vulnerability. The ultimate goal of the NASA Langley program is an assessment of the magnitude of the risk.

In order to estimate the risk, ORI has developed a stochastic model that replicates many possible aircraft accidents with fire, and estimates the dollar costs associated with the subsequent release of the fibers, their downwind transport under different meterological conditions, their transfer into offices, factories, and homes, and subsequent failures of vulnerable equipment. The model was used to estimate the risk associated with accidents at several major U.S. airports. These results were later combined to provide an initial estimate of the total risk to the nation.

The results were obtained using a variety of input parameters that were, in all cases, the best estimates available to the NASA-ORI team for the time periods of most interest to NASA: 1985 and 1993. The results indicate that the risk, expressed as the probability that the annual cost associated with equipment failures following an accident exceeds some stated amount, appears relatively small. However, the results indicate that, in view of the uncertainty with regard to many of the input parameters, further investigation appears warranted. In addition we have shown that the model results still exhibit some uncertainty in the high cost-low probability range where there is, of course, considerable interest.

The model developed and reported on in this document provides an economical means of developing these additional required estimates for a variety of different sets of input specifications.

Detailed analysis of the possible impact of accidents at Washington National Airport indicates an expected (average) annual impact of $110 for 1985 and $1,200 for 1993. The 1993 results indicate the probability that the damage in any one year will exceed $100,000 is .0024, while for $1,000,000 it is .0001. There is some uncertainty with regard to many of the inputs that are necessary in treating this problem. If we assume that these uncertainties correspond to a factor of ten in the product of the amount of fiber released in the aircraft fire, the effect of downwind diffusion, and the intake into buildings, we estimate that the risk would then be approximately .01, that the annual impact would exceed $100,000 and .002 for exceeding $1,000,000. This amount of uncertainty in the factors associated with the problem is by no means unreasonable.

The examination of worst-case accidents generated by the random selection of specific parameters clearly shows that effects of the accident leading to release of graphite fibers can be felt at considerable distances downwind from the accident site. For example, a simulated 1993 accident at Washington National Airport resulted in an impact greater than $4,000,000; more than half of this was due to the calculated effect on business and industry in Baltimore.

The individual airport risk is a function of the level of aircraft operations at the airport and the amount of business and industry at risk, that is, in the geographical area surrounding the airport. For O'Hare Airport at Chicago, the nation's busiest, for example, the expected (average) annual risk is $300 for the 1985 scenario and $2,700 for the 1993 scenario. The probability that the total impact will exceed $500,000 is .0002 for 1985 and .0015 for 1993. For the 1993 case the probability is .0004 that the annual impact will exceed $1,000,000 and estimated as .00001 that is will exceed $10,000,000.

These results may also be presented in terms of individual accidents; the average impact associated with aircraft accidents at O'Hare Airport is estimated to be $18,200 for 1993, while 0.2 percent of the accidents had an estimated impact greater than $1,000,000.

The results for the national risk profile indicate that the expected annual national impact is approximately $2,800 for 1985 and $29,000 for 1993. For the 1993 scenario we estimate that the probability of exceeding an annual national impact of $1,000,000 (in 1976 dollars) is approximately .005 and decreases to .0001 for $10,000,000.

This report describes the ORI work in some detail. The following chapter describes the model in broad outline form. Chapter III describes the results obtained from the analysis of historical accident data, used to develop several of the model inputs. Chapter IV describes the sub-model developed to predict the behavior of the plume resulting from a fire associated with an aircraft accident. Following this, we describe the methods used to model the downwind transport and diffusion of the fibers released at the accident scene, (Chapter V). Chapter VI discusses the transfer of fibers from the exterior to the interior of structures. In Chapter VII we present equipment failure models to treat particular segments of business and industry. Next, in Chapter VIII, the methods for costing out the equipment failures are derived.

Results of the study are presented in some detail in the remaining sections of the report. Chapter IX describes the results for the Washington National Airport - Washington DC metropolitan area at several levels of detail, from an individual simulated accident to the statistics developed over many replications, including a description of the ten most costly accidents. Sensitivity of the results to major changes in the amount of composite material on board the aircraft is investigated. Chapter X presents additional results for the individual airport investigations; these include the comparison of several airports, and the discussion of statistical error bounds for the simulation results. Chapter XI describes the methods used to generate the national risk profile, presents the results and develops the associated statistical confidence limits.

II. OVERVIEW OF TECHNICAL APPROACH

BASIC APPROACH

Method

The basic approach embodied in the ORI risk assessment technique is that of the Monte Carlo simulation. This method was essentially dictated by the following factors:

- The problem is affected by many variables
- It was difficult to identify in advance the values of these variables associated with the "worst cases."
- It was important to obtain information about the statistical distribution of the results, and this is difficult to do analytically.

The complete model, which is exercised in each simulation, comprises several individual modules. These form the backbone of the complete model as well as the structure for this report.

The major problem elements are illustrated in Figure 2.1. Each is discussed briefly in this section of the report and then described in more detail in subsequent sections. Overlaying each accident-outcome calculation are several operations required to establish the conditions associated with the accident and to compute the desired statistics. These are illustrated

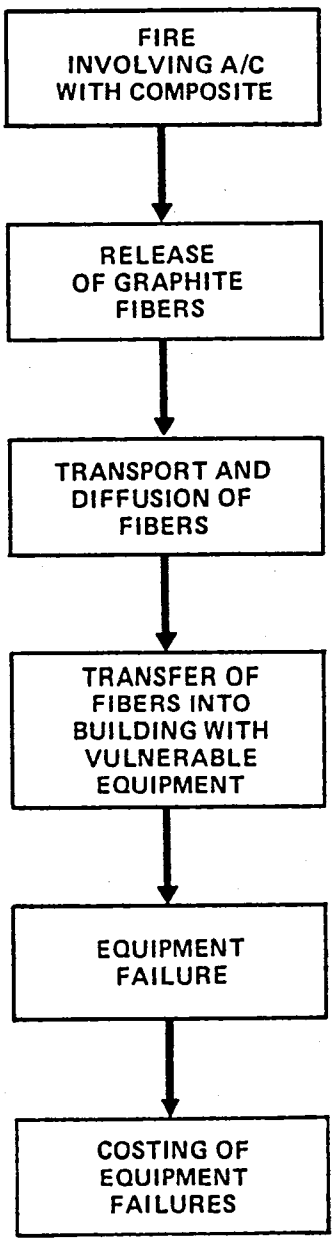

FIGURE 2.1. MAJOR ELEMENTS OF RISK ANALYSIS SCENARIO

in the aggregate in Figure 2.2. For each sample, or replicated year, any fire accidents that occur with attendant release of graphite fibers are simulated and their impact assessed. The year is replicated many times in order to develop probablistic estimates of the annual impact.

Underlying Assumptions

The ORI strategy described in this section makes use of several assumptions that are required for the implementation of the model. All aircraft in the time periods covered by the analysis are considered to be members of a limited number of categories, defined primarily by aircraft size. National historical accident data describing the relative frequency of an accident during particular operational phases are assumed to be applicable to all airports being analyzed in the future; the expected number of accidents at an airport is proportional to the number of operations. The geographical area surrounding the airport is defined in terms of a data base, primarily the County Business Patterns, which presents economic information on a county-by-county basis. Each county is described for the model as a set of points, each of which is surrounded by a circle, such that the circles cover the county. The industry and households within the circle are assumed to be uniformly distributed over the area enclosed by the circle. Each type of business is defined, for purposes of calculating damage and its cost impact, by its two-digit Standard Industrial Classification code number, by which information is categorized in the County Business Patterns.

AIRPORT-URBAN AREA RISK ASSESSMENT MODEL

In this section each of the major model elements is described. These model elements and their interrelationships are illustrated in Figure 2.3. Each model element is described in order. The model can treat several airports in sequence, but the description here is limited to the processing of one airport. At the start of the calculation, the model is set up to run a given number of replications (samples); it takes the necessary actions to initialize for the first replication. After that, random samples are drawn and accidents occur, as described below.

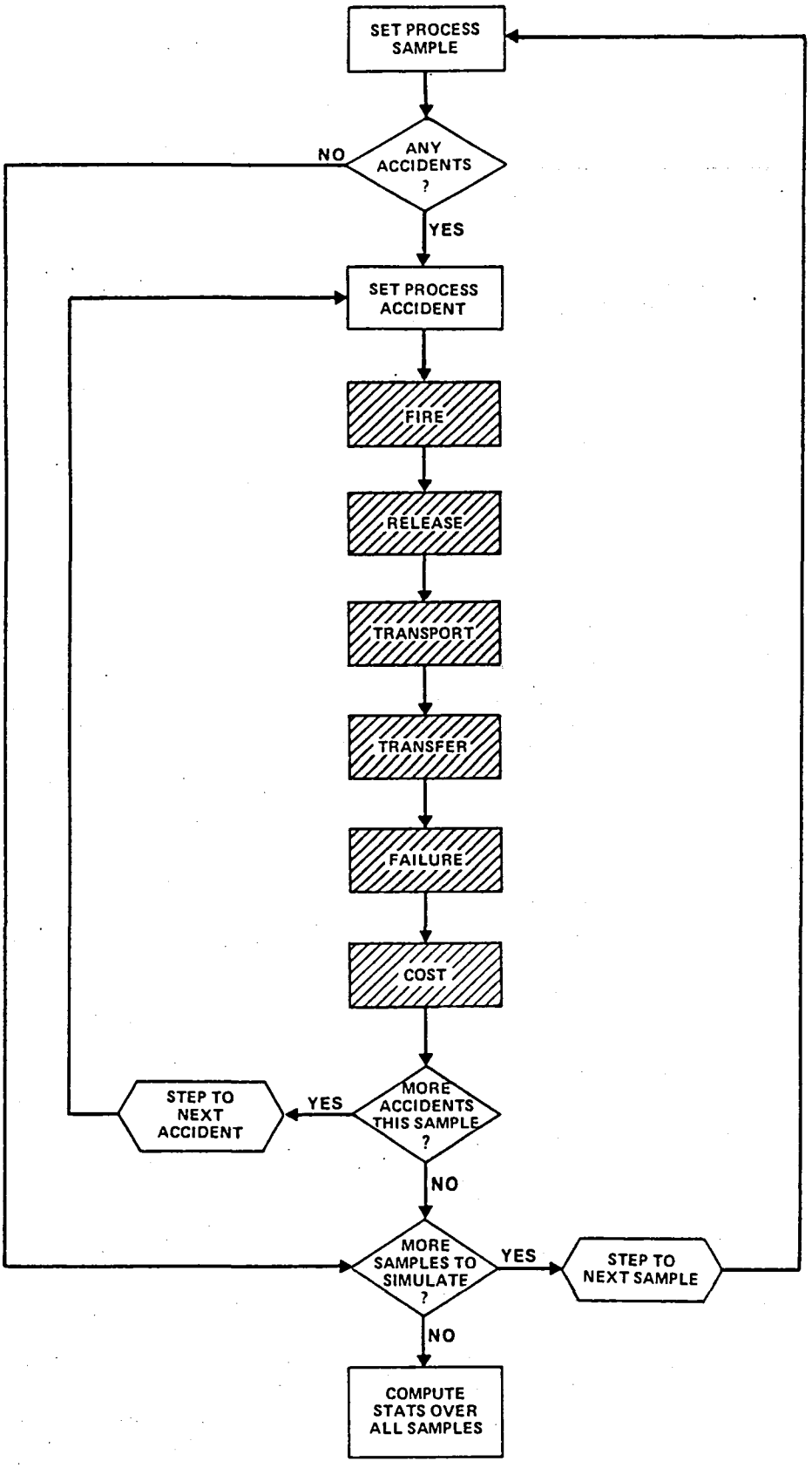

FIGURE 2.2. FLOWCHART ILLUSTRATING ACCIDENT-RELATED EVENTS EMBEDDED IN SIMULATION PROCESS

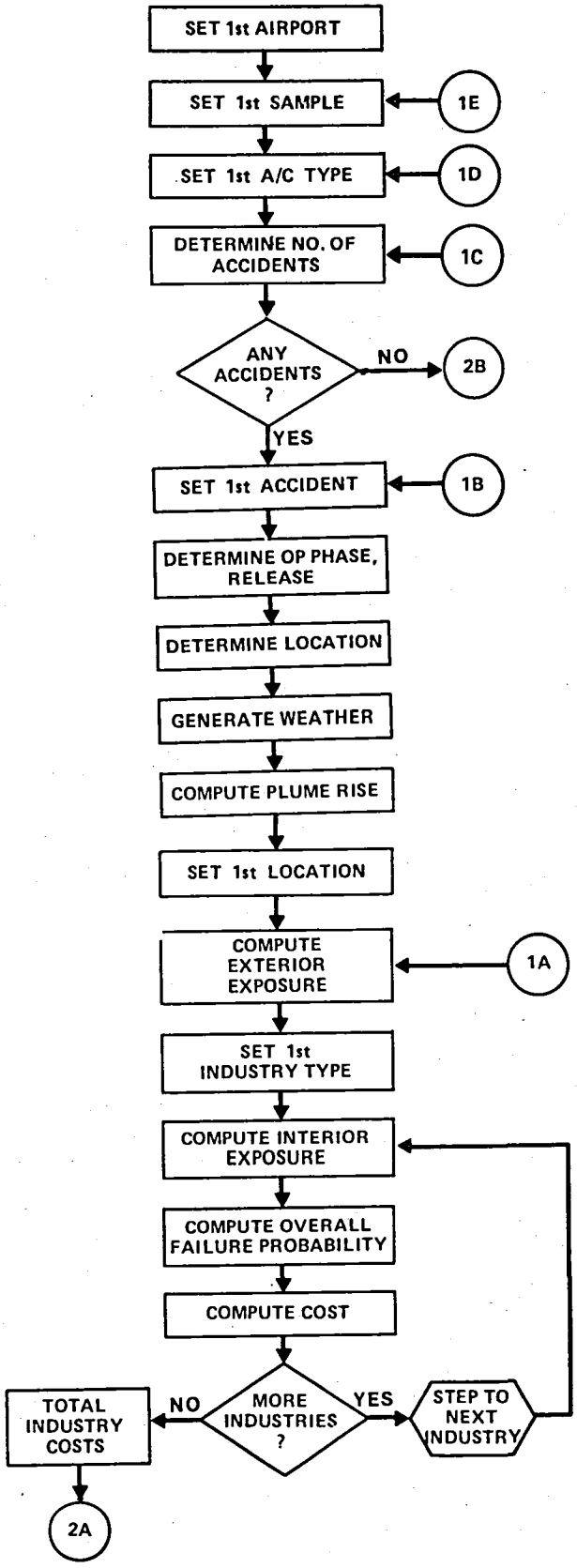

FIGURE 2.3a. FLOWCHART 1 FOR ORI AIRPORT RISK ASSESSMENT MODEL

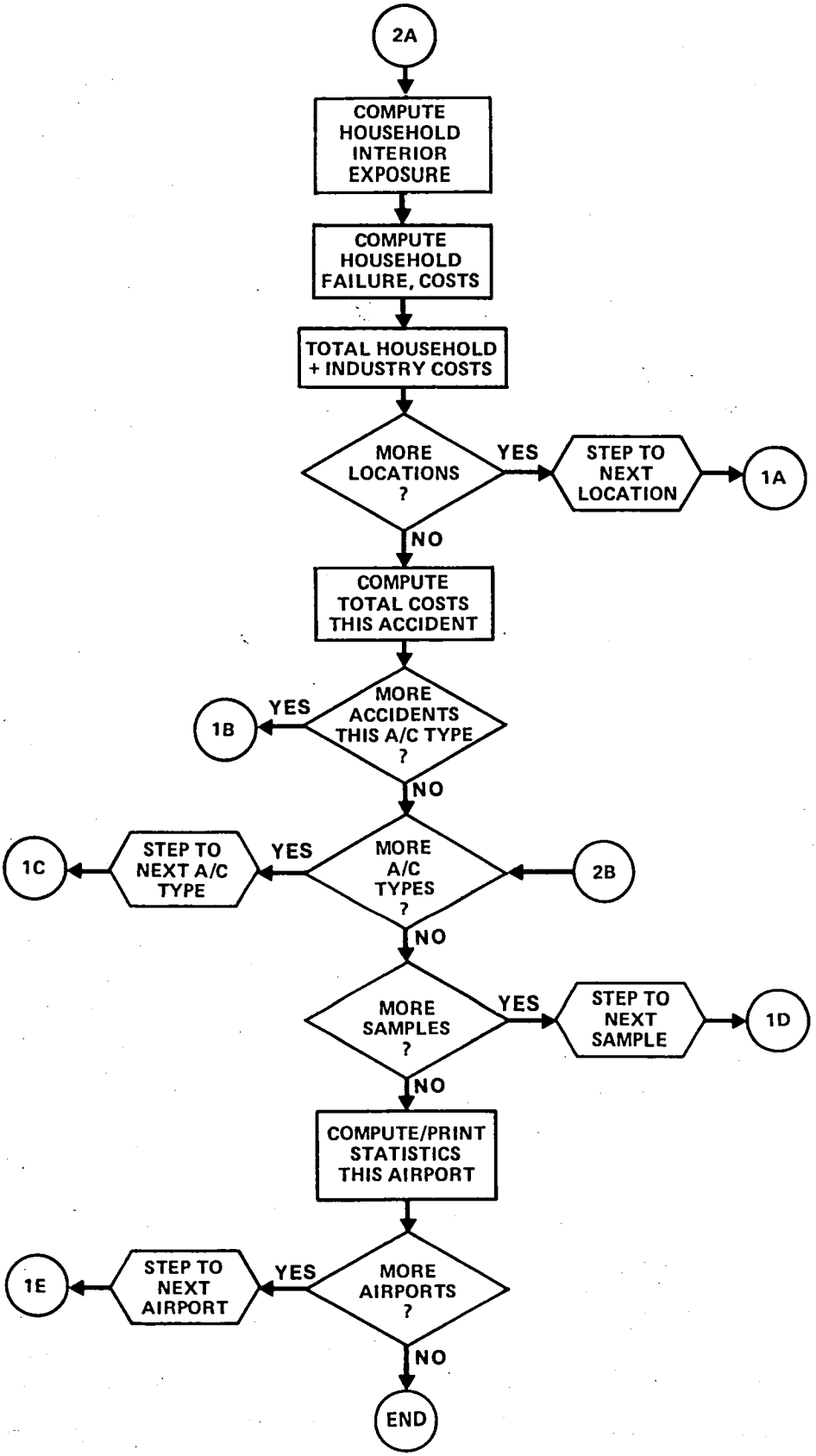

FIGURE 2.3b. FLOWCHART 2 FOR ORI AIRPORT RISK ASSESSMENT MODEL

Generate Accident

The computer model computes the number of accidents that will take place during the simulated year at this airport for each aircraft category. This calculation is a random process based on the assumption that the actual number of accidents is described by a Poisson distribution. The mean is estimated by taking the ratio of the number of operations of one type of aircraft at this airport to the total number of operations in the United States, and multiplying this ratio by the expected national annual accident rate. For generality, however, the complete model can consider all accidents, later deciding on the basis of reference to input data whether the accident led to a fire and possible release of graphite fibers. In the calculations reported here, we restricted our attention to accidents with fire. Further, we deal only with aircraft that have graphite composite material in their structures; therefore, the national accident rate used in calculating the expected number of accidents is the rate for graphite-fiber aircraft accidents with fires. Sample calculations of this rate, and comparisons of random draws from the Poisson distribution with expectations are presented later in the report.

Once the model computes the number of accidents for the aircraft type being considered, we determine the operational phase during which the accident took place; this is a random assignment based on experiential data drawn from accident files at the National Transportation Safety Board. For each operational phase and aircraft type the model assigns an accident location, which is also a random draw from accident location distributions developed by analysis of the NTSB data. At the end of the accident generation routine we then have the aircraft type, the operational phase during which the accident took place, and the associated accident location. The model is now ready to compute the subsequent movement of graphite fibers released in the fire that followed the accident, but first must determine certain associated variables, as described below.

Compute Weather Details

The actual weather conditions which are required as input to the model are the surface wind speed and direction, and the associated

atmospheric stability conditions. Fortunately, the joint distribution of these variables is available in a data base maintained at ORI under a joint EPA-FAA contract. This distribution is read into the computer for each airport being investigated. The probability distribution gives the frequency with which each combination of wind direction, wind speed range, and stability class occurred in the past. Some consideration was given to biasing this distribution towards poor weather conditions, since accidents are more likely to occur in bad weather than in good. After some discussion, the decision made was to consider all weather conditions, without bias in favor of poor weather conditions; it was estimated that the difference in final results would be less than a factor of two. With these weather data at hand, the model is ready to do the two calculations described next.

Compute Plume Height

At this step in the program, the model computes the height to which the fire plume will grow before stabilizing. This height is based on the aircraft class, the operational phase during which the accident took place, and the weather conditions selected earlier. It was recognized that many different random elements are present in this stage of the process, but, because of the uncertainty regarding them, we limited ourselves to using one set of stabilized plume heights for each combination of aircraft class and weather stability condition at the time of the accident. This method will tend to reduce the final variance, when compared to a wider range of plume height values. The aircraft size determines the size of the subsequent pool fire, or rate of energy release, which, with the meteorological stability condition, determines the behavior of the fire plume.

Compute Downwind Exposure

The model uses the weather details obtained earlier and the fire plume height generated in the last routine as inputs to the downwind exposure calculation. The other major input, which is the amount of graphite fiber released due to the fire is also determined here. Although the actual value is a random variable we have assumed that the fraction of the aircraft actually involved in the fire is fixed for each operational phase; the

fraction of fiber in the aircraft structure that is involved in the fire is assumed to be equal to the fraction of the aircraft that is involved in the fire. Further, we used the generally-accepted value of 20 percent of this fiber as the amount subsequently released as single fibers. These methods were adopted due to the unavailability of more precise aircraft-fire data; the use of probability distributions while introducing more variance would also have introduced more uncertainty and required more replications. The actual exterior exposure values are computed at points within a set of representative circles covering the region around the airport out to a range of at least fifty miles. This set-up is illustrated schematically in Figure 2.4 for a case in which one circle is used for an entire county; in many cases more than one circle was required. For each representative circle the model calculates the exterior exposure at the central point and at points two-thirds of the radius to the east, west, north, and south of the central point, in order to establish values representative of the area. The equipment failure and resulting cost impact calculations described below are also done for each of these points. The basic transport and diffusion model is characterized as a Gaussian plume model with some modifications. The principal modifications made were to include the effects of the fallout of the graphite fibers and partial reflection at the earth's surface.

Compute Interior Exposure

The model assumes that each residential unit and each type of business or industry at each of the key points for which the exposure is computed can be characterized by a typical building or type of enclosure. Each type of business-industry and each residential unit has associated with it a set of input parameters that determine how the exposure inside the building is related to the exposure outside the building. These values are developed from standard air conditioning and heating manuals. By referring to these parametric values the model determines the exposure interior to typical buildings for each class of business or industry (or particular parts of these buildings if this is pertinent). This set of assumptions also tends to reduce variance, but is reasonable in terms of the introduction of uncertainty and associated computational requirements.

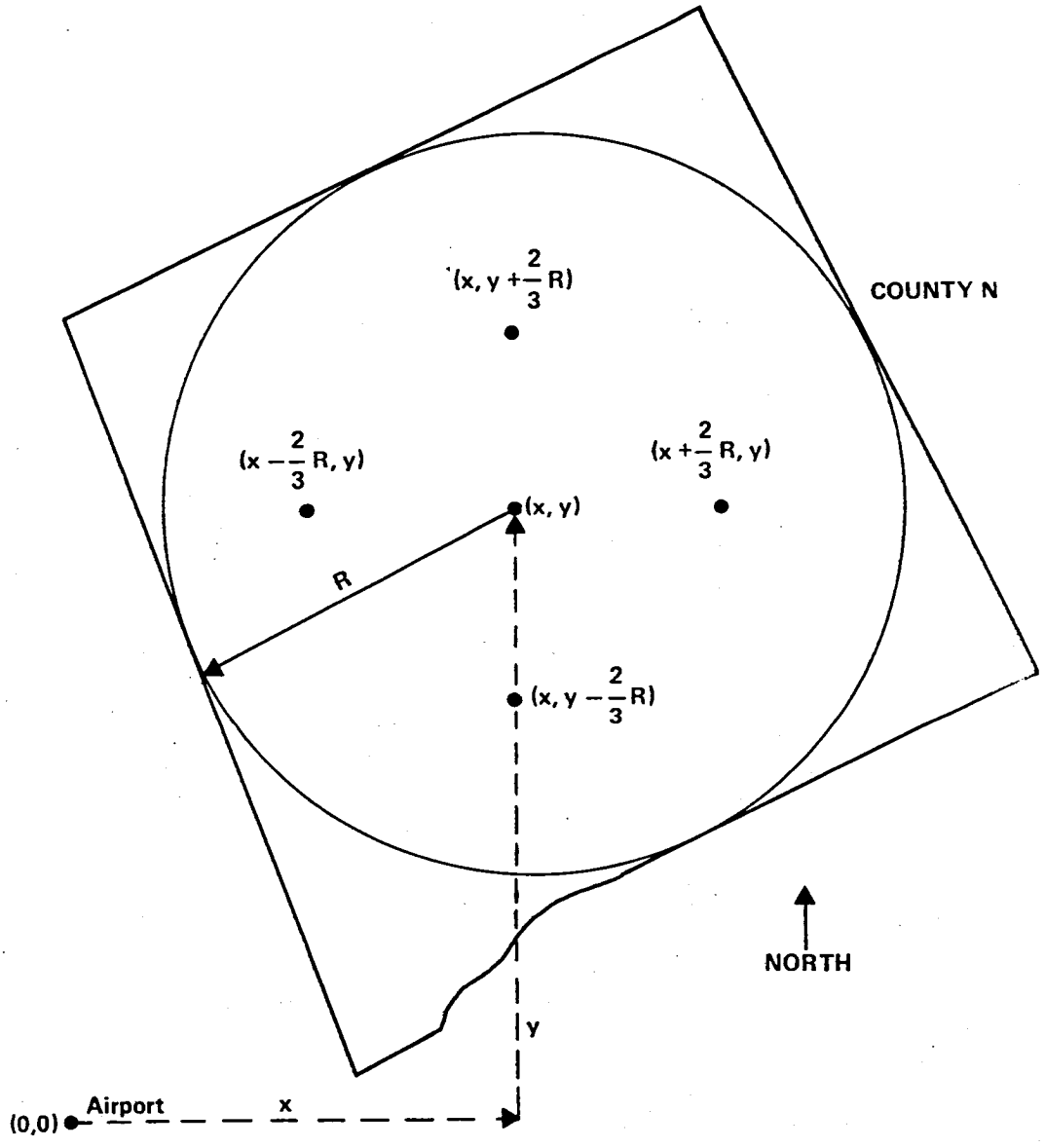

FIGURE 2.4. SCHEMATIC SHOWING LOCATION OF HYPOTHETICAL COUNTY RELATIVE TO AIRPORT

Compute Failures

The model assumes that each individual vulnerable equipment obeys an exponential failure law. The input structure for each business-industry type describes the set of equipments within the typical building and the way they are related to each other. From the interior exposure values and the input failure parameters for each of these individual equipments the model computes the probability that an individual factory or business establishment in each category would have failed. Similarly, the probability that household equipment would have failed is computed for each typical household class at each of the characteristic points in the geographic area. This is done for all business-industry categories and types of residence at each characteristic location.

Compute Cost

For each residential unit the impact is estimated on the basis of the fraction of the equipments expected to be damaged and a standard repair cost. In the case of business and industry the impact is based on the assumption that all impact can be proxied by the likelihood that a complete failure would result in one day's lost business or production. The probability of failure of one type of business or industry is used as an estimate of the fraction of all businesses of that type near (within a distance of the order of R/3 as shown in Figure 2.4) that location that would have been affected. The model then allocates to each type of business its share, based on its fraction of the national payroll, of the Gross Domestic Product for that type of business. The estimated impact in dollars, at one point, is the sum over all businesses of the product of the Gross Domestic Product allocated to each business and the failure probability for that type of business at that location. The calculation is carried out for all points in the geographical area surrounding the airport. This is essentially an expected value calculation; for the airports of most interest, where business and industry are relatively dense this method is not expected to yield results that are significantly different from a completely randomized calculation, while saving considerable computational effort.

The computation of the interior exposure, resulting failures, and their cost impact -- is done for all industries, and residential unit types at all of the pre-defined points within the circle representing a county or a portion of a county. Once the computations are made for one of the clusters representing a county or portion of a county, the model moves on to the next geographical area and its component circles. The computations are repeated there for that location's industries and residential units, using the value of exposure for that location. When all geographical areas have been completed, we have the estimate of the total cost impact of one accident. The model then determines whether it has finished processing all accidents that occurred in the simulated year (sample) for that aircraft type. If not, the next accident is processed exactly as described above until the total cost impact is generated. This is done for all the aircraft types considered for the year being simulated to obtain the total estimated impact of graphite fiber incidents during the year. The model then draws another sample by generating the number of accidents during another replication of the year under investigation. When the pre-set number of replications have been made the model has the information it needs to compute selected statistics over all samples. These include the frequency distribution of annual costs and the risk profile. Detailed results describing the ten most costly accidents are also available.

NATIONAL RISK PROFILE

The total national risk can be estimated in several ways. One method is to model the entire nation, at least as represented by some set of airports. The national model can be exercised in exactly the same way as the single airport model. The number of accidents in the country is generated and accidents assigned to individual airports. A replication would consist of simulating the total national impact by adding the costs incurred at each of the representative airports. This method is considered relatively costly in terms of computational effort. Other methods would develop the individual risk profiles for a number of airports and then combine the risk profiles to prepare a national risk profile. One such

approach is a variant of the national model in which individual output results are randomly drawn from distributions previously computed in single airport analyses. Another method is the straightforward combining of risk profiles previously obtained from individual airport analyses. This process, by which several probability distributions are combined to yield the probability distribution of a new variable which is the sum of the individual variables, is a convolution. In order to develop individual airport results which are of considerable significance in their own right, en route to the national risk estimate, this is the method we adopted.

A computational algorithm was prepared to perform the convolution, using as input the frequency distributions of the accident impact cost for several airports. This model can treat any number of airports to generate the probability distribution of total national cost impact: the national risk profile. If necessary, one airport can be convoluted with itself to estimate the impact of several similar airports.

III. AIRCRAFT ACCIDENT DATA

Several factors associated with aircraft accidents are required as input to the risk assessment calculation. We need to determine the probability that an aircraft will catch fire during an accident near each airport of interest, since graphite fibers are only released as the result of a fire involving composite material. We need some description of the locations of these accidents, and the resulting fires, relative to the airport. We need some estimate of the fraction of graphite composite in the aircraft structure that will be involved in the fire, and the resulting amount of fiber that will be released in the size range that we expect to constitute a risk. Each of these aspects of the aircraft accident problem is discussed in this section of the report.

AIRCRAFT ACCIDENTS INVOLVING FIRE

Aviation accidents that have been reported by the National Transportation Safety Board (NTSB) for the eleven-year period 1966 to 1976 were reviewed. The basic data source was the NTSB's Annual Review of Aircraft Accident Data, one volume for each of the eleven years. The Annual Review is published each year for commercial civil aviation (the certificated air carriers) as well as for general aviation. The scope of our investigation caused us to restrict attention to the commercial aviation statistics only. Although the data are summarized in the annual reports, and although the data are also available on

magnetic tape, it is still necessary to turn to more fundamental sources of information.

Table 3.1 summarizes the gross statistics from the accident briefs as reported in the NTSB's Annual Review series. A total of 594 accidents was reported in the course of the eleven years, and of these, 136 involved fires. That is, 23 percent of the reported accidents involved fires.

TABLE 3.1

SUMMARY OF U.S. AIR CARRIER ACCIDENTS[1]

Year	No. of Accidents Reported	No. of Accidents with Fire
1966	75	13
1967	70	21
1968	71	17
1969	63	6
1970	55	16
1971	48	11
1972	50	14
1973	42	9
1974	47	12
1975	45	9
1976	28	8
TOTALS	594	136

It is possible to draw a trend line through these data, as some investigators have, and show that the number of accidents per year will approach zero within a few years. We have taken a more realistic approach and assumed that there will always be some accidents. The actual number would realistically be a function of many variables, for example, the experience associated with the introduction of new aircraft. In view of these considerations, we have assumed that the total number of accidents involving fires in the United States will "level off" at six per year. This combines the well-documented downward trend with the notion that the number is not likely to reach zero. We have retained

[1]NTSB, Annual Review of Aircraft Accident Data, 1966-1976.

this estimate throughout the calculations, using it both for the 1985 and 1993 scenarios. With expected increases in air traffic during the intervening years, this implies a continued decrease in the national aircraft accident rate, but avoids the introduction of one more variable parameter into the comparison of our results for 1985 and 1993.

In the simulation model described later in the report it was necessary to allocate an appropriate fraction of the six fire accidents estimated to occur nationally to each airport being processed. For this allocation we assumed that the expected number of accidents at an airport in one year is given by the expression:

$$\frac{\text{Number of operations at this airport}}{\text{Total number of operations in the U.S.}} \times 6$$

Further, rather than estimate the number of accidents nationally for each aircraft type we are concerned with, we chose to apply essentially the same relationship for each aircraft type. That is, the expected number of accidents involving fires for a specific type of aircraft is obtained by multiplying the expected number of accidents at the airport by the ratio of operations at the airport by the aircraft type of interest to all operations at the same airport. This is equivalent to replacing the numerator above by the number of operations of the specific aircraft type at the specific airport.

To summarize, then, the expected number of accidents at the airport is assumed to be proportional to the number of operations at that airport. In a separate analysis we demonstrated that more than 70 percent of the variance in the accident distribution was accounted for by the number of operations. For the purposes of this study, in view of the questionable accuracy of many of the other inputs, we considered this result sufficient confirmation of the proposed method.

In the ORI Risk Assessment Model the number of accidents in any sample is obtained by making a random draw from a Poisson distribution. The probability of exactly k accidents with fire in a year at one airport involving a particular class of aircraft with carbon fiber is given by:

$$p(k;\lambda) = \frac{e^{-\lambda}\, k}{k!} \qquad (3.1)$$

where λ is the mean annual fire-fiber accident rate at the airport. That is, λ given by:

$$\frac{\text{No. of operations at airport, aircraft category of interest}}{\text{Total U.S. operations, all commercial aircraft}} \times 6 \times \text{Fraction of aircraft in category with fiber} \quad (3.2)$$

The Poisson distribution is often used for estimating accident incidence and other related random events. The distribution, because of its special utility in this regard, was once known as the "law of small numbers or rare events."[2]

FRACTION OF AIRCRAFT CONSUMED BY FIRE

In examining the data describing accidents accompanied by fire in the NTSB Annual Reviews, as well as tabular summaries generated by the accident abstracts included in the NTSB-prepared computer tape, we determined that many of the details necessary at this stage of the analysis were not available in these two media. It was necessary to review more basic accident data, much of which was available at the NTSB Headquarters. In particular, it was necessary to develop estimates, for future input to the computer, of the fraction of an aircraft that might be consumed by fire following an accident. It was particularly desirable to relate these estimates to aircraft type, if feasible, and operational mode during which the accident took place. It was clear from a preliminary review of the summary data that many of the accidents accompanied by fire might be such that liberation of graphite fibers could not reasonably be expected.

The NTSB maintains two data sources that are "more basic" than the published annual summaries or the tabulated summary data: the Aircraft Accident Reports (known as the "Blue Books") and the actual file of raw accident data containing on-the-spot reports from many sources. It was possible to review several years' worth of accidents involving fires with the aid of the information in these two sources. Unfortunately, some earlier accidents with little damage did not rate the preparation of a "Blue Book," while several that had been prepared were no longer available. Our concern for problems of inhomoge-

[2]W. Feller, 1950. An Introduction to Probability Theory and Its Application, John Wiley, New York, P 158 et seq.

neity of the data associated with going too far back in time led us to forego the hunt for accident files earlier than those maintained at the NTSB Headquarters. Accordingly, our review of raw accident data spanned the years 1972 through 1976. We covered those accidents that had previously been identified as accompanied by fire or explosion. This comprised a total of 52 accidents that had been identified in the Annual Reviews for these years. In the "Blue Books" and the basic accident files we were able to find 34 of these. A summary of our findings with regard to the possibility of graphite fiber release as a result of the accident appears below. Here we have indicated the number of "possibles" out of the total number of fire accidents reviewed. The scoring of "possible" means that, in the judgment of our accident review team, graphite fibers might have been released in the accident, given that there were fibers in the structure of the aircraft. Of course, no fibers were released in any of these accidents since there were none present. The preliminary results were:

- 1972 -- Six accidents reviewed; six possibles
- 1973 -- Seven accidents reviewed; six possibles
- 1974 -- Seven accidents reviewed; five possibles
- 1975 -- Six accidents reviewed; two possibles
- 1976 -- Eight accidents reviewed; six possibles.

In summary, 25 out of the 34 accidents involving fire for which detailed data were available, were judged to be potential graphite fiber release accidents.

Some of the details underlying the exclusion of specific accidents from the "possible" category are worth noting. Brief accounts of these excluded fire accidents, focusing on the reasons for deciding that they would not lead to graphite fiber release, follow:

- 1973 -- Aircraft ran off the runway after landing. A small fire in the right engine was extinguished by the aircraft's own fire-extinguishing equipment.
- 1974 -- An in-flight fire in the number two engine was extinguished by the engine's own fire bottles.
  -- An accident was found to be caused by an explosion due to sabotage. There was no fire.

- 1975 -- Prior to take-off there was a fire due to overheated wires; extinguished and aircraft resumed operation.
  - -- Prior to take-off the number-3 engine caught fire. The fire was put out "immediately" by ground mechanics.
  - -- A flash fire in the area of the tail pipe of the number-1 engine was under control in seconds. The fire effects were limited to the landing gear tires and wheels.
  - -- Fire prior to take-off was limited to the APU and lasted only 5 to 10 seconds.
- 1976 -- In-flight fire in number-2 engine was self-extinguished.
  - -- The use of a power carbide saw by rescue personnel caused a fire. The fire was extinguished in seconds.

AMOUNT OF GRAPHITE FIBER RELEASED

The number of graphite fibers that might be released as a result of an aircraft accident involving fire depends on several factors. Among the more obvious factors are how much graphite fiber material (more precisely, perhaps: how much composite material, and what fraction of the composite is graphite fiber) is used in the aircraft structure, and how much of the composite material is actually involved in the fire. If the composite material is used in identifiable parts of the aircraft, the factors of particular interest to us are whether that portion of the aircraft would be involved in a fire resulting from an accident, and, if involved, what fraction of the fiber therein would be liberated.

As part of NASA's Aircraft Energy Efficiency (ACEE) program, the aviation industry is currently developing a number of aircraft structure components using graphite fiber composites. Components including rudder, ailerons, and elevators could be used in 1980-1983 production aircraft. Structures such as the vertical fin and the horizontal tail will probably not be in production before 1983. There is apparently no current development program to apply carbon composite materials to the wing structures of production commercial aircraft. Such composite structures are not expected to be available before 1985, at the earliest. Composite wing structures for aircraft about the size of the DC-9

or the Boeing 727 might contain about 1,800 kilograms of carbon epoxy composite material. We have noted, for example, that in several accidents the tail section was separated from the rest of the aircraft during the early stage of the accident. If all of the composite material in such an aircraft were in the tail structure, and the fire were confined completely to the main fuselage, then no graphite fiber would have been released in those accidents. A parallel study by the air frame manufacturers is underway to provide more details of the type outlined above for past accidents.

At present, with future applications of composite material not completely firm, and the detailed data describing involvement of specific aircraft structural elements in fires resulting from accidents unavailable, we have made an assumption equivalent to: the composite material is used uniformly throughout the aircraft structure. The actual amount of graphite contained in composite material projected for aircraft by aircraft size (type) is shown in Table 3.2. These values were developed collectively by NASA, Boeing, McDonnell-Douglas, and Lockheed, and were essentially adopted by ORI and other investigators as standard values for the Phase I risk assessment calculations. Our basic assumption is that if one-half of the aircraft is involved in a fire, one-half of the composite material on board is involved in the fire. Table 3.2 also shows the fraction of commercial aircraft in each size category that is expected to have graphite composite material in their structure. Further, the available data reported by other NASA/Langley-sponsored investigators suggest that about 20 percent of the carbon in that composite material will actually be released as single short fibers in the size range that poses a threat to electric and electronic equipment downwind. Again, this 20-percent factor was adopted as standard for all calculations.

FRACTION OF AIRCRAFT CONSUMED BY FIRE

Table 3.3 summarizes the available information for each of the aircraft fire accidents reviewed by the ORI team. For each accident the table shows the operational phase during which the accident took place, the weather at the accident site, the amount of fuel on board, the duration of the fire, the extent of damage as estimated by the NTSB investigators, and the fraction of aircraft structure consumed in the fire, as estimated by the ORI accident review team. In each case we have reported the original NTSB file number which enables any investigator to retrieve the complete docket for that accident.

TABLE 3.2

PROJECTED FUTURE USE OF CARBON FIBER IN COMMERCIAL AIRCRAFT

Aircraft Category		1985		1993	
Size	Current Examples	Fraction Carrying Fiber	Fiber Per Aircraft (Kilograms)	Fraction Carrying Fiber	Fiber Per Aircraft (Kilograms)
Large	DC-10, L-1011, 747 727, 757, 767, 707	.33	454	.50	2041
Medium	DC-8	.20	136	.60	680
Small	737, DC-9	.33	91	.50	454

The ORI estimates of fraction of structure consumed by the fire were based on the narrative reports prepared by NTSB investigators, and the examination of all relevant data in the complete accident file, which occasionally included photographs. One finding is that, in all cases examined, some portion of the aircraft escaped complete destruction by fire. As an example of how the fraction of aircraft consumed was estimated, consider the 1976 accident with file number 1-0020 (cf. Table 3.3).

The following is an excerpt from a 1976 accident "Blue Book."[3]

"Fire erupted in the left side of the aircraft after the left main landing gear traversed the ditch and severed the left main landing gear's attaching structure on the left main fuel tank's rear bulkhead. Fuel escaped from this tank, burned and caused massive damage to the left side of the fuselage and inboard section of the left wing. The cabin interior was damaged heavily throughout by smoke and soot."

---

[3] National Transportation Safety Board, Aircraft Accident Report, Texas International Airlines, Inc., Douglas DC-9-14, N9104, Stapleton International Airport, Denver, Colorado, November 16, 1976, Report Number NTSB-AAR-77-10.

TABLE 3.3

SUMMARY OF AIRCRAFT FIRE-ACCIDENT DATA

YEAR	FILE NO.	A/C TYPE	OPERATIONAL PHASE	WEATHER AT ACCIDENT SITE	FUEL ON BOARD (POUNDS)	FIRE DURATION	AIRCRAFT STRUCTURE CONSUMED (PERCENT)*	DAMAGE EXTENT†
1972	1-0002	DC-9	Landing	rain	NR	3 min.	50	Destroyed
	1-0003	DC-9-14	Landing Go-around	none	22,000 (jet A)	NR	80	Destroyed
	1-0005	CV-580 DHC-6	In-flight, cruise	none	NR	NR	30 30	Destroyed Destroyed
	1-0016	L-1011	In-flight	none	43,000	flash fire	10	Destroyed
	1-0017	DC-9	Take-off, initial climb	fog	22,000 (jet A)	19 min.	60	Destroyed
	1-0048	B-737	Final Approach	fog		20-30 min.	50	Destroyed
1973	1-0011	DC-9	Final Approach	fog	13,000	20 min.	80	Destroyed
	1-0015	DC-8	Take-off	NR**	NR	NR	10	Minor
	1-0017	CV-600	In-flight	rain	NR	NR	20	Destroyed
	1-0018	DC-8	Landing	drizzle	70,000		70	Destroyed
	1-0019	B-737	Landing	rain	NR	≈ 0	≈ 0	Substantial
	1-0026	DC-10-30	?	rain	182,000	> 3 min.	40	Substantial
	1-0041	F11227B	Landing	rain	4,830 (jet A)	NR	20	Destroyed
1974	1-0001	B-707	Landing	rain	69,000	> 14 min.	90	Destroyed
	1-0008	Lockheed 382	In-flight	rain	40,500 at take-off	NR	60	Destroyed
	1-0012	B-707	Landing	fog	hydraulic fluid burned	25 min.	60	Destroyed
	1-0013	DC-10	Climb to cruise	NR		0	0	Substantial
	1-0020	DC-9-31	Landing	fog		10 min.	80	Destroyed
	1-0024	B-707	In-flight	clear		No fire - explosive device	80	Destroyed
	1-0029	B-727	Landing	rain			80	Destroyed
1975	1-0002	B-727	Parked	NR			Wiring Overheated	Substantial
	1-0006	B-727	Landing	rain	11,300	8 min.	50	Destroyed
	1-0019	L-1011	Starting Engines	NR	NR	NR	0	None
	1-0029	B-727	Taxi	fog	NR	12 min.	20	Substantial
	1-0032	DC-10	Take-off	haze	155,000	∿ sec.	0	Substantial
	1-0037	DC-10	Taxi	rain	NR	NR	0	None
1976	1-0003	B-727	Landing	fog/snow	35,000	4 hrs.	50 (classic bent-over plume)	Destroyed
	1-0005	B-727	Landing	clear	14,100	40 min.	80 (plume several 100 ft high)	Destroyed
	1-0009	L-1011	Descending	NR	NR	NR	0 (electrical fire)	Substantial
	1-0012	B-727	Take-off	clear	NR	NR	10	Substantial
	1-0015	DC-6	Take-off	rain	9,600 (av. gasoline)	∿ sec.	0	Destroyed
	1-0020	DC-9	Take-off	clear	18,300	7 min.	15	Substantial
	1-0024	DC-10	Landing	NR	NR		20	Substantial
	1-0025	L-188	Landing	NR	(5,000 gallons transported)	1 day	50	Destroyed

* Estimated by ORI accident review team

† Estimated by NTSB accident team

NR Not reported

In addition, other reports in the investigative file showed that the fuselage was burned through on the left side in the area of the left wing roots. The left wing root and fairing were burned. The left overwing exist was almost completely consumed by fire. In this instance, the investigative file contained the statement that about 25 percent (such percentages are rarely given) of the fuselage on the left side was consumed in the fire, which was extinguished in 7 minutes. This led to the ORI team's estimate of 15 percent overall fire damage to the aircraft. The NTSB report characterized the damage to the aircraft as "substantial."

We were clearly interested in the relationship of the fraction of aircraft destroyed by fire and the operational phase. Due to the limited data, some aggregation was done in seeking to establish this relationship. In the "take-off" category we included taxi prior to take-off as well as ascent to cruise level. In "landing" we included descent from cruise level and taxi after landing. The intent was to separate the operation of the aircraft into time categories that would segregate periods when there were large amounts of fuel on board (take-off) from those with relatively little fuel (landing). Of the 34 accidents with fire that were reviewed in detail, we were able to classify 17 as "landing" accidents and 7 as "take-off" accidents. The remainder were either unassignable due to data gaps, or clearly not in these operational phases.

Based on our analysis of the data summarized in Table 3.3 and these definitions, we estimated the distribution by operational phase of accidents involving fires that could potentially result in the release of graphite fibers to be:

- Static -- 0
- Taxi -- 0
- Take-off -- 20%
- In-Flight -- 20%
- Landing -- 60%

These results are discussed further below.

The data indicate that the fraction of aircraft consumed by fires during landing accidents is significantly greater than for take-off accidents. The estimated median fraction of aircraft consumed is 50 percent for landing and 20 percent for take-off. This suggests that the amount of fuel on board, typically far less on landings than on take-offs, is not critical to the determination of consumption by fire. More important, perhaps, is the impact associated with an emergency landing and the higher probability of the crash being off the airport resulting in decreasing accessibility for fire and rescue equipment. The fraction-of-aircraft-consumed data for in-flight accidents were even more sparse than indicated earlier. As a reasonable value based on the few documented cases, we selected the value of 30 percent of the aircraft involved in fire for accidents occurring during the in-flight phase.

FIRE DURATION

Another question of interest is the duration of any fire resulting from an aircraft accident, and its relationship to phase of operation. The frequency data for fire duration following landing and take-off accidents from the NTSB reports indicate that the median fire duration is 20 minutes for landing accidents and 2.5 minutes for take-off accidents. The data set is extremely limited, implying that relatively little confidence can be placed in the numerical results, but longer durations for landing accidents are consistent with the earlier finding of greater consumption by fire in landing accidents. The frequency distribution based on the cases available is shown in Figure 3.1.

The conclusion based on necessarily restricted analyses of limited data is that the fire hazard, and consequent release of graphite fibers, is greater for landing than take-off accidents. There are considerably more landing accidents with fire than take-off accidents with fire; the percentage consumption by fire is considerably greater for landing accidents than take-off accidents; and, probably correlated with the previous finding, landing-accident fires last longer than take-off accident fires.

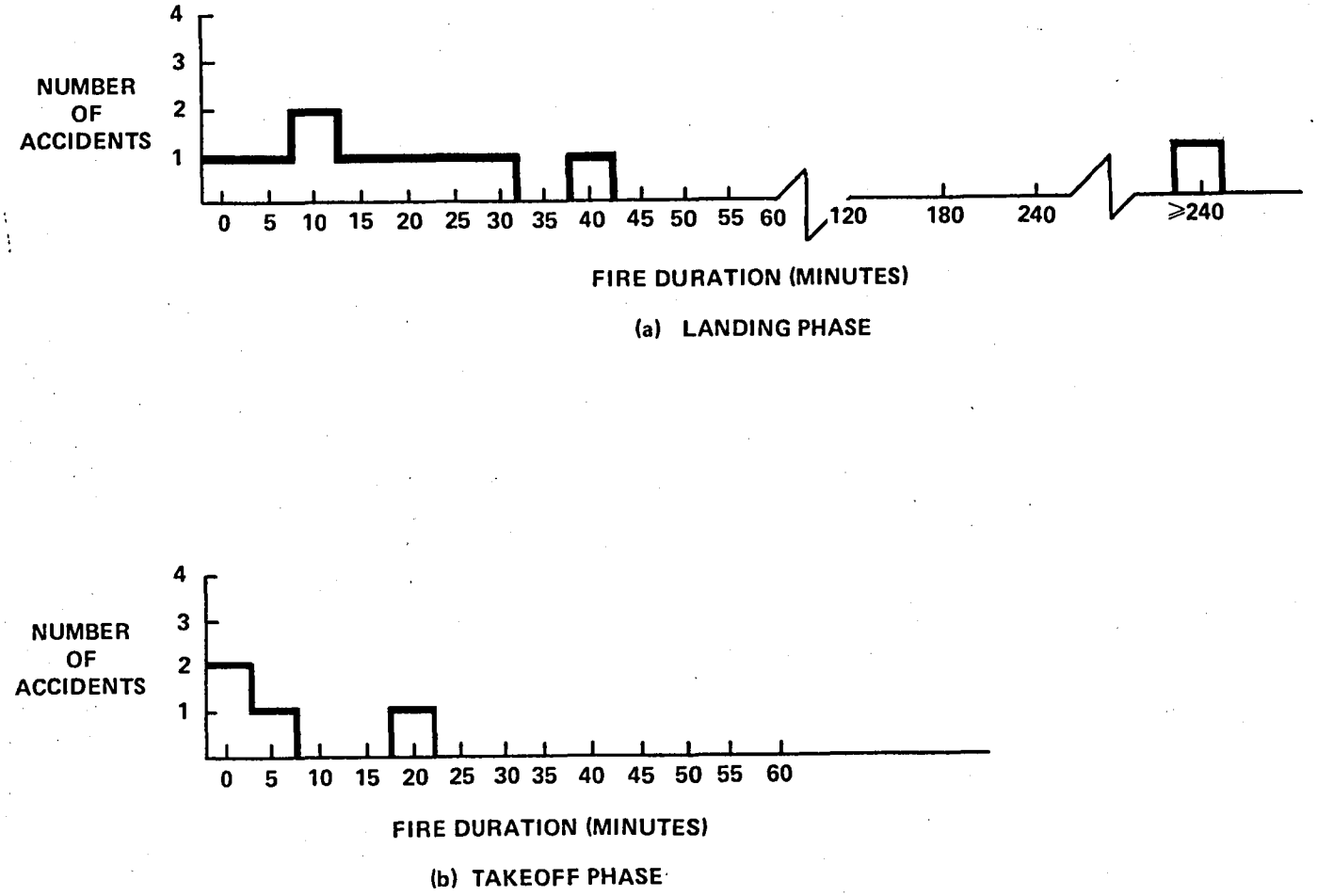

FIGURE 3.1. FREQUENCY DISTRIBUTION FOR FIRE DURATION

Stanford Research Institute (SRI) has written a detailed report which also characterizes aircraft accidents involving fires.[4] The period for which they studied the accident data was 1963-1974, whereas we generally reviewed data for 1966 to 1976, and concentrated our analysis on 1972 to 1976. Their reported distribution of accidents involving fire over operational phase is consistent with ORI's findings. Landing accidents predominate, and the static and taxi phases are relatively insignificant contributors to the overall accident set.

The SRI study, like the basic NTSB data source, gives degree of destruction by fire only in the qualitative terms: destroyed, substantial, minor, and none. Thus, it is not possible to use SRI findings to supplement ORI's numerical estimates of percent of aircraft destroyed by fire.

AIRCRAFT ACCIDENT LOCATIONS

In developing the distribution of aircraft accident locations we separated the categories of in-flight and landing accidents which we had tended to lump in the analysis discussed to this point. We recognized, as will be shown later, that true landing accidents tend to be nearer the airport and in-flight accidents tend to be distributed over greater distances from the airport.

Table 3.4 gives the proximity to the "nearest runway of the airport" for 33 accidents involving fire that occurred in the years 1972 to 1976.* One accident that had been included in some of the earlier analyses was in fact an explosion due to sabotage (without fire) and it was decided to exclude it from this portion of the analysis. Only two of the 33 accidents involving fire took place under "static" conditions and two took place during the "taxi" phase. This supports our decision to simplify the analysis by assigning zero probability to accidents involving fire during the static or taxi phases. Further, it seems very unlikely that "on-airport" fires during these operational phases would be allowed to burn for more than a few seconds before fire-fighting equipment came to extinguish them.

---

[4]"An Analysis of Aircraft Accidents Involving Fires," G.V. Lucha, M.A. Robertson, and F.A. Schooley, SRI, May 1975, NASA CR 173690.

*Note that miles are used as the units because this is how original data are reported.

TABLE 3.4

AIRPORT PROXIMITY FOR AIRCRAFT ACCIDENTS WITH FIRE*

YEAR	FILE NO.	DISTANCE FROM AIRPORT (MILES)	OPNL PHASE
1972	1-0002	0	L
	1-0003	0	L
	1-0005	>5	I/F
	1-0016	>5	I/F
	1-0017	0	T/O
	1-0048	<2	L
1973	1-0011	0	L
	1-0015	0	T/O
	1-0017	>5	I/F
	1-0018	>5	L
	1-0019	0	L
	1-0026	0	L
	1-0041	<3	L
1974	1-0001	0	L
	1-0008	?	I/F
	1-0012	0	L
	1-0013	>5	I/F
	1-0020	<4	L
	1-0029	>5	L
1975	1-0002	0	S
	1-0006	<¼	L
	1-0019	0	S
	1-0029	0	T
	1-0032	0	T/O
	1-0037	0	T
1976	1-0003	0	L
	1-0005	0	L
	1-0009	>5	I/F
	1-0012	0	T/O
	1-0015	<1	T/O
	1-0020	0	T/O
	1-0024	0	L
	1-0025	0	L

Legend:

L = Landing
T/O = Takeoff
I/F = In-flight
T = Taxi

* 34 accidents from 1972 to 1976 previously selected for damage analysis, but one case of sabotage explosion dropped. Distances are to nearest runway of the airport.

Six of the reported accidents with fire took place during the take-off phase. As Table 3.4 shows, five out of six took place on the runway (distance to runway was zero miles) and the sixth took place less than a mile from the runway. It seems logical that take-off accidents will either occur on the runway or just beyond the end of the runway. Lacking specific data, we have assigned uniform probability for locations of take-off accidents with fire from the beginning of the runway to a distance of one mile beyond the far end of the runway.

Seventeen of the accidents with fire were landing accidents. Eleven of these took place on the runway. The remaining six were distributed as follows:

1 within 1/4 miles of the runway
1 within 2 miles of the runway
1 within 3 miles of the runway
1 within 4 miles of the runway,

while 2 were more than 5 miles away from the end of the runway.

Thus, combining the one landing accident that was within one-quarter mile of the runway with the eleven that were on the runway, we conclude that approximately two-thirds of all landing accidents with fire occur on the runway. For computer modeling purposes, we assume that these accidents are distributed uniformly along the runway with a total probability of two-thirds. Since we have no data to distinguish undershoots from overshoots, we arbitrarily assume landing accidents are equally likely to be undershoots or overshoots with probability equal to one-half for each type. Based on the crude proximity data for the sample of six landing accidents that occurred off the runway we assign the off-runway accidents uniformly within a six-mile band short of the runway and another six-mile band just beyond the runway.

Of the six in-flight accidents with fire reported in Table 3.4, the site of one is not given, and the other five all took place at distances greater than five miles from the airport runway. We have assumed symmetry so that half the in-flight accidents end up short of the runway and half

beyond the runway. We impose a five mile zone just short and just long of the runway where no in-flight accidents occur. And then we assume there is a 15-mile band beyond the five mile zone where the in-flight accidents do occur with uniform probability.

IV. FIRE AND RELEASE OF GRAPHITE FIBERS

The graphite-fiber release starts with an aircraft accident leading to a fire. The "typical" accident envisioned is fed by the aircraft fuel. As a result of the fire some fraction of the aircraft is consumed. Chapter III reviewed the correlation between aircraft operational phase (take-off, landing etc.) and the amount of damage caused by fire. It was noted that official sources, such as the National Transportation Safety Board, do not prepare quantitative estimates of the amount of damage caused by fire and, of course, there is essentially no information available on the amount of composite material that would be involved in the fire.

In the absence of detailed estimates of future use of carbon fiber composite material in commercial aircraft components, we introduced the assumption that the fraction of composite material in the aircraft structure that would be involved in the fire is equal to the estimated fraction of the aircraft involved in the fire. This is essentially equivalent to assuming that the composite material is used uniformly throughout the aircraft. Further, as described in Chapter III, it is expected that 20 percent, by weight, of the carbon in the composite material would be released as single fibers in the size range of interest during the fire. These assumptions reduce the variance of the final results, but some insight into their impact can be obtained from the sensitivity tests reported in Chapter IX.

As a consequence of the fuel-fed fire a hot buoyant plume is formed that rises to a "stabilization" height which is a function of the energy available to feed the fire, the wind speed, and the atmospheric stability. The released graphite fibers enter the buoyant plume and travel to the stabilization height, which is reached at a particular downwind stabilization distance. The solution to the physical problem of the rise of the buoyant plume was formulated by Gary Briggs. The results appear in the next section.

PLUME HEIGHT CALCULATION

Calculation of the plume rise (or elevation), H, at stabilization from an open fire follows the work of Briggs.[1] The height of the plume, in meters, is given by:

$$H = 2.9(F/us)^{1/3}. \qquad (4.1a)$$

for stable conditions, where u is the mean wind speed in meters per second.

For neutral or unstable conditions we have

$$H = 1.6F^{1/3}u^{-1}x^{2/3}, \text{ when } x < 3.5x^* \qquad (4.1b)$$

$$H = 1.6F^{1/3}u^{-1}(3.5x^*)^{2/3}, \text{ when } x > 3.5x^* \qquad (4.1c)$$

where:

$$x^* = 14F^{5/8}, \text{ when } F < 55$$

$$x^* = 34F^{2/5}, \text{ when } F > 55$$

The buoyancy flux parameter F, appearing in the above equation, is given by

$$F = \frac{gQ_R}{\pi C_p \rho T}$$

[1] Some Recent Analyses of Plume Rise Observations, Gary A. Briggs, paper presented at the 1970 International Air Pollution Conference of the International Union of Air Pollution Prevention Associates.

where:

g = acceleration of gravity, 9.8 m sec^{-2}

Q_R = heat emission rate, kcal sec^{-1}

C_p = specific heat of air at constant pressure, 0.2391 kcal $kg^{-1}(^oK)^{-1}$

ρ = atmospheric density, 1.293 kgm^{-3}

T = ambient temperature, (273.2 + temp $^oC)^oK$.

The atmospheric stability parameter, s, is defined by:

$$s = \frac{g}{T} \frac{\partial \theta}{\partial z}$$

where:

$\frac{\partial \theta}{\partial z}$ = gradient of potential temperature, $0.35^o km^{-1}$ for stable conditions (value appears in CRSTER code for subroutine BEH072).[2]

In order to use the Briggs formulas, we must specify Q_R, the heat emission rate for a burning aircraft. For this specification we are indebted to Bart Bartram of NUS Corporation.[3] Bartram has shown that Q_R may be approximated by:

$$Q_R = RA\rho E \qquad (4.2)$$

where:

R = fuel burning rate, 0.047 ft/min

A = fuel dispersion area, 481.74 ft^2

ρ = fuel density, 48.7 lb/ft^3

E = fuel heat content, 18,400 BTU/lb

---

[2] User's Manual for Single-Source (CRSTER) Model, EPA, July 1977, EPA-405/2-77-013.

[3] Unpublished Communication, 1978.

The fuel burning rate was determined empirically by Los Alamos Scientific Laboratories for JP-4 jet fuel[4]; more recent experiments conducted by NASA, reported after the ORI calculations were complete, indicate that this value may be too high, by as much as a factor of two (cf. the following section, "Layer Penetration.") The fuel dispersion area is an estimate of the area below the wing tanks on a B-737 aircraft. Using these data we find that $Q_R = 3.3575 \times 10^5$ BTU sec^{-1} (or 8.4614×10^4 kcal sec^{-1}) for a B-737 type aircraft.

Substituting the above values, we find that Equation (4.1a) becomes $H_{B-737} = 400\ u^{-1/3}$ for stable air at 70^0 F and $H_{B-737} = 380\ u^{-1/3}$ for stable air at 20^0 F. For unstable or neutral conditions, at either 20^0 or 70^0 F, equations (4.1b) and (4.1c) become $H_{B-737} = 4800\ u^{-1}$.

Since the B-737 is designated as a small transport type, we need a means to extend the plume-rise calculations to medium (707-type) and large (747-type) transport aircraft. We note in Equation (4.1) that H is proportional to $F^{1/3}$ for stable conditions and F is directly proportional to Q_R. It follows that H is therefore proportional to $Q_R{}^{1/3}$.

Equation (4.2) shows that Q_R is proportional to the area of the burning pool, the fuel deposited on the ground from the airplane's fuel tanks. For the B-737, a small transport type, the fuel dispersion area was set equal to the area below the wing tanks. Since the wing tanks comprise most of the wing structure, excluding ducts along the leading edge and control surfaces and voids in the trailing edge, this area is proportional to the area of the wing. Further a wing chord is typically approximately proportional to the wing span, so that the area subtended by the fuel tanks may be considered proportional to the square of the wing span. We have used this proportionality relationship in extrapolating Equation (4.2) to other aircraft. It then follows that the maximum plume height obeys the relationship:

$$H = K(\text{wing span})^{2/3}.$$

Then the height of the plume for any aircraft fire, H_{AC}, can be obtained from the height calculated for a B-737 aircraft, given by Equation (4.1) (defined

---

[4] R. K. Clarke, et al., 1976. Severities of Transportation Accidents, Sandia Laboratory, SLA-74-001.

as H_{737}). In stable atmospheric conditions the result is:

$$H_{AC} = H_{737} \left[\frac{(\text{Wing Span})_{AC}}{(\text{Wing Span})_{737}}\right]^{2/3}$$

In unstable or neutral conditions H is proportional to:

$$F^{1/3}F^{4/15} = F^{3/5}$$

Then H may be estimated from:

$$H_{AC} = H_{737} \left[\frac{(\text{Wing Span})_{AC}}{(\text{Wing Span})_{737}}\right]^{6/5}$$

These relationships thus enable us to determine plume rise for accidents involving different aircraft for any combination of wind speed and stability conditions. Typical values of the calculated plume heights under different conditions are given in Table 4.1.

LAYER PENETRATION

It is pointed out in Chapter V that there are occasions when the calculated plume rise is greater than the mixing layer height. When these cases occurred in the simulated accidents the plume height was set equal to the layer height. That is, "punching through" was forbidden. In the "real world," whether punching through occurs is problematic. For instance, L. Lavdas, of the Forest Service, has suggested that it is unlikely.[5] On the other hand, Table 4.2 from Pasquill[6] shows, for a limited set of data, instances of both penetration and nonpenetration of inversions. The values of Q_R are of the same order of magnitude as those that concern us here. The bottom of the inversion as shown in Table 4.2 is the mixing layer height, as the term is used in this report.

It would be important to evaluate the "punch through" or penetration problem with greater care if the graphite-fiber problem turned out to be

---

[5] Letter from Lavdas, USDA, Forest Service, Macon, Ga., to R. Greenstone, ORI, Inc., 26 October 1978.

[6] F. Pasquill, Atmospheric Diffusion (2d edition), John Wiley & Sons, New York, 1974.

TABLE 4.1

TYPICAL PLUME HEIGHTS (METERS)
(MODERATE WIND SPEED = 10 m/sec)

Aircraft Category	Wing Span (meters)	Stability Condition	
		Stable	Neutral/ Unstable
Large	59	257	685
Medium	44	180	480
Small	29	108	289

TABLE 4.2

DATA ON PENETRATION OF INVERSIONS BY HOT PLUMES
After Briggs (1969)

Date	Time	Q_R (10^7 cal/sec)	u (m/sec)	Plume Height (m)	Inversion height (m)		Penetration ?
					Bottom	Top	
May 25	1825	1.97	9.0	295	145	180	Yes
					325	475	No
July 20	0552-0559	0.98	10.5	350	255	275	Yes
					365	395	No
	0617-0820	1.11	7.3	360	540	580	No
July 21	0600-0724	1.13	4.3	360	410	450	No
	0828	1.64	2.7	510	240	280	Yes
					360	410	Yes
September 8	0648-0930	1.66	7.5	410	360	400	?
	1000-1020	1.77	5.4	560	620	650	No
	0640-0705	1.20	9.6	350	360	400	No
	0747-0850	1.54	9.1	370	260	300	Yes
					370	410	No
September 9	0930-1000	2.13	9.6	390	420	530	No

Source: F. Pasquill, Op.Cit.

severe. Our model of the physical processes involved in fiber transport (see Chapter V) indicates that there will be no graphite fiber at the ground as long as the plume is above the layer. The plume stays above the layer until its center of gravity drops through as a result of gravitational settling of the fibers. This phenomenon is represented by the tilted-plume model we have adopted, as described in Chapter V.

V. DOWNWIND TRANSPORT AND DIFFUSION OF FIBERS

MODEL SELECTION

Background

For this risk assessment study we wished to use a downwind transport and diffusion model that captured all of the significant physical elements of the problem. At the same time we wanted a model that could be easily adapted to our use. We hoped to use one that required a relatively small amount of input meteorological data and was relatively modest in its requirements for computer time. In examining relatively sophisticated models we recognized the associated liabilities in terms of cost associated with data preparation and computing time. We also concluded that this model need not provide results that were significantly more accurate than those that could realistically be expected from other parts of the complete risk assessment modeling chain.

A review of existing models with the above considerations in mind led us to a choice between the widely used EPA Turner Model[1] and the H.E. Cramer model[2]. We selected the Turner Workbook approach. The basic Cramer model

---

[1] D. Bruce Turner, Workbook of Atmospheric Dispersion Estimates, EPA, 1970.

[2] R.K. Dumbould and J.R. Bjorklund, NASA/MSFC Multilayer Diffusion Models and Computer Programs -- Version 5, H.E. Cramer Co., Inc., Salt Lake City, Utah, NASA CR-2631, December, 1975.

is not significantly different from the Turner model in the sense that they are both Gaussian plume models. The multilayer version of Cramer's model referenced here offers a degree of refinement that appears to go beyond the requirements of, and the data availability for, the present study. To use the multilayer model, one must have the appropriate meteorological characteristics for the various atmospheric layers being modeled. Since we are postulating accidents we would require data for typical multilayer atmospheric structures at various airport-associated accident sites around the country.

To determine typical multilayer atmospheric structures for each of a number of potential accident sites would require a significant meteorological investigation. The results would probably have to be given in terms of standard synoptic situations or by season of the year. In view of their detailed input data requirements, and associated costs, it appeared wisest to reject relatively sophisticated approaches, as exemplified by the Cramer model; the same argument applies to primitive equation models which depend on the numerical integration of the hydrodynamic equations of motion. Instead, a more readily applied model as exemplified by the Turner Workbook was selected. This model is also generally accepted by professionals in the pollution control field.

EPA Standard (Turner) Model

Turner's model (the present "standard" EPA model) provides for net downwind transport of material in the form of a plume that diffuses simultaneously in the crosswind and vertical directions. The initial source can be elevated at a specified height.

The atmosphere is characterized as being in one of several stability classes, with the most stable condition having the lowest mixing height (inversion level), and the least stable having the greatest mixing height. Dispersion parameters that govern the rate of crosswind and downwind diffusion are associated with each specified stability class. The dispersion parameter is smallest for the most stable atmospheric conditions and greatest for the most unstable condition. The magnitude of each dispersion parameter increases

with downwind distance from the source; the functional relationship for different stability categories is provided by the well-known Pasquill-Gifford dispersion curves. They are used in this ORI report in a form adapted from an EPA computer program called CRSTER[3]. These subjects are discussed in more detail below.

The ORI Transport and Diffusion Model

The plume rise calculations, performed separately, give the source height, which is then used explicitly in the transport and diffusion model. Plume rise calculations were discussed in Chapter IV. When the the independent plume rise calculations lead to plume heights greater than the height of the mixed layer, the plume rise is arbitrarily restricted to the layer height. In other words, heated plumes do not "punch through" the layer, as discussed in Section V.

As described below, the ORI model has features not included in the standard Turner model. It provides for finite particle settling through use of a "tilted plume" model. Also, the model permits less-than-perfect reflection of the diffusing cloud from the ground through introduction of a reflection coefficient, as shown by Cramer.

---

[3] User's Manual for Single-Source (CRSTER) Model, EPA, July 1977, EPA-450/2-77-013.

GENERAL MATHEMATICAL MODEL

The most general form of the ORI meteorological transport and diffusion equation is:

$$D(x,y,z,H') = \frac{Q}{2\pi\sigma_y\sigma_z u} \exp\left[-\frac{1}{2}\left(\frac{y}{\sigma_y}\right)^2\right] \left\{\exp\left[-\frac{1}{2}\frac{(z-H')^2}{\sigma_z^2}\right] + r \exp\left[-\frac{1}{2}\frac{(z+H')^2}{\sigma_z^2}\right]\right\} \quad (5.1)$$

where:

$D(x,y,z,H')$ = dosage at x,y,z (receptor location) in particle-sec m^{-3} for the particle size of interest

x = downwind distance from source to receptor, meters

y = crosswind distance from source to receptor, meters

z = elevation of receptor, meters

u = mean wind speed, m sec^{-1}, from release altitude to plume stabilization altitude, H.

Q = total number of particles in the size range of interest released

σ_y = standard deviation of the wind speed in the crosswind direction, as a function of x and the stability class, in meters

σ_z = standard deviation of the wind speed in the vertical, as a function of x and the stability class, in meters

r = reflection coefficient, the fraction of particles that are reflected from the ground surface, dimensionless parameter

Equation (5.1) makes use of the effective plume height, H'; this is the elevation of the plume central axis at any downwind distance, given by:

$$H' = H - (v_s / u) x \quad (5.2)$$

where:

H = elevation of plume at plume stabilization, meters

v_s = particle settling speed, $msec^{-1}$, for the selected particle size

The ORI Equation (5.1) for dosage is essentially the same form as Turner's Equation (3.1) for concentration when the height, z, is set equal to zero. To show this precisely we note that there is no settling considered by Turner so that H'=H. Total reflection is assumed so that r in Equation (5.1) may be set equal to one. The two exponential terms involving σ_z represent diffusion away from the "true" source at H and an "image" source at -H. If we set

$$r = 1$$

$$v_s = 0$$

and

$$z = 0$$

we have the conditions for no gravitational settling of the diffusing particles, perfect reflection of the particles at the ground surface, and have set the receptor for which the dosage is being estimated at ground level; these are the conditions assumed by Turner. Then, Equation (5.1) becomes:

$$D(x,y,0,H) = \frac{Q}{\pi\sigma_y\sigma_z u} \exp\left[-\frac{1}{2}\left(\frac{y}{\sigma_y}\right)^2\right]\exp\left[-\frac{1}{2}\left(\frac{H}{\sigma_z}\right)^2\right] . \qquad (5.3)$$

which is identical to Equation (5.10) presented in Turner's Workbook.

MODEL IMPLEMENTATION

In this section we describe the actual methods used to adapt and modify Equations (5.1), (5.2), and (5.3) to capture the key elements of the problem at hand, as well as to make them amenable for computer application in a Monte-Carlo simulation. The major model adaptations are discussed in turn below, along with the development of the appropriate input data. It should be noted that the model programmed and used is somewhat more general than the one published by Turner.

Elevated Virtual Source

It is necessary to develop methods to provide a source of fibers some distance from the scene of the aircraft accident and fire that is liberating the fibers. Here "distance" is typically some vertical elevation of the fire plume, and some downwind distance at which the plume is said to be stabilized. At this point we may say that Equation (5.1) "takes over." It is customary in many applications of these diffusion methods to compute the plume size at stabilization, and then determine the location of an upwind virtual point source from which a diffusing plume could be expected to grow, according to the diffusion model being used, to the actual size previously computed for plume stabilization. In this case the virtual point source will certainly be upwind of the plume stabilization point, and either upwind or downwind from the accident site. In view of the large uncertainties present in many other phases of the complete risk calculation, and the insight that leads us to be concerned with effects some miles downwind from the accident site, we have chosen to arbitrarily set the virtual point source directly over the accident - fire site. The calculation of the plume height at stabilization has been discussed previously, and is,of course modeled in the full calculation. In this application, then, we approximate the actual elevated downwind finite source by a virtual point source directly over the accident site.

The Tilted Plume Model

Ample experimental evidence exists to show that the graphite fibers we are interested in fall out with a non-neglible terminal velocity, variously estimated to be in the range of two to three centimeters per second. The diffusion and transport literature clearly indicates that fall rates of this magnitude have a significant impact on the downwind concentrations. These effects were also demonstrated in other calculations made for NASA Langley, principally those by Trethewey and Cramer. In order to incorporate these effects into our calculations we have adopted the method presented by Van der Hoven[4]. Van der Hoven proposed that the effect of gravitational settling of diffusing particles could be modeled by treating the plume as if it were tilted at an angle whose tangent is given by the ratio of the settling speed, v_s, to the mean horizontal wind speed, u. The decrease in height of the plume centerline as the plume moves downwind is then given by $(v_s/u)x$, where x is the downwind distance from the virtual point source. The resulting centerline height H' would eventually reach a value of zero and then become negative as x increases. The model guards against this result by setting H' equal to zero for all values of x at which H' would otherwise have a negative value; this in effect prevents the tilted plume from "going underground."

Dispersion Parameters

Equation (5.1) requires input values of the dispersion parameters, σ_y and σ_z, as functions of the downwind distance, x, and the prevailing stability conditions. The standard in this case is provided by the well-known Pasquill-Gifford curves, presented, for example, in Turner and shown here as Figures 5.1 and 5.2. Several investigators have recently questioned their universal applicability; the reader is referred to Pasquill's recent work on this subject[5]. In view of the fact that no generally accepted modification of the Pasquill-Gifford curves yet exists, and that Cramer has indicated, in discussions held at NASA Langley, that simple modifications of

---

[4] Meteorology and Atomic Energy 1968, David H. Slade, Editor, AEC, July 1968. (See section 5-3, "Deposition of Particles and Gases.")

[5] Pasquill, F., Atmospheric Dispersion Parameters in Gaussian Plume Modeling, Part II, "Possible Requirements for Change in the Turner Workbook Values," EPA, Research Triangle Park, June 1976, EPA-600/4-76-0306.

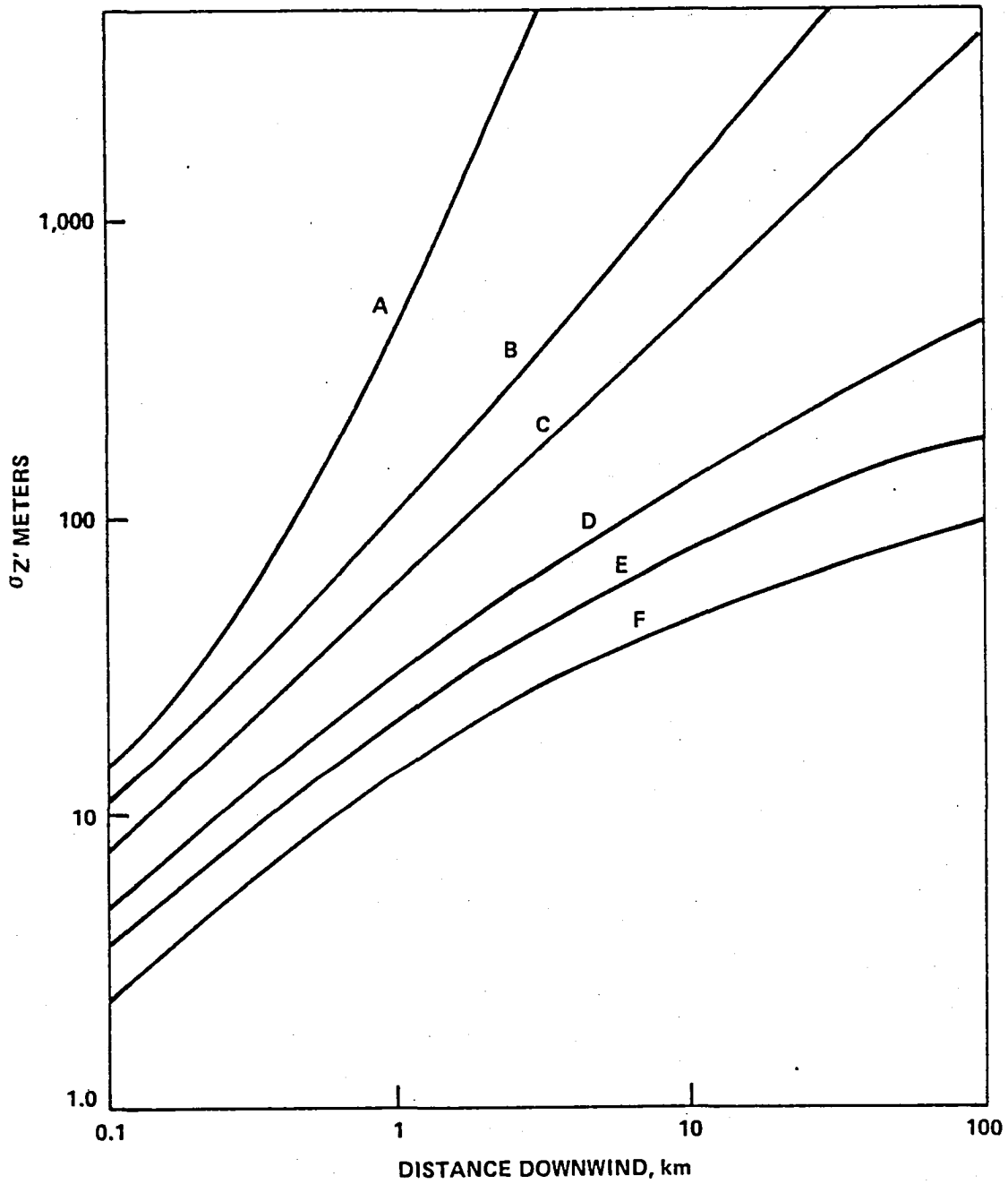

FIGURE 5.1. VERTICAL DISPERSION COEFFICIENT, σ_z, AS A FUNCTION OF DOWNWIND DISTANCE FROM THE SOURCE

(A = least stable, F = most stable)

Source: Turner, op. cit.

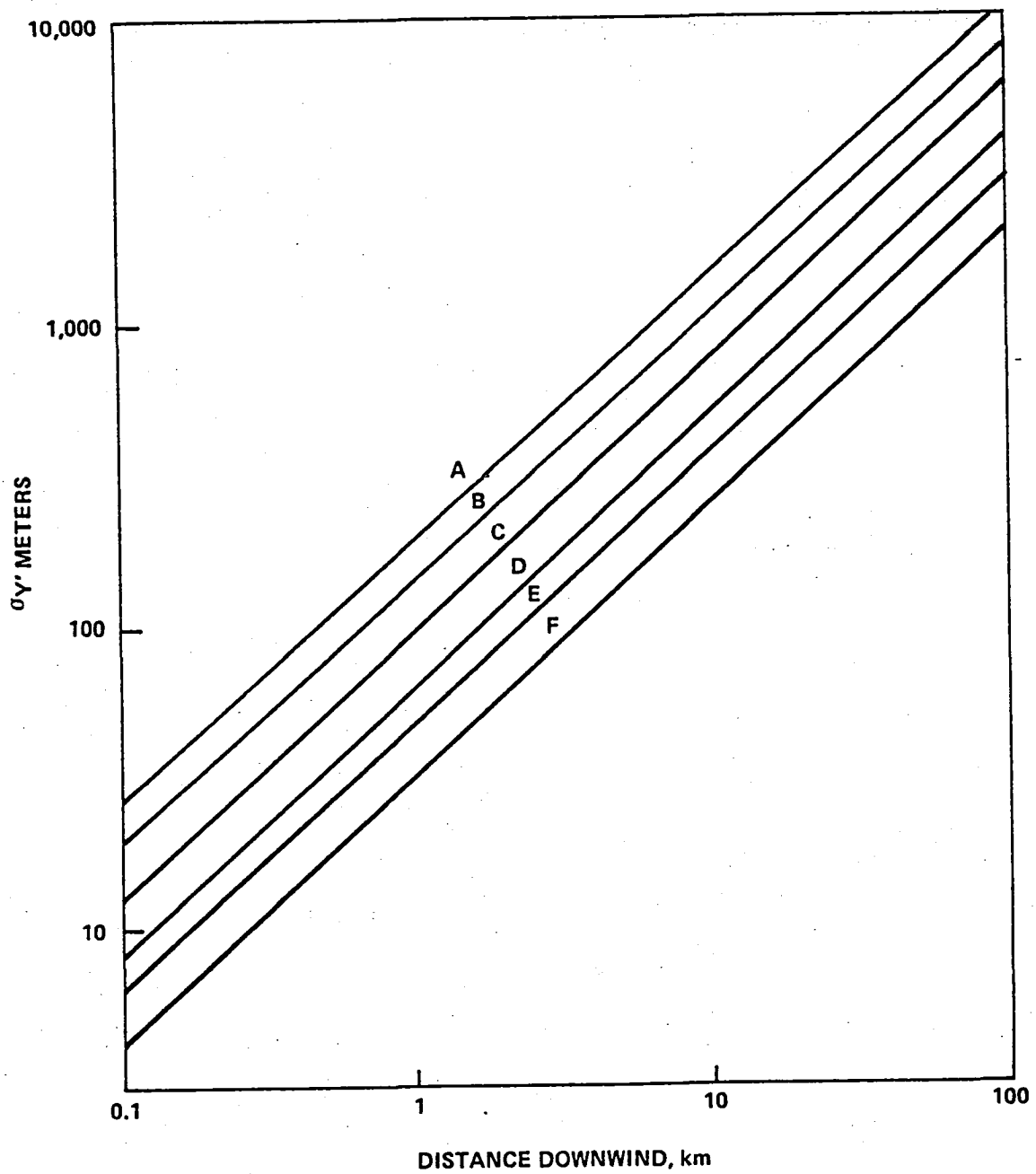

FIGURE 5.2. HORIZONTAL DISPERSION COEFFICIENT, σ_y, AS A FUNCTION OF DOWNWIND DISTANCE FROM THE SOURCE

(A = least stable, F = most stable)

Source: Turner, op. cit.

these curves can handle most unusual meteorological-topographical situations, we have essentially adopted these curves for our calculations. The ORI risk assessment model uses a computational subroutine -- SUBROUTINE SIGMA -- from the Single Source (CRSTER) Model developed by Turner and available from the EPA.[6]

Mean Wind Speed

The mean wind speed to be used in Equation (5.1) is most conveniently related to the surface wind speed reported in standard meteorological data. The wind speed at any height, h, can be related to the surface wind speed, usually measured at an elevation of seven meters, by a power law:

$$u = u_0 (h/7)^p \qquad (5.4)$$

where u_0 is the surface wind speed in meters per second.

The required mean wind speed must be representative of the layer in which the carbon fibers are dispersing. It is standard practice to use the wind speed at the plume height for this purpose, on the grounds that the plume will disperse above and below that height. In this case Equation (5.4) may be written:

$$u = u_0 (H/7)^p \qquad (5.5)$$

If the actual plume height is lower than seven meters, it is set equal to seven. (In other words, $u = u_0$ if $H < 7$.) For plume heights greater than seven meters, the value of u used in Equation (5.1) is then dependent on u_0, H, and p. The exponent p depends, in turn, on the stability conditions. It is assigned specific values, for the different Pasquill-Gifford stability classes, as shown in Table 5.1, adapted from EPA's CRSTER model.[6]

---

[6] EPA, July 1977, op. cit.

TABLE 5.1

VALUES OF WIND PROFILE EXPONENT

Pasquill-Gifford Stability Class	Exponent, p
A	0.10
B	0.15
C	0.20
D	0.25
E	0.30
F	0.30

Effect of Inversion

The effect of an inversion lid (mixing height = H_m) above a neutral or unstable layer may be taken into account in two ways. First, at downwind distances where H' is greater than H_m, it may be assumed that no particles will reach receptors (dosage equals zero) at the surface. Since the plume is tilted, H' decreases with increasing downwind distance, and where $H' < H_m$ dosage calculations can be made using Equation (5.1). In most cases, though, rather stringent physical conditions must be met for the plume to "punch through" the inversion. Observations indicate that this typically does not occur. It is therefore considered most reasonable to assume that if the computed plume height H is greater than the height of the inversion H_m, it can be set equal to the inversion height. Indeed the ORI risk assessment model does this.

Further, when the vertical range over which the plume is mixed becomes equal to the depth of the mixed layer (below the inversion), it can be assumed that this mixing results in a relatively uniform distribution of particles in the vertical. The model therefore, following Turner, makes the distribution of graphite fibers uniform in the vertical, from the ground surface to the base of the inversion, when σ_z becomes larger than 1.6 H_m. For relatively low elevations of receptor points, it is reasonable to set z = 0

in Equation (5.1) to yield the following simplified equation for the dosage:

$$D(x,y,0,H') = \frac{Q(1+r)}{2\pi\sigma_y\sigma_z u} \exp\left[-\frac{1}{2}\left(\frac{y}{\sigma_y}\right)^2\right] \exp\left[-\frac{1}{2}\left(\frac{H'}{\sigma_z}\right)^2\right] \cdot \quad (5.5)$$

Then, following Turner[7], if mixing results in an essentially uniform distribution of the fibers in the vertical we can replace

$$\frac{(1+r)}{2\pi\sigma_y\sigma_z} e^{-\frac{1}{2}\left(\frac{H'}{\sigma_z}\right)^2}$$

by

$$\frac{(1+r)}{5.0133\,\sigma_y H_m} .$$

(note that $2\sqrt{2\pi} = 5.0133$) and obtain:

$$D(x,y,0,H') = \frac{Q(1+r)}{5.0133\,\sigma_y H_m u} \exp\left[-\frac{1}{2}\left(\frac{y}{\sigma_y}\right)^2\right] . \quad (5.6)$$

Equation (5.6) is used in the model whenever $\sigma_z > 1.6\ H_m$.

Specification of Mixing Height Values

The meteorological data is provided in the form of a frequency distribution of the combination of stability class, wind speed and direction; this data set does not include values of the mixing height. The actual value to be used in calculating downwind transport and diffusion of graphite fibers must be specific to the airport and meteorological conditions used in the particular Monte-Carlo run.

In our search for useful data we were led to a paper by Holzworth[8] which gives mean (climatological) mixing heights for 62 National Weather Service stations in the contiguous United States. For example, Holzworth's Table B-1 gives the mean annual mixing height for afternoons in Washington,

---

[7] Turner, op. cit.

[8] George Holzworth, Mixing Heights, Wind Speeds, and Potential for Urban Air Pollution Throughout the Contiguous United States, EPA, January 1972.

D.C., as 1570 meters. (The corresponding value for Los Angeles -- Santa Monica is actually the site of the weather observations -- is 814 meters.) These values are mean annual mixing heights, and we were still faced with the problem of generating values that were specifically associated with appropriate wind direction, speed and stability class values.

The problem of developing appropriate values of the mixing height for different stability conditions, given the mean annual mixing height, is addressed in a paper by K. L. Calder[9]. Calder, based on the analysis of available data and theoretical arguments, recommends that, for Pasquill-Gifford stability class A, the mixing height should be set equal to 1.5 times the Holzworth climatological value. For stability classes B, C, and D the mixing height is set equal to the Holzworth value. For stability classes E and F the mixing height is set equal to 100 meters. This method gives the results for Washington, D.C., and Los Angeles (Santa Monica), California, shown in Table 5.2 as examples.

TABLE 5.2

SAMPLE MIXING HEIGHTS FOR DIFFERENT STABILITY CONDITIONS
(Meters)

Stability Class	Washington, D.C.	Los Angeles (Santa Monica)
A	2355	1221
B	1570	814
C	1570	814
D	1570	814
E	100	100
F	100	100
Climatological Mean	1570	814

[9] K. L. Calder, "A Climatological Model for Multiple Source Urban Air Pollution, Appendix D" to A. D. Buse and J. R. Zimmerman, User's Guide for the Climatological Dispersion Model, EPA-73-024, December 1973.

Other Input Specifications

In the description provided here of the ORI transport and diffusion model used in the overall risk assessment calculations, many of the necessary input parameters have been, perforce, defined. In this section we briefly note those input data sets that have not been explicitly covered above.

- Wind speed and direction, with stability class, are available in a frequency distribution for all of the airports for which risk assessment calculations were made. This data base (the fundamental source is the STAR data provided by the National Climatic Center) is maintained by ORI as part of its work under a joint FAA-EPA aircraft engine emission study. For each of the four seasons, and the entire year, the data provide, for each Pasquill-Gifford stability class, for each of the sixteen principal wind directions, the frequency with which the surface wind speed was observed in any of five class intervals. In implementing the model we assumed the wind direction to be uniformly distributed within each of the 22.5-degree sectors centered about each of the sixteen principal wind directions, to avoid any systematic error due to geographical area center locations relative to the airport location.

- Based on available data reported by several investigators, the value of the settling speed, v_s, has been set equal to 0.02 meters per second.

- On the basis of our discussions with Trethewey and Cramer at the meeting arranged by the Project Officer at NASA Langley, we have used a reflection coefficient, r, equal to 0.7. This implies some reflection, but allows for some adherence of the fibers to surface roughness elements, which in the cases of particular interest are probably building sides, etc.

The input value of Q, the mass of fiber released in the simulated accident is, of course, the principal input to the transport and diffusion calculation. Its development was discussed previously in Section IV.

VI. TRANSFER OF FIBERS INTO INTERIOR OF STRUCTURES

This section of the report documents the development of the methods and inputs used to estimate the penetration of carbon fibers into representative buildings and structures.

BASIC PROCESSES

When a building or equipment enclosure is impinged on by a plume of carbon fibers, some of the fibers may enter the building or enclosure through air conditioning or other ventilation systems and by various air leakage paths. Once inside the building or enclosure, fibers will be removed by fallout and through leakage paths back to the outside. If inside air is recirculated and filtered, additional fibers will be removed by this method. The concentration of active fibers (e.g. those actually producing failure stresses on equipments in a building or enclosure) at any time may be determined from equations describing the net flow. These have been developed in a relatively simple form by Slade.[1]

The leakage and recirculation paths may be defined for typical buildings and enclosures using standard design factors and ventilation rates contained in handbooks. Examples of these are the Handbook of Air Conditioning

---

[1] Slade, Meteorology and Atomic Energy, Eq. (7.83), p. 365, 1968.

System Design[2] and the Standard Handbook of Mechanical Engineers.[3] Fallout of fibers may be estimated simply on the basis of known fiber fall rates and the area upon which fibers are being deposited.

ORI MODELING APPROACH

If a building or enclosure is impacted by a cloud of carbon fibers with an average concentration $\bar{X}$, the rate of change of the amount of active fibers inside the building or enclosure is given by:

$$dq = v_i \bar{X} dt - v_o\left(\frac{q}{s}\right)dt - v_s a\left(\frac{q}{s}\right)dt - v_r\left(\frac{q}{s}\right)dt \qquad (6.1)$$

where:

q = number of active fibers in building or enclosure at time (t)

$\bar{X}$ = average concentration of fibers outside building or enclosure at time (t)

v_i = rate at which fiber-borne air enters the building, or enclosure through both the air conditioning system and through all sources of leakage

v_o = rate at which fiber-borne air leaves the building, including that removed by recirculation

v_s = fall rate of carbon fibers

v_r = rate at which fibers are removed by recirculation filtering

s = volume of building or enclosure

a = area of space subject to fallout.

The above terms are defined in more detail as required during subsequent development in this section.

Equation (6.1) may be rearranged into the following form:

$$dt = \frac{dq}{v_i \bar{X} - v_o\left(\frac{q}{s}\right) - v_s a\left(\frac{q}{s}\right) - v_r\left(\frac{q}{s}\right)} \qquad (6.2)$$

---

[2] Carrier Air Conditioning Co., Handbook of Air Conditioning System Design, McGraw-Hill Book Co., 1965.

[3] Standard Handbook for Mechanical Engineers, Baumeister & Marks, McGraw-Hill, 1967.

or:

$$\frac{dt}{s} = \frac{d(\frac{q}{s})}{v_i\overline{X} - v_o(\frac{q}{s}) - v_s a(\frac{q}{s}) - v_r(\frac{q}{s})} \quad . \tag{6.3}$$

Now, for convenience, let

$$A = v_o + v_s a + v_r$$

so that Equation (6.3) can be more easily written as:

$$\frac{dt}{s} = \frac{d(\frac{q}{s})}{v_i\overline{X} - A(\frac{q}{s})} \quad . \tag{6.4}$$

Equation (6.4) is most conveniently integrated for two special cases as shown in the next two subsections of this chapter.

Inside Concentration During Build-up Phase

The first special case to be considered is the build-up of the concentration of graphite fibers inside a building starting at the time the leading edge of the graphite fiber plume first hits the exterior of the building. For convenience let the time when this occurs be defined as

$$t = 0$$

at which time the interior concentration of fibers is also zero:

$$\frac{q}{s} = 0.$$

In this case Equation (6.4) can be integrated to yield:

$$\frac{t}{s} = \frac{1}{A} \ln \left[\frac{v_i\overline{X}}{v_i\overline{X} - A(q/s)} \right] \tag{6.5}$$

In the more conventional exponential format this equation may be written:

$$\frac{q}{s} = \frac{v_i\overline{X}}{A} \left[1 - e^{-(A/s)t} \right] \tag{6.6}$$

Interior Concentration During Decay

The second special case to be considered for Equation (6.4) is that describing the behavior of the concentration of graphite fibers within an enclosure after the exterior plume has passed. If we define the time at which the cloud just passes the exterior of the structure as

$$t = T$$

then the exterior concentration at this time (and later times) is

$$X = 0.$$

The differential equation, Equation (6.4), takes the special form:

$$\frac{dt}{s} = -\left(\frac{1}{A}\right) \frac{d(q/s)}{(q/s)} \tag{6.4a}$$

which may be integrated to yield:

$$\frac{t-T}{s} = -(1/A)\ln \left[\frac{q(t)/s}{q(T)/s}\right] . \tag{6.7}$$

This may also be written in the exponential form as:

$$\frac{q(t)}{s} = \frac{q(T)}{s} e^{-(A/s)(t-T)} . \tag{6.8}$$

In this case we have made explicit the dependence of the fiber count, q, on time in order to differentiate between its value for time t from its value at the specific time of cloud passage, T.

Calculation of Interior Exposure

The exposure is defined mathematically as the integral of the concentration over time. For convenience we introduce a term E(0,T) for the

interior exposure at time T, and assume that the concentration was zero prior to time zero. The exposure at time T can then be written:

$$E(0,T) = \int_0^T \frac{v_i \overline{X}}{A} \left[1 - e^{-(A/s)\tau} \right] d\tau \ . \qquad (6.9)$$

We lose very little generality with regard to the complete risk assessment calculation if we assume that the exterior concentration actually has the constant value $\overline{X}$ from time t = 0 until time t = T. This is particularly true because the transport and diffusion model, described in Section V of this report, actually treats the cloud of fibers in such a way that we may think of it as causing a sharp rise in exterior concentration to a constant level until the cloud passes, followed by a sudden drop to zero concentration. With this assumption it is a relatively straightforward matter to integrate the expression in Equation (6.9) to provide the following result:

$$E(0,T) = \frac{v_i \overline{X}}{A} \left[T + \frac{s}{A} \left(e^{-\frac{A}{s} T} - 1 \right) \right] \qquad (6.10)$$

In analogous fashion it is possible to write an integral for the exposure due to the fibers interior to the structure after the exterior cloud has passed. We consider some time long after the exterior plume has passed, and consider this to be t = ∞ for our purposes. The exposure experienced after the exterior plume has passed is defined as $E(T,\infty)$ and is given by:

$$E(T,\infty) = \int_T^\infty e^{-(A/s)(\tau - T)} d\tau \qquad (6.11)$$

which may be integrated to yield:

$$E(T,\infty) = (s/A)\ (q/s)\ T \ . \qquad (6.12)$$

The total interior exposure due to the passage of the exterior plume can be written as:

$$E(0,\infty) = E(0,T) + E(T,\infty). \qquad (6.13)$$

We evaluate this expression by using the results just obtained, namely Equations (6.10) and (6.12):

$$E(0,\infty) = \frac{v_i \overline{X}}{A} \left[T + \frac{s}{A} \left(e^{-(A/s)T} - 1 \right) \right] + \left(\frac{s}{A} \right) \frac{q(T)}{s} \quad . \tag{6.14}$$

Now we note that Equation (6.6) can be written, for time T, as:

$$\frac{q(T)}{s} = \frac{v_i \overline{X}}{A} \left[1 - e^{-(A/s)T} \right] . \tag{6.6a}$$

This can now be substituted into Equation (6.14), after which, if terms are appropriately combined, we obtain:

$$E(0,\infty) = \frac{v_i \overline{X}}{A} \; T \quad . \tag{6.15}$$

The exterior exposure, due to our assumption that the concentration is a constant value $\overline{X}$ over a time period of length T, is simply given by:

$$E_o = \overline{X} T$$

so that the interior and exterior exposures are related by:

$$\frac{E}{E_o} = \frac{v_i}{A} = \frac{v_i}{v_o + a v_s + v_r} \quad . \tag{6.16}$$

which may be termed the "penetration factor."

Penetration Factors

Equation (6.16) forms the principal basis for our calculation of interior exposure values which are used, in turn, to compute the failure probabilities for specific equipments, as described in Section VII, which

follows. Each of the terms appearing in that equation is discussed in more detail below:

- The rate at which fiber-borne air, v_i, enters the building or other enclosure includes that which enters through the air conditioning system and that which enters via leakage. The air entering through the air conditioning system is obtained from the air conditioning airflow, v_{ac}, and the filter efficiency, EFF, as follows:

$$v_{acf} = v_{ac} (1 - EFF). \tag{6.17}$$

- The rate at which fiber-borne air enters the building or other enclosure via leakage, v_l, is obtained from standard air conditioning planning factors for various combinations of types of doors and windows, in different types of buildings, located in different climatic zones, for different wind conditions. Then:

$$v_i = v_{acf} + v_l . \tag{6.18}$$

- The rate at which fiber-borne air leaves the building, v_o, assuming conservation of mass, is equal to the total of the air entering the building through the air conditioning or ventilating system and the air entering the building via leakage:

$$v_o = v_{ac} + v_l . \tag{6.19}$$

- For the fall rate, v_s, we have used the nominal value of 4 feet per minute, or 2 centimeters per second for all calculations; this appears to be in accord with current observational data.

- The rate at which fibers are removed by recirculation, v_r, accounts for fibers removed by recirculation filters plus that which deposits in the ductwork. The rate at which fibers are removed in the recirculation system is obtained from the product of the recirculation rate, v_{rr}, and the filter efficiency, while that which is deposited out is estimated by the product of the fall rate, v_s, and the effective area of the recirculation system, a_r:

$$v_r = v_{rr} (EFF) + v_s a_r . \tag{6.20}$$

Multiple Enclosures

In some instances there can be several enclosures in series in the penetration path, for example an equipment housing may be located inside of a building. In this case, the penetration factors are multiplied together to arrive at an effective overall factor. This operation tacitly assumes that the result derived in Equation (6.16) holds even if the exterior concentration cannot be characterized as a square wave. Intuitively, this assumption appears reasonable in the present context.

CHARACTERIZATION OF TYPICAL STRUCTURES

The sizes, shapes, and types of buildings and equipment enclosures of interest to this study are, of course, nearly infinite in variety. However, if it is assumed that these buildings and enclosures have been designed to generally accept heating and ventilation standards, they can be defined by a few rather standard categories. It is assumed that all buildings and equipment enclosures can be adequately defined by one or more of the following categories:

1. Small Equipment Building or Van
2. Medium Equipment Building
3. Large Equipment Building or Factory
4. Equipment Room inside a building
5. Utility Room
   a) filtered
   b) unfiltered
6. Hospital Operating Room, Intensive Care Area
7. Switchgear Cabinet
   a) filtered
   b) unfiltered
8. Electronic Equipment Enclosure - forced air
   a) filtered
   b) unfiltered
9. Electronic Equipment Enclosure with louvers
   a) filtered
   b) unfiltered
10. Residence
    a) air conditioned
    b) not air conditioned
11. Business/Office Building.

Design Factors

Table 6.1 shows the design factors associated with each category of building or enclosure defined above. These design factors are used to determine the air conditioning flow rates, filter efficiencies, and air leakage rates used in Equation (6.16) et seq. The sizes of buildings and enclosures have been arbitrarily selected. It should be noted that enclosure size is not critical as long as the associated ventilation rate is reasonable for that size enclosure.

The types and numbers of doors and windows were selected on the basis of building type and size. It is assumed that the addition of doors and windows for larger buildings of the same type would result in approximately constant leakage per volume (i.e., leakage effects are independent of building size once a basic design is selected). The size and type of doors and windows are selected from those shown in Table 44, pp. 1-95 of the Handbook of Air Conditioning System Design.[4] Industrial doors are well fitted metal doors with weatherstripping. Hospital doors and business doors are selected from Table 41E, pp. 1-91. The leakage rate through business doors is based on an average occupancy rate of 5 people per 2400 square feet and 2.5 CFM leakage per person.

The ventilation rates shown in Table 6.1 are based on standards contained in the Handbook of Air Conditioning System Design[5] and in the Standard Handbook for Mechanical Engineers.[6] Ventilation rates for electronic equipment, in cubic feet per minute, are approximated by:

$$\text{ventilation rate} = \frac{\text{power consumption in watts}}{\text{required temperature reduction in degrees F.}}$$

Typical electrical and electronic equipment must be kept within about 20 degrees Fahrenheit of the ambient temperature so that a ventilation rate of approximately 1.5 cubic feet per minute (CFM) per watt consumed is a reasonable value to assume.

---

[4] Op. cit.

[5] Ibid.

[6] Op. cit.

TABLE 6.1
DESIGN FACTORS FOR TYPICAL ENCLOSURES

Enclosure Category	Size W x L x H (feet)	Doors Facing Wind			Windows Facing Wind			Ventilation Rate(CFM)	Filter Eff.*
		No.	Size	Type	No.	Size	Type		
1. Small Equipment Building or Van	15 x 30 x 15	1	3' x 7'	Industrial/ Weatherstrip	0			300	85% AFI 95% CF
2. Medium Equipment Building	30 x 60 x 10	2	3' x 7'	Industrial/ Weatherstrip	2	3' x 5'	Industrial Casement 1/64" Crack	1000	85% AFI 95% CF
3. Large Equipment Building or Factory Building (per floor)	100 x 300 x 10'	3	3' x 7'	Industrial/ Weatherstrip	20	3' x 5'	Industrial Casement 1/64" Crack	3000	80% AFI 90% CF
4. Equipment Room in Building (one exterior wall)	30 x 60 x 10	2	3' x 7' Interior/ Exterior Vestibule	Factory Type Interior and Exterior	5	3' x 5'	Industrial Casement 1/64" Crack	1000	85% AFI 90% CF
5. Utility Room	30 x 60 x 10	1	3' x 7'	Factory Type Exterior/ 1/8" Crack	0	- -	- -	500	a - 85% AFI 95% CF b - None
6. Hospital Operating Room, Intensive Care Area	20 x 25 x 10	2	3' x 7' with Vestibule	Swinging Door	0	- -	- -	1000	Double at 95% CF Each
7. Switchgear Cabinet (From Westinghouse Catalog 55-000)	5 x 3 x 7	0	- -	- -	0	- -	- -	a - 300 b - 1 Assumed Leakage	85% AFI 95%CF None
8. Electronic Equipment Enclosure (with forced air)	2 x 1 x 1/2	--	- -	- -	0	- -	- -	30 (20 watts)	a - 85% AFI 95% CF b - None
9. Electronic Equipment Enclosure (with louvers)	2 x 1 x 1	0	- -	- -	0	- -	- -	3 (2 watts)	a - 85% AFI 95% CF b - None
10. Residences	40 x 30 x 8	1	3' x 7'	Glass - Avg. Fit 3/16" Crack	4	4' x 7'	Residential Casement 1/32" Crack	a - 300 b - None	85% AFI 95% CF
11. Business (Small)	60 x 40 x 10	1	3' x 7'	Swinging	All Windows Sealed			500	85% AFI 95% CF

* Two types considered: Dry Type Glass Wool: 85% AFI, 95% CF
Viscous Impingement: 80% AFI, 90% CF

The effectiveness of filters with respect to carbon fibers of various size is not accurately known. Comparisons of American Filter Institute values for standard filter types with available graphite fiber tests on similar filters indicate the approximate relations shown in Table 6.2.

TABLE 6.2

COMPARISON OF REPORTED FILTER EFFECTIVENESS WITH EFFECTIVENESS IN FILTERING GRAPHITE FIBERS (percent)

Effectiveness Reported by AFI	Graphite Fiber Effectiveness
80	90
85	95
95	99
99	99.9

Penetration Parameter Values

Table 6.3 summarizes the data obtained from the several sources referenced above for the different enclosure types defined here. These are shown for buildings in typical temperate zone climatic regimes for different values of the wind speed. In implementing these values for the computer model it was determined that the "fallout term" tended to dominate in computing numerical values of the ratio shown in Equation (6.16). The values were therefore relatively independent of wind speed. For this reason a standard 10 mile-per-hour wind speed was assumed to be blowing directly at external windward doors and windows. In addition, the following assumptions were introduced:

- The "air conditioning" for enclosure types 7b, 9a, 9b is by natural convection through louvers at recommended values.
- Leakage of air into electrical and electronic enclosures (other than that which is intended through louvers) is neglected.

TABLE 6.3

VENTILATION RATES (CFM) FOR TYPICAL ENCLOSURES
AT VARIOUS WIND SPEEDS

Enclosure Category	0 mph*		5 mph		10 mph		15 mph		20 mph	
	V_i	V_o	V_i	V_o	V_i	V_o	V_i	V_o	V_i	V_o
1	15	300	24	309	25	310	33	318	41	326
2	50	1000	69.6	1020	80	1030	95.6	1046	115.8	1066
3	300	3000	343	3043	390	3090	450	3150	516	3216
4	50	1000	61	1011	73	1023	88	1038	104	1054
5a	25	500	89	564	153	628	217	692	285	760
5b	500	500	564	564	628	628	692	692	760	760
6	2.50	1000	4.25	1002	6.00	1000	7.70	1005	9.43	1007
7a	15	300	Infiltration thru cabinet neglected							
7b	1	1	Switchgear assumed inside building							
8a	1.50	30	Leakage is assumed to be zero							
8b	30	30	Leakage is assumed to be zero							
9a	0.15	3	Leakage is assumed to be zero							
9b	3	3	Leakage is assumed to be zero							
10a	15	300	131	416	262	550	372	657	527	812
10b	0	0	416	416	550	550	657	657	812	812
11	25	500	30	505	37.5	512.5	45	520	55	530

*These values also apply to pressurized enclosures.

With these additional minor assumptions, the input parameters for calculating the transfer function, or effect of ventilation on allowing exterior fibers to enter buildings or other structures, are those shown in Table 6.4. The relationship of these building and other enclosure types to different facilities modeled in each of the airport-urban complexes treated in the risk assessment calculations is established in the next section of this report. There it is shown that each class of business or industry may be characterized as being located in one or more of the types of enclosures described in this section. The use of these one-to-one relationships between business type and building type reduces the input data variability and thus tends to reduce the variance of the final results. On the basis of resources available for this analysis, and the expected difficulty in improving on this assumption, it was considered most appropriate to make this assumption and accept the consequences. The calculation of the failure probabilities for specific equipment in particular classes of enclosures is combined with the calculation of the transfer of fibers from the outside to the inside of those enclosures.

TABLE 6.4

INPUT PENETRATION PARAMETER VALUES FOR SELECTED BUILDING AND ENCLOSURE TYPES *

Building or Enclosure Type	Penetration Factors								
	v_{ac}	(1-EFF)	v_{acf}	v_1	v_i	v_o	av_s	v_o+av_s	$v_i/(v_o+av_s)$
1	300	.05	15	10	25	310	1800	2110	.01180
2	1000	.05	50	30	80	1030	6000	7020	.00989
3	300	.10	300	90	390	3090	100,000	103090	.00378
4	1000	.05	50	23	73	1023	6000	7023	.01040
5a	500	.05	25	128	153	628	6000	6628	.02310
5b	500	1.00	500	128	628	628	6000	6692	.09380
6	1000	.0025	2.50	3.50	6.0	1000	6000	7000	.00086
7a	300	.05	15	0	15	300	60	360	.04170
7b	1	1.00	1	0	1	1	60	61	.01640
8a	30	.05	1.50	0	1.50	30	4	34	.04410
8b	30	1.00	30	0	30	30	4	34	.88200
9a	3	.05	0.15	0	0.15	3	4	7	.02140
9b	3	1.00	3	0	3	3	4	7	.42800
10a	300	.05	15	247	262	550	4000	4550	.05800
10b	0	1.00	0	530	550	550	4000	4500	.11100
11	500	.05	25	12.5	37.5	512.5	9600	10112.5	.00370

*All ventilation rates are in cubic feet per minute.

VII. FAILURE OF INDIVIDUAL AND COLLECTIVE EQUIPMENTS

DESCRIPTION OF FAILURE MODELS

Use of Exponential Model

The probability of failure of equipment which is exposed to carbon fibers is obtained from the exponential expression:

$$P_F = 1 - \exp\left[-E/\overline{E}\right] \tag{7.1}$$

Where:

P_F = probability of failure of equipment

E = exposure level in the immediate vicinity of the vulnerable equipment, in fiber-seconds per cubic meter

$\overline{E}$ = average exposure level causing a failure

The U.S. Army Ballistics Research Laboratory (BRL) at Aberdeen, Maryland has tested the exponential model against a large number of test results and has shown that the experimental data show a close fit to the exponential failure law.[1,2] ORI also completed a log-linear plot of e^{-ct} as a function of time-to-failure (t) for various concentrations (c). This analysis, performed during ORI's previous Phase I work using data from the Ford Aeronautics

---

[1] Have Name Vulnerability of the Improved Hawk System, BRL Report No. 1964, Shelton & Moore, Feb. 1977.

[2] ORI discussions with BRL, Aug. 15, 1978.

generic target tests showed a linear relationship except for large values of the time-to-failure, for which data were sparse. For our purposes, then, Equation (7.1) is considered to adequately describe the probability of failure for a single piece of equipment as a function of exposure.

Incorporation of Penetration

The values of exposure used in Equation (7.1) are those directly impinging on the vulnerable equipment. When this equipment is located within a building and/or enclosure, the value of the internal exposure may be obtained from the outside exposure by multiplying the external exposure by the appropriate penetration factor(s) (as described in Section VI):

$$E = E_o \, KP \tag{7.2}$$

where:

E = inside exposure

E_o = outside exposure

$KP = \dfrac{v_i}{v_o + av_s + v_r}$ = penetration factor (Sec. VI).

When an equipment is doubly enclosed, for example, when equipment is in a cabinet that is inside a building, an overall penetration value is obtained from:

$$KP_i = (KP_b) \cdot (KP_e) \tag{7.3}$$

Where:

KP_i = overall penetration factor for equipment (i)

KP_b = penetration factor for building

KP_e = penetration factor for enclosure

Development of Failure Constants

Since the penetration factors and the mean exposure to failure, $\overline{E}$, are constants for any particular piece of equipment in a particular enclosure (where enclosure describes the building type as well as any box the equipment is in) we can define a single failure parameter:

$$K_{ij} = KP_j/\overline{E}_i \tag{7.4}$$

Where:

K_{ij} = overall failure parameter for equipment of type i in an enclosure of type j

KP_j = penetration factor for an enclosure of type j

E_i = mean exposure to failure for equipment of type i

The parameter K_{ij} may now be substituted into Equation (7.1) to yield a useful relationship giving the probability of failure for equipment of type i in an enclosure of type j for any value of the exposure recorded exterior to the enclosure:

$$P_{F,ij} = 1 - \exp(-K_{ij} E_o) \tag{7.5}$$

Treatment of Equipment Configurations

The failure probabilities for individual equipments may now be combined to cover various series, parallel, or series-parallel configurations found in typical facilities. It is first convenient to define the reliability of a particular piece of equipment in a particular class of enclosure as:

$$R_{ij} = 1 - P_{F,ij} \tag{7.6}$$

Then we can write, for several pieces of equipment in series:

$$\begin{aligned} P_{FS,j} &= 1 - R_{1j} R_{2j} \cdot \cdot \cdot \cdot \\ &= 1 - (e^{-K1j E_o})(e^{-K2j E_o}) \cdot \cdot \cdot \cdot \\ &= 1 - e^{-(K_{1j} + K_{2j} + \cdot \cdot \cdot \cdot) E_o} \end{aligned}$$

This is the probability that at least one of the equipments in series fails. For situations in which several equipments are in parallel (redundant configurations), the probability of failure for the aggregate is given by:

$$P_{FP,j} = P_{F,1j} \cdot P_{F,2j} \cdot \cdot \cdot \cdot \cdot \tag{7.7}$$

Series-parallel equipment configurations are treated by first converting parallel combinations into an aggregate equivalent and then computing failures for the resulting series configurations.

A standard configuration from which all facilities may be synthesized is shown in Figure 7.1. "PRI" represents the primary source of power from the public utility. When this source fails, power at the facility must be obtained from a local auxiliary power supply, "AUX," if such a supply is available. Box "SW" refers to service switchgear which handles incoming power at the facility. Common equipment includes central computers, central communications, etc. The failure of common equipment results in an overall failure of the facility. Distributed components account for parallel assembly lines or other parallel production elements so that the failure of a distributed module would reduce facility capacity or production without causing a complete facility outage.

The probability of no input power at the facility (P_{NP}) is obtained from:

$$P_{NP} = P_{PRI} + (1 - P_{PRI}) \cdot (P_{SW}) \tag{7.8}$$

where:

P_{PRI} = probability of failure of primary power

P_{SW} = probability of failure of switchgear

The probability of no power inside the facility (P_{NPI}) is given by:

$$P_{NPI} = P_{NP} \cdot P_{AUX} \tag{7.9}$$

where P_{AUX} is the probability that the auxiliary power system fails. The probability that there is power inside the facility is equal to:

$$P_{PI} = 1 - P_{NPI}$$

The probability that there is power inside the facility but that the facility is down due to a failure of the common module is equal to:

$$P_{PI} \cdot P_{FC}$$

where P_{FC} is the probability of failure of the common module.

Similarly, the probability that there is power inside the facility and that the common module has not failed, but that the facility's production

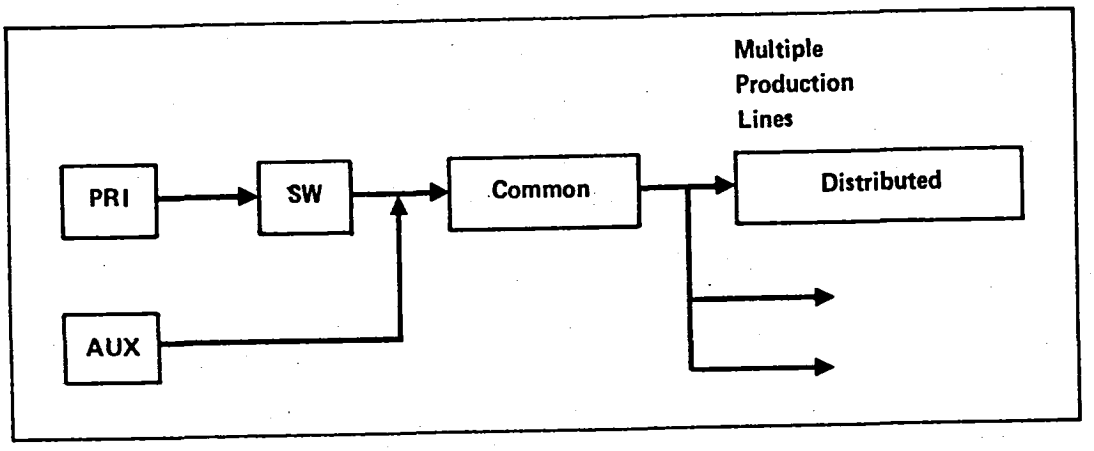

FIGURE 7.1. STANDARD CONFIGURATION
FOR MODELLING FACILITY POWER FLOW

or output is reduced due to a failure of one of the distributed modules is estimated by:

$$P_{PI} (1 - P_{FC})P_{FD}$$

where P_{FD} is the probability of failure of one distributed module: for example, one of several production lines operating in parallel.

By carefully summing up the terms of the relationships developed above, we find that the probability of no output or production from any single distributed module is equal to:

$$F = P_{NPI} + P_{PI} P_{FC} + P_{PI} (1 - P_{FC})P_{FD} \qquad (7.10)$$

Now, the probability that exactly n out of a total of N distributed modules remain in production--do not fail --is given by:

$$R(n,N) = \binom{N}{n} (1 - P_{FD})^n (P_{FD})^{N-n} .$$

In this case the fractional capacity associated with the n distributed modules that do not fail is n/N. We may therefore write, for the expected capacity or production obtainable from the distributed modules:

$$\sum_{n=0}^{N} \left(\frac{n}{N}\right) \binom{N}{n} (1 - P_{FD})^n (P_{FD})^{N-n}$$

$$= \left(\frac{1}{N}\right) N (1 - P_{FD}) = 1 - P_{FD}$$

The fraction of production lost due to failures of the distributed modules may therefore be estimated by P_{FD}, the probability of failure of one distributed module, and Equation (7.10) can be used to estimate the fraction of production or output lost due to failures at the facility. If the equation were applied to many identical facilities we would expect the overall result to be essentially the same as if each facility's degradation were obtained by a random sampling procedure. In actual analyses, however, the equation is applied to a variety of facility-types at one location, and this may result in some reduction of variance in the final results.

RELATIONSHIP OF INDUSTRIES AND POPULATION CENTERS TO EQUIPMENT ENSEMBLES

Methodology

In any center of population, i.e., urban area, close to a major airport, there is a wide range of facilities measured by type and/or size. There is also great variability in types and configurations of equipment across facilities, or even within facilities of a particular type. The only approach considered practical for this study was to define "typical" facilities which are believed to best represent specific facilities in existence in the geographical area being studied during the time frame of interest. Failure computations were then addressed to these typical facilities. To provide the basis for defining the typical facilities it was decided to make use of a classification scheme already well established for other, quite different reasons: the U.S. Census Bureau Standard Industrial Classification (SIC) Codes. It is recognized that in some cases there can be a bigger difference between two facilities characterized by the same SIC Code than between facilities with different code numbers. However, these code numbers do provide a standardized basis for facility definition and have the advantage of being directly relatable to population centers for which census data are readily available. Further, as shall become evident below, in Section VIII of this Report, this decision makes a great body of data developed for economic analysis available for use in estimating the dollar impact of a graphite fiber incident. A partial list of SIC numbers and corresponding business types is shown in Table 7.1. The industry categories shown are those that figured prominently in the study.

The types of individual equipments and their groupings into typical facility configurations (of the type typified generally by Figure 7.1) were prepared after a broad literature review, supported by a number of site visits, and further augmented by discussions with representatives of several major industries and government agencies. These data and information-gathering activities are summarized here. Documents covered in the literature review, primarily periodicals in order to obtain up-to-date information, included:

- IEEE Spectrum 1970 to Present
- Instruments and Control Systems 1970 to Present
- Production Engineering (formerly Automation) 1970 to Present
- Computers and Automation 1975 to Present

TABLE 7.1
SELECTED LIST OF SIC CODE NUMBERS

SIC Code	Major Industry Group
	Manufacturing
20	Food and kindred products
22	Textile Mill Products
23	Apparel and other textile products
24	Lumber and wood products
25	Furniture and fixtures
27	Printing and publishing
28	Chemicals and allied products
29	Petroleum and coal products
30	Rubber and misc. plastics products
33	Primary metal industries
34	Fabricated metal products
35	Machinery, except electrical
36	Electric and electronic equipment
37	Transportation equipment
38	Instruments and related products
	Transportation and other public utilities
45	Transportation by air
48	Communication
49	Electric, gas, and sanitary services
	Wholesale trade
50	Wholesale trade-durable goods
51	Wholesale trade-nondurable goods
	Retail trade
52	Building materials and garden supplies
53	General merchandise stores
54	Food stores
55	Automotive dealers and service stations
56	Apparel and accessory stores
57	Furniture and home furnishings stores
58	Eating and drinking places
59	Miscellaneous retail
	Finance, insurance, and real estate
60	Banking
61	Credit agencies other than banks
62	Security, commodity brokers and services
63	Insurance carriers
	Services
73	Business services
80	Health services
99*	Government

* Defined by ORI

- Data Processing 1975 to Present
- Electronic Communication 1975 to Present
- Machine Design 1975 to Present

Visits were made to the following facilities in the Washington, D.C. metropolitan area:

- Washington National Airport
- Holy Cross Hospital, Silver Spring, Md.
- Montgomery General Hospital, Olney, Md.
- Radio Station WTOP, Wheaton, Md.

Discussions were held with representatives of the following specific industries and government agencies:

- Potomac Electric Power Company
- Edison Electric Company
- IEEE Substation Design Group
- Department of Energy/Energy Research and Development Agency
- Federal Power Commission
- Westinghouse Substation Design Group
- Department of Health, Education, and Welfare/ Bureau of Medical Devices
- General Electric Medical Devices Division

In addition, several visits were made to the Ballistics Research Laboratory (BRL), Aberdeen, Maryland, for general discussions on the subject of equipment vulnerability, the review of test procedures used at that facility, and the review of specific exposure-to-failure results.

The equipment types finally defined for each SIC code-typical facility were then compared with the types of equipment that had been covered in the BRL test program. Mean exposure-to-failure values were selected for those equipments tested that most closely matched the equipments defined for each typical industrial-commercial facility, as well as residences. Once the task of defining the typical facility for each required SIC code number was completed, the numbers of each facility-- business or industrial unit --in each county or other geographical area of interest were obtained directly from published Bureau of Census data, primarily the County Business Patterns.

These data were necessarily supplemented in some cases by personal contacts with Census Bureau personnel. The methods used to assess the consequences of industrial-commercial failures and their associated costs are described in Section VIII of this report.

Description of Typical Facilities

Specific types of industries and related facilities are described in Appendix A. Appendix A serves as a baseline from which configurations and vulnerability factors for each required SIC Code were derived; the appendix contains the following information:

- Descriptions of specific configurations
- Description of equipment components
- Rationale for assigning enclosure types
- Rationale for assigning mean exposure-to-failure values.

Standardized configurations for the various SIC Codes, based on variations of Figure 7.1, are described below and illustrated in Figure 7.2:

- Electric Utility; SIC 49; Figure 7.2a. The station consists of common communications and controls together with a number of parallel bays, each consisting of a switchgear panel and high voltage equipment.

- Small Light Industry; SIC 20,23,24,27,38; Figure 7.2b. These industrial plants are assumed to have no auxiliary power. The following specific changes were made to the general configuration shown in Figure 7.2b for each of the SIC numbers shown:

  - SIC 23,38: replace service switch with power distribution
  - SIC 20,38: servo circuits as shown
  - SIC 24 : replace interface unit + servo with high voltage motor controls and heavy duty motors
  - SIC 23,27: power directly from controller to small motors
  - SIC 24 : no controller

- Large Light Industry: SIC 22,25,34,35,36; Figure 7.2c. Large light industries are similar to small light industries except that auxiliary power is assumed to be available. The following variations of Figure 7.2c were introduced:

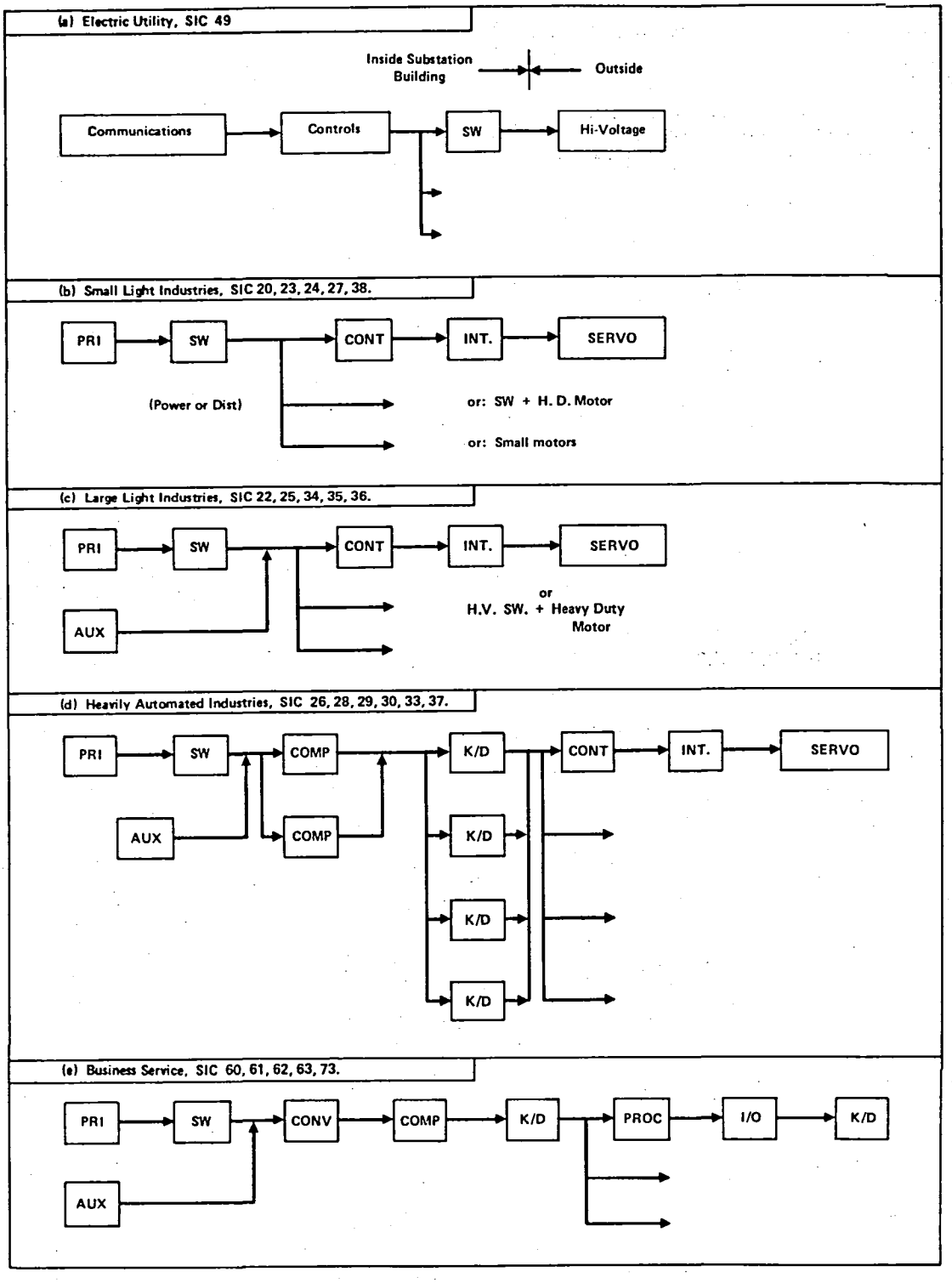

FIGURE 7.2. CONFIGURATION OF EQUIPMENT FOR SPECIFIC INDUSTRY GROUPS IDENTIFIED BY SIC NUMBER

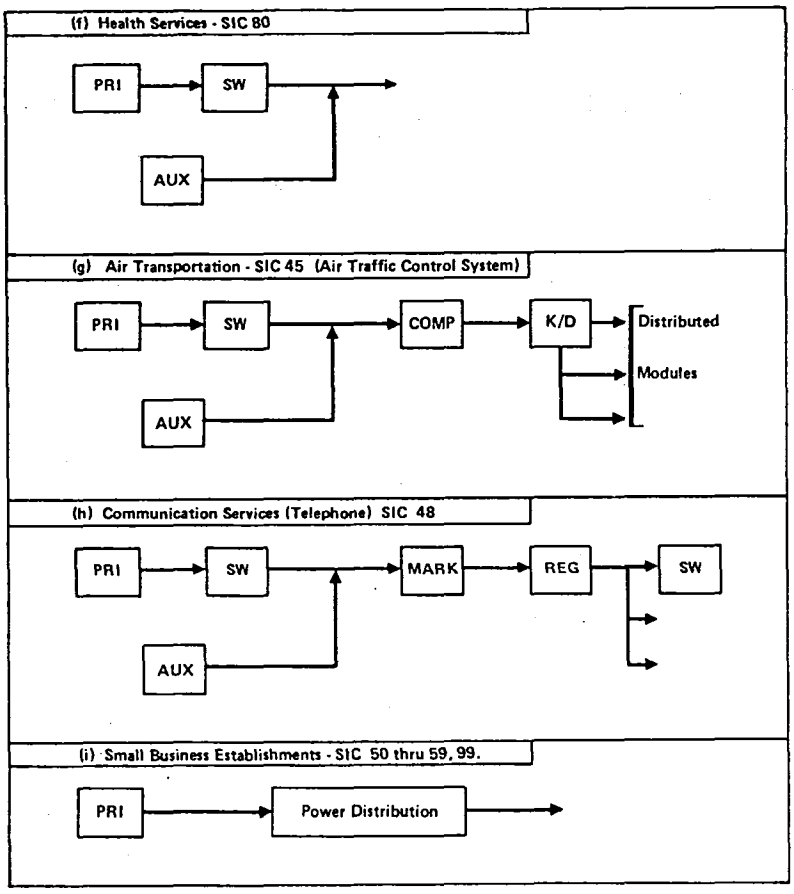

FIGURE 7.2. (CONCLUDED) CONFIGURATION OF EQUIPMENT FOR SPECIFIC INDUSTRY GROUPS IDENTIFIED BY SIC NUMBER

-- SIC 22,36: interface units and servos as shown
-- SIC 25,34,35: replace interference units and servos with high voltage controls and motors
-- SIC 34,35,36: line controller
-- SIC 25 no line controller

- Heavily Automated Industry: SIC 26,28,29,30,33,37; Figure 7.2d. Heavily automated industries are similar to large light industries except that they have a common module consisting of computers in parallel, together with keyboard/displays which are also in parallel. SIC 28,29,30 and 37 are assumed to have production lines dominated by servo systems while SIC 26 and 33 are assumed to have production lines dominated by high voltage motor controls (switchgear) and heavy duty motors.
- Business Services: SIC 60,61,62,63,73; Figure 7.2e. Business service facilities are assumed to have a single central computer with associated power converter and keyboard/display. Distributed modules consist of data terminals (keyboard/display) together with local processors and input-output interface units.
- Health Services: SIC 80; Figure 7.2f. Health service facilities are assumed to be vulnerable only to power outages, and to possess auxiliary power. It is assumed that medical devices and other vulnerable "production" units are in highly protected environments.
- Air Transportation: SIC 45; Figure 7.2g. Air traffic control consists of power units together with central computing facilities. The distributed modules actually consist of RADARS, ILS, VORs, Communications, etc. These are highly redundant, well filtered, and have local (site) auxiliary power, and on this basis were not included in the computerized model. Off-line calculations showed that the risk to such facilities could be neglected.
- Communication Services (Telephone): SIC 48; Figure 7.2h. A very simplified telephone central office is assumed to consist of one common marker and register equipment serving a number of trunk frames and line frames via relay switches.

- Small Businesses; SIC 50-59,99; Figure 7.2i.
  Small business establishments are assumed to be vulnerable only from the standpoint of power outage. The only vulnerable equipment within the establishment are power distribution circuits.

- Private Residences
  Residences with and without air conditioning are considered, using a fraction of occurrence based on type of county (urban, rural). The only equipments considered to be vulnerable were television sets and high-fidelity equipment. Electric toasters are vulnerable but, because of their relatively low replacement cost, they were not included in the calculation. On the other hand, toasters do appear to constitute a potential shock hazard; this effect was not included in the calculations reported here. The considerable uncertainty surrounding this problem made it virtually impossible to attempt to quantify the phenomenon. It is a subject that clearly requires more attention in further analysis of the carbon fiber risk.

Implementation for the Simulation Model

The computer program that determines the impact of each simulated aircraft accident and associated release of graphite fibers uses Equation (7.10) to estimate the probability that each business or industry in the geographical area of interest is affected. One of the major efforts in this project has been the characterization of each business-industry sector, defined by an SIC number, by a specific set of equipments installed in a specific type of structure. The results for the physical plant were described earlier, and the equipment problem has been covered in this section. Once these definitions have been arrived at, we have, in effect, defined a set of K_{ij} (cf Equation (7.4)) for each class of equipment in each class of building.

Failure parameters were prepared for each SIC number by using expressions (7.3) and (7.4) for each equipment-enclosure combination defined for each relevant SIC number. In terms of the configurations illustrated in Figure 7.2, the

following generalized equipment categories were defined:

- service switch, or power distribution panel
- auxiliary power system
- common equipment module
- distributed equipment module.

It was found that, for computer input specification, it was useful to define a set of input parameters less abstract than those relying on the "ij" notation. Accordingly, the following set of failure parameters were defined; these correspond to the K_{ij} defined by Equation (7.4), and are prepared for each SIC number needed for each airport-urban area simulated:

- $K_{F,SW}$ Input failure parameter for service switch, input power panel, or transformer
- $K_{F,AUX}$ Input failure parameter for auxiliary power system
- $K_{F,C}$ Input failure parameter for common equipment module
- $K_{F,D}$ Input failure parameter for distributed equipment module.

In order to accommodate the wide variety of actual configurations shown in Figure 7.2 and described above within the general structure of power flowing into a generalized interface (transformer and/or switch panel), an auxiliary power system in parallel to a common module, and then to a parallel set of distributed modules, several strategies were adopted, as listed below:

- If no auxiliary power system is available, the auxiliary power system is treated as "always failed" by assigning an essentially infinite failure parameter
- If the facility being modelled has no service power interface $K_{F,S}$ is set equal to zero; i.e., it can never fail
- If the facility has no common equipment, $K_{F,C}$ is set equal to zero; it can never fail
- If the facility has no distributed modules, $K_{F,D}$ is set equal to zero; they can never fail
- If the facility has several equipments in parallel, to insure a high degree of redundancy, collectively these are assumed not to fail; the failure parameter for this stage is set equal to

zero. When tested with model-generated values of the exterior exposure and other input parameters, this approximation was of the same order as those tolerated elsewhere in the analysis.

SUMMARY OF FAILURE PARAMETERS

The tables which follow summarize the equipment and equipment module failure parameters, and enclosure characteristics. These are based on the facility and equipment designations contained in Appendix A and the methods described in this section.

Mean Exposure-to-Failure Levels

Failure exposure levels for individual equipments at each type of facility are shown in Table 7.2. These equipments are those shown previously in Figures 7.2. Note that the primary power referred to under each facility is the power source represented by the public utility (SIC 49). Note that electric motors are assumed to not be vulnerable (based on limited test data).

Facility Equipment Enclosures

Table 7.3 shows the enclosure categories associated with each SIC Code for the equipments shown in Figure 7.2. When an enclosure is located inside a building (double enclosure), the building category is listed under level 1 and the equipment enclosure category is listed under level 2. Enclosure categories were defined in Section VI. Note that Table 7.3 reflects many of the SIC special cases within the broad industry categories discussed previously.

Facility Failure Parameters

The facility failure parameters, $K_{F,SW}$, $K_{F,AUX}$, $K_{F,C}$, and $K_{F,D}$ for each pertinent SIC number are obtained by applying Equations (7.3) and (7.4) to each equipment for each SIC number, and then using the methods described above to relate individual equipment types to overall failure parameters. The mean exposure-to-failure values are obtained from Table 7.2, the enclosure types from Table 7.3, and the penetration factors

TABLE 7.2
MEAN EXPOSURE-TO-FAILURE VALUES FOR TYPICAL EQUIPMENTS BY SIC NUMBER

Facility and SIC Code	Facility Equipment	Mean Exposure to Failure (Fiber-sec/Meter ^{3})
Electric Utility SIC-49	Communications	5×10^6
	Common Controls	7×10^8
	High Voltage Switch Gear	7×10^5
	High Voltage Bus	1.6×10^7
Light Industries Small = SIC-20, 23, 24, 27, 38 Large = SIC-22, 25, 34, 35, 36	Primary Power	(SIC-49)
	Service Switch Gear	7×10^5
	Power Distribution	1.5×10^6
	Auxiliary Power	2.2×10^5
	Controller	1×10^7
	Small Motors	(Not Vulnerable)
	Interface Units	1.4×10^5
	High Voltage Motor Controls	1.4×10^5
	Servo Motor Circuits	1×10^8
Heavily Automated Industries SIC-26, 28, 29, 30, 33, 37	Primary Power	(SIC-49)
	Service Switch Gear	7×10^5
	Auxiliary Power	2.2×10^6
	Computer	5×10^5
	Keyboard/Display	4.5×10^5
	Controller	1×10^7
	Interface Units	1.4×10^5
	Servo Motor Circuits	1×10^8
	High Voltage Motor Controls	1.4×10^5
	High Voltage Motors	(Not Vulnerable)
Business Service SIC-60, 62, 63, 73	Primary Power	(SIC-49)
	Service Switch Gear	7×10^5
	Auxiliary Power	2.2×10^6
	Converter	1×10^6
	Computer	5×10^5
	Keyboard/Display	4.5×10^5
	Processor	1×10^7
	I/O Interface	1×10^7
	Keyboard/Display	4.5×10^5
Health Service SIC-80	Primary Power	(SIC-49)
	Service Switch Gear	7×10^5
	Auxiliary Power	2.2×10^6
Communication Service (TELE) SIC-48	Primary Power	(SIC-49)
	Service Switch Gear	7×10^5
	Auxiliary Power	2.2×10^6
	Marker/Connectors	1×10^7
	Registers	1×10^7
	Relay Switches	7×10^5
Small Business SIC-50-59, 99	Primary Power	(SIC-49)
	Power Distribution	1.5×10^6
Residential:	High Fidelity Set	6.6×10^5
	TV Set	1.7×10^7

TABLE 7.3
ENCLOSURE TYPES FOR SIC-CODED BUSINESS AND INDUSTRY EQUIPMENTS

Facility SIC Code	Equipment or Equipment Module	Enclosure Type	
		Level 1	Level 2
Electric Utility	Communications & Controls	1	–
SIC-49	High Voltage Switch Gear	1	7b
	High Voltage Bus	–	–
Small Light Industry	Service Switch Gear	5b	7b
SIC-20, 24, 27	Power Distribution	2	–
SIC-23, 38	Controller & Servo	2	–
SIC-20, 38	Servo Interface Unit	2	7b
SIC-20, 38	Controller	2	–
SIC-23, 27	Motor Control Switch Gear	2	7a
SIC-24			
Large Light Industry	Service Switch Gear	5b	7b
SIC-22, 25, 34, 35, 36	Auxiliary Power	5b	–
SIC-22, 36	Controller & Switch & Servo	3	–
SIC-25, 35	Motor Control Switch Gear	3	7a
SIC-34, 35, 36	Line Controller	3	–
Heavily Automated Industry	Service Switch Gear	5b	7b
SIC-26, 28, 29, 33, 37	Auxiliary Power	5b	–
	Computers & Keyboard/Displays	4	–
SIC-26, 33	Controller & Motor Control Sw.	3	–
SIC-28, 29, 30, 37	Controller & Switch & Servo	3	–
Business Service	Power Distribution & Auxiliary Power	5a	–
SIC-60, 61, 62, 63	Conv. & Comp. & Keyboard/Displays	4	–
SIC-73	Processor & I/O & Keyboard/Displays	4	–
Air Transportation	Service Switch Gear	5b	7b
SIC-45	Auxiliary Power	5b	–
	Computer & Keyboard/Displays	4	–
Health Services	Service Switch Gear	5b	7b
SIC-80	Auxiliary Power	5b	–
Communications (TELE)	Service Switch Gear	4	7b
SIC-48	Auxiliary Power	4	–
	Marker & Register	4	9b
	Line Switches	4	–
Small Business	Power Distribution	11	–
SIC-50-59, 99			
Residential With Air Conditioning	HIFI & TV Set	10a	–
Without Air Conditioning	HIFI & TV Set	10b	–

Note: Enclosure types are defined in Table 6.1

from Table 6.2. The technique is illustrated by the following example for SIC 20:

1. From Figure 7.2 it can be seen that SIC 20 has service switchgear but no auxiliary power, no common equipment, and distributed modules consisting of controllers, interface units and servo circuits.

2. From Table 7.2 the following mean-exposure-to-failure values are obtained (in units of fiber-seconds per cubic meter):

   - service switchgear; $\overline{E} = 7 \times 10^5$
   - controller; $\overline{E} = 1 \times 10^7$
   - interface unit; $\overline{E} = 1.4 \times 10^5$
   - servo circuits; $\overline{E} = 1 \times 10^8$

3. From Table 7.3 it can be seen that service switchgear has two enclosures, Type 5b and Type 7b; controller + servo are in a single Type 2 enclosure, while the servo interface unit is inside a Type 7b enclosure within a Type 2 enclosure.

4. Table 6.2 shows the following penetration factors:

   - Type 2; $E/E_0 = .00989$
   - Type 5b; $E/E_0 = .0938$
   - Type 7b; $E/E_0 = .0164$.

5. Applying Equations (7.3) and (7.4) (cf p. 7-15):

$$K_{F,SW} = (\text{Penetration Factor, 5b}) \cdot (\text{Penetration Factor, 7b}) \cdot (1 \div \text{service switch failure parameter})$$
$$= (.0938)\ (.0164)\ (1 \div 7 \times 10^5) = .22 \times 10^{-8}$$

$$K_{F,C} = 0$$

$$K_{F,D} = (\text{Penetration Factor 2})\ [(1 \div \text{controller mean exposure-to-failure}) + (\text{Penetration Factor 7b})\ (1 \div \text{interface mean exposure-to-failure}) + (1 \div \text{servo mean exposure-to-failure})]$$
$$= (.00989)\ \left[(1 \div 10^7) + (.0164)\ (1 \div 1.4 \times 10^5) + (1 \div 10^8)\right] = .22 \times 10^{-8}$$

VIII. COSTS ASSOCIATED WITH EQUIPMENT FAILURES

This section of the report presents ORI's methodology for determining the costs associated with equipment failures resulting from an aircraft accident involving the release and subsequent dispersion of graphite fibers. These costs may be divided into two categories:

- cost of cleanup and repair of affected electrical equipment
- impact due to business and industry "dislocation."

BUSINESS-INDUSTRY IMPACT

The major goal in developing the methodology to use in this part of the model was to provide a rational means of relating impacts in dollar values to graphite fiber incursions and the resulting equipment failures. A secondary but still large factor was the requirement that the method selected enable us to make use of available data. Several potential methods clearly required the collection of substantial amounts of data, so that candidate methods were screened rather critically against the data availability criterion. We argued that economic losses resulting from equipment failures consist primarily of lost production, sales, and wages. We also recognized that, at least on the national level, the Gross National Product (GNP) measures the grand total of all goods and services produced in the country in one year. A related measure, the Gross Domestic Product (GDP) is a more useful measure for our purposes since it includes all goods and

services produced within the united States in a somewhat more rigorous way then the GNP. The value of goods and services produced by American corporations overseas is included in the GNP but excluded from the GDP; similarly the GDP includes goods and services produced in the United States by foreign corporations.

The selection of these measures as the major inputs for the cost calculations makes available a wealth of data collected primarily for other purposes. For example, projections of the national economy are typically made in terms of the growth of the GNP, and in many cases, for particular economic sectors. More pertinent to our requirements is the information tabulated by the Department of Commerce on a routine basis; it provides national gross domestic product values for individual industries classified by their two-digit Standard Industrial Classification (SIC) designations. Sample SIC numbers were shown in Table 7.1 previously. With these data available at the national level, we sought to develop a method of allocating an appropriate fraction to each local area for which risk assessment calculations were to be made. This allocation was made on the basis of the ratio of the local payroll for a particular industrial sector to the national payroll in the same sector. Again this operation was facilitated by the availability of a major data base: the Bureau of Census publication County Business Patterns. These reports provide the number of establishments in different size groups, payroll, and employment for each SIC-coded business and industry category. A sample excerpt from this document appears in Figure 8.1. The basic assumption required in order to apply this allocation scheme is that the local productivity as measured by output per payroll dollar is equal to the national average productivity.

The risk assessment model thus assumes that the impact of a carbon fiber incident on the economy can be measured by the fraction of the local GDP allocated to a particular industry over the period of time that the industry is "down." In the absence of any other information we assumed that the down time would be of the order of one day and that cleanup costs could be satisfactorily represented by the GDP impact calculation. That is, we felt that the cleanup costs would be no more than of the same order of magnitude as that measured by the impact calculation. In view of the

Table 2. Counties—Employees, Payroll, and Establishments, by Industry: 1976—Continued

(Excludes government employees, railroad employees, self-employed persons, etc.—see "General Explanation" for definitions and statement on reliability of data. Size class 1 to 4 includes establishments having payroll but no employees during mid-March pay period. "D" denotes figures withheld to avoid disclosure of operations of individual establishments; the other alphabetics indicate employment-size class—see footnote.)

SIC code	Industry	Number of employees for week including March 12	Payroll ($1000)		Number of establishments, by employment-size class									
			First quarter	Annual	Total	1 to 4	5 to 9	10 to 19	20 to 49	50 to 99	100 to 249	250 to 499	500 to 999	1000 or more
	GLOUCESTER—Continued													
734	Services to buildings	259	252	1 320	20	9	6	2	2	1	-	-	-	-
7349	Building maintenance services, nec	212	208	1 132	14	6	5	1	1	1	-	-	-	-
738	Miscellaneous business services	189	336	1 611	39	28	6	3	2	-	-	-	-	-
7399	Business services, nec	55	111	549	12	7	4	1	-	-	-	-	-	-
75	Auto repair, services, and garages	200	382	1 829	63	50	11	2	-	-	-	-	-	-
752	Automotive repair shops	168	326	1 394	49	40	7	2	-	-	-	-	-	-
7531	Top and body repair shops	70	167	664	13	9	3	1	-	-	-	-	-	-
7538	General automotive repair shops	71	116	491	25	23	1	1	-	-	-	-	-	-
76	Miscellaneous repair services	180	467	2 064	37	27	4	4	2	-	-	-	-	-
769	Miscellaneous repair shops	129	358	1 572	19	11	3	3	2	-	-	-	-	-
7699	Repair services, nec	95	287	1 289	14	9	2	1	2	-	-	-	-	-
79	Amusement & recreation services	211	237	1 189	25	15	2	3	5	-	-	-	-	-
793	Bowling and billiard establishments	(B)	(D)	(D)	4	1	-	1	2	-	-	-	-	-
7933	Bowling alleys	(B)	(D)	(D)	4	1	-	1	2	-	-	-	-	-
799	Misc. amusement, recreational services	104	132	817	17	12	1	2	2	-	-	-	-	-
80	Health services	2 291	5 314	23 070	135	85	33	10	2	2	1	1	1	-
801	Offices of physicians	326	1 391	5 669	61	37	17	7	-	-	-	-	-	-
802	Offices of dentists	118	261	1 280	35	27	7	1	-	-	-	-	-	-
805	Nursing and personal care facilities	320	601	2 624	4	-	1	-	-	2	1	-	-	-
806	Hospitals	(G)	(D)	(D)	2	-	-	-	-	-	1	1	-	-
81	Legal services	195	465	2 006	56	46	9	3	-	-	-	-	-	-
82	Educational services	238	306	1 155	14	3	4	5	1	1	-	-	-	-
821	Elementary and secondary schools	196	271	1 008	8	-	2	4	1	1	-	-	-	-
83	Social services	351	374	1 559	33	17	8	4	2	1	1	-	-	-
831	Social services nec	(C)	(D)	(D)	30	15	8	4	2	1	-	-	-	-
836	Residential care	(C)	(D)	(D)	3	2	-	-	-	-	1	-	-	-
86	Membership organizations	346	378	1 504	56	33	17	5	1	-	-	-	-	-
863	Labor organizations	54	46	187	4	2	1	1	-	-	-	-	-	-
866	Religious organizations	239	274	1 065	41	23	13	4	1	-	-	-	-	-
89	Miscellaneous services	179	457	1 875	31	21	6	3	1	-	-	-	-	-
891	Engineering & architectural services	106	296	1 222	13	8	2	2	1	-	-	-	-	-
893	Accounting, auditing & bookkeeping	67	141	594	15	10	4	1	-	-	-	-	-	-
—	Nonclassifiable establishments	(B)	(D)	(D)	51	49	1	1	-	-	-	-	-	-
	HUDSON													
	Total	183 837	481 548	2 005 992	10 794	6 507	1 701	1 086	863	347	209	55	24	8
—	Agricultural services, forestry, fisheries	(B)	(D)	(D)	20	16	3	1	-	-	-	-	-	-
07	Agricultural services	(B)	(D)	(D)	20	16	3	1	-	-	-	-	-	-
—	Mining	(B)	(D)	(D)	3	2	-	1	-	-	-	-	-	-
—	Contract construction	4 179	14 727	68 967	560	400	68	37	20	11	3	1	-	-
15	General contractors and operative builders	689	1 789	10 474	149	113	15	8	6	2	-	-	-	-
151	General building contractors	542	1 459	8 485	75	51	8	8	6	2	-	-	-	-
16	Heavy construction contractors	852	3 568	17 766	25	11	7	2	2	1	1	1	-	-
161	Highway and street construction	(F)	(D)	(D)	12	6	3	-	1	1	-	1	-	-
162	Heavy construction, except highway	(E)	(D)	(D)	13	5	4	2	1	-	1	-	-	-
17	Special trade contractors	2 638	8 369	40 727	386	271	66	27	12	8	2	-	-	-
171	Plumbing, heating, air conditioning	484	1 890	8 926	88	65	16	5	-	1	1	-	-	-
172	Painting, paper hanging, decorating	263	881	4 662	32	26	3	2	-	-	1	-	-	-
173	Electrical work	482	1 880	7 957	64	40	11	8	4	1	-	-	-	-
174	Masonry, stonework, and plastering	306	1 172	4 661	53	39	7	4	2	1	-	-	-	-
1741	Masonry and other stonework	115	348	1 992	40	33	3	3	1	-	-	-	-	-
1742	Plastering, drywall and insulation	179	788	2 595	8	2	3	1	1	1	-	-	-	-
175	Carpentering and flooring	119	331	1 594	33	29	3	-	1	-	-	-	-	-
1751	Carpentering	89	271	1 224	23	21	1	-	1	-	-	-	-	-
176	Roofing and sheet metal work	176	441	2 417	46	33	11	1	1	-	-	-	-	-
179	Misc. special trade contractors	762	2 857	11 689	56	28	13	8	4	5	-	-	-	-
1791	Structural steel erection	60	202	682	6	3	-	2	1	-	-	-	-	-
1793	Glass and glazing work	(B)	(D)	(D)	8	5	2	1	-	-	-	-	-	-
1794	Excavating and foundation work	(B)	(D)	(D)	2	1	-	-	1	-	-	-	-	-
1795	Wrecking and demolition work	237	717	3 982	11	4	2	1	2	2	-	-	-	-
1796	Installing building equipment, nec	199	966	3 943	8	3	1	2	-	2	-	-	-	-
1799	Special trade contractors, nec	150	454	2 066	20	11	8	-	-	1	-	-	-	-
—	Manufacturing	72 041	203 059	848 989	1 626	501	258	258	312	184	83	23	14	3
20	Food and kindred products	7 376	25 185	101 476	89	19	13	17	16	7	11	3	2	1
201	Meat products	1 647	6 139	23 681	15	-	2	2	5	1	4	1	-	-
2011	Meat packing plants	(F)	(D)	(D)	6	-	1	1	2	-	2	-	-	-
2013	Sausages and other prepared meats	1 092	4 099	17 342	9	-	1	1	3	1	2	1	-	-
203	Preserved fruits and vegetables	669	1 737	7 535	9	1	1	3	2	1	-	-	1	-
2034	Dehydrated fruits, vegetables, soups	(B)	(D)	(D)	1	-	-	-	-	1	-	-	-	-
2035	Pickles, sauces, and salad dressings	(F)	(D)	(D)	3	-	-	1	1	-	-	-	1	-
2038	Frozen specialties	(B)	(D)	(D)	4	1	-	2	1	-	-	-	-	-
204	Grain mill products	207	633	2 917	8	1	3	1	1	2	-	-	-	-
2047	Dog, cat, and other pet food	(B)	(D)	(D)	2	1	-	-	-	1	-	-	-	-
2048	Prepared feeds, nec	117	384	1 353	4	-	2	1	-	1	-	-	-	-
205	Bakery products	887	3 218	12 029	21	7	3	5	2	1	2	1	-	-
2051	Bread, cake, and related products	(F)	(D)	(D)	20	7	3	5	2	1	1	1	-	-
2052	Cookies and crackers	(C)	(D)	(D)	1	-	-	-	-	-	1	-	-	-

A 0–19, B 20–99, C 100–249, E 250–499, F 500–999, G 1,000–2,499, H 2,500–4,999, I 5,000–9,999, J 10,000–24,999, K 25,000–49,999, L 50,000–99,999, M 100,000 or more

FIGURE 8.1 EXCERPT FROM COUNTY BUSINESS PATTERNS, 1976, FOR NEW JERSEY

estimated cleanup costs presented below, this assumption appears justified. It is recognized, however, that cleanup and restart costs are probably sensitive to industry type and this problem should receive additional attention in the future.

The next major step in developing the costing algorithm is the introduction of an expected value calculation. The calculation described in Section VII of this report is done for a particular small area. It is an estimate of the probability that a unit -- building or plant -- of a particular class of business or industry would have failed as a result of the graphite fiber incident. We then use it as an estimate of the fraction of that industry or business at that location that would be "knocked out" as the result of the graphite fiber incident.

The method of calculating the impact in dollars for a particular location is to use the results of the calculations described in Section VII, $P_{F,SIC}$, the probability of failure of a plant or business facility in a particular SIC number category in the following algorithm:

$$\text{Business-Industry Impact} = \sum_{SIC} \frac{LP_{SIC}}{NP_{SIC}} \; GDP_{SIC} \; P_{F,SIC} \qquad (8.1)$$

National-level inputs from the Department of Commerce provide the national payroll broken out by SIC number, NP_{SIC}, and the Gross Domestic Product broken out by SIC number, GDP_{SIC}. Available data for counties surrounding the particular airport include the payroll for each SIC-coded business and industry; the local input for each individual geographical area is defined as LP_{SIC}.

In order to treat the government "business" impact we defined a new SIC number 99 for that industry. The national payroll and Gross Domestic Product were both assigned the value one, i.e.,

$$NP_{99} = GDP_{99} = 1$$

so that the resulting local domestic product for that class of business is equal to the local payroll only. The government payroll for each county is also reported in County Business Patterns.

The model computes the failure probability for each business and industry category at one location. The resulting costs are then computed at that location, using Equation (8.1). This provides the sum over all categories of business and industry at that location, which is then adjusted to account for the one-day impact assumption. The model then does the household impact costing at that location.

HOUSEHOLD IMPACT

In order to compute the costs associated with the repair of household appliances we estimated the fraction of households that are air conditioned, defined by FAC. Using the methods described in Section VII, we obtained the failure probabilities for household appliances in air conditioned and non-air conditioned households. The overall failure probability depends on the ventilation parameters for typical residences that are air conditioned and those that are not air conditioned, and the mean exposure-to-failure for the equipment in question. If the resulting failure probabilities are $P_{F,AC}$ in the air conditioned household and $P_{F,NAC}$ in the non-air conditioned household, then the estimated cost to repair all damaged equipments of a particular class at all households in the geographical area is given by:

$$\text{Repair Cost} \times \text{Number of Households} \times \text{Number of Equipments per Household} \{P_{F,AC}FAC + P_{F,NAC}(1 - FAC)\}$$

The locations and numbers of residential units were obtained from the latest (1977) Bureau of Census publication, County and City Data Book. Based on a general consensus of the NASA-ORI risk assessment team members, our attention was limited to household television and high fidelity equipment. Other household equipments are reported to be relatively invulnerable. In many cases we were able to use local information sources to estimate the fraction of households that are air conditioned; in any case we applied judgmental factors to adjust this factor as a function of geography. The grand average number of television sets and high fidelity sets (or low fidelity music systems) appears to be about one each per household. Where local information was available we were able to adjust this ratio, but no generally available data source was identified as a result of contacts made with national organizations. Cleanup and repair costs for residential television sets and home music systems were developed from an informal survey of local service shops, as well as some conversations with the national

industry groups. The typical average cost to clean and repair a home television set is estimated to be fifty dollars; the average cost to clean and repair a stereo or high fidelity unit is estimated to be seventy-five dollars. While these costs are relatively modest, the general position of those in the business was that these repair costs were typical of equipment that would be repaired; in many cases a potentially higher repair cost for poor equipment would result in a similar outlay for new equipment.

DEFINITION OF GEOGRAPHICAL AREAS

The description of the method used to define geographical locations at which the impact calculations are made is placed here since it is to a large extent dictated by the selection of the cost impact method just described. The use of a method that has as one of its major advantages the availability of a ready-made data base, also carries with it something of a disadvantage - namely, the fact that the data base is primarily at the county level. The individual county is not a uniformly defined entity in the United States. Fortunately the County Business Patterns does completely span the United States. That is, where an individual city, for example, Fairfax City, in the Virginia suburbs of Washington, D.C., is not a true county, it is nevertheless reported in the County Business Patterns as a separate entity. Further, counties are not of uniform size, business or population density, etc.

In adapting the household and business data for computer input, we subdivided the counties into smaller, essentially homogeneous geographical units. In some cases different divisions were made for household data and business-industry data. In each case the center of the county or sub-county geographical unit was selected and a representative circle inscribed within the area. The input data set includes the coordinates of the center and the associated radius. The exposure and resulting impact calculations were made at five points within the circle. These points are the center and points a distance equal to two-thirds of the radius to the east, west, north and south of the center. The two-thirds value was selected as a result of the argument that, if the counties were equally spaced squares, say, these values would result in an equally spaced mesh. Our first inclination to use points on the circumference of the circle was discarded since it could

have resulted in calculations made at the same points, selected as representative of neighboring counties. In each case one-fifth of the input industrial business-industry payroll associated with the geographical unit is allocated to each of the five points. The calculation described in the preceding section is performed for each of the five points and totalled. Thus the result is an average of the impact over the geographical area, where the average is made after the final cost calculation. This method retains the necessary area sensitivity of the risk pheonomenon which is lost if all the business or industry is considered located at only one point. In that case we would tend to have a strongly binary risk mechanism.

The concept is illustrated schematically in Figure 2.4, and by an actual example in Figure 8.2. This figure shows how Howard County, Maryland was defined for purposes of the graphite fiber risk assessment model input structure. The upper map in Figure 11 shows the location of Howard County relative to the Washington National Airport and the Washington, D.C., Baltimore, Maryland, and Wilmington, Delaware SMSA's. Those SIC code numbers associated with manufacturing were located within the circle about the industrial center encompassing the industrial sites shown on the lower map. Those businesses identified as service-oriented, and wholesale and retail trade were placed within the circle about the point identified as the commercial center. Residential units were divided between the two points defined as "residential" and "commercial and residential."

CLEAN-UP AND REPAIR COSTS

The ORI risk assessment team contacted representatives of several agencies participating in the national graphite fiber risk assessment program in its search for information concerning the cost of clean-up and repair of damaged electrical and electronic equipment. Although we determined that standard clean-up procedures appear to have been established, the cost and effectiveness of these procedures has not been thoroughly documented.

In the absence of repair and clean-up cost estimates, ORI team members worked with the maintenance staff at Washington National Airport to develop original estimates of the labor required, and the associated cost, to

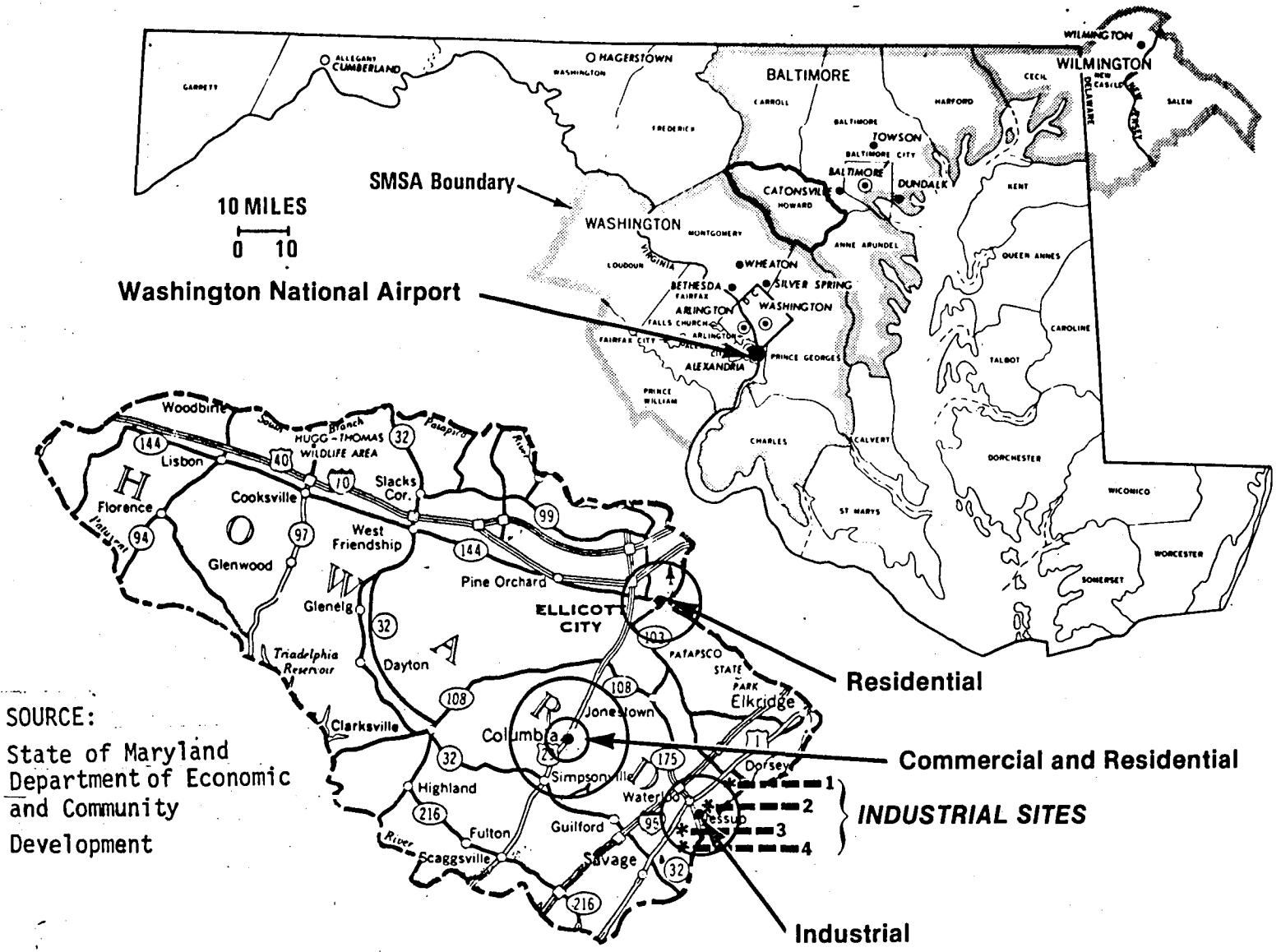

FIGURE 8.2 DESIGNATION OF AREAS FOR EXPOSURE AND COST COMPUTATIONS: HOWARD COUNTY, MARYLAND (LOWER) IDENTIFIED BY DARK BORDER IN MAP OF WASHINGTON-BALTIMORE AREA (UPPER).

TABLE 8.1

ESTIMATED CLEAN-UP AND REPAIR COSTS*
AIR TRAFFIC CONTROL EQUIPMENT

Equipment	Labor in Man Hours	**Cost ($)
Terminal Board	1	$ 13
Motor or Generator	3	39
Processor	24	312
Computer	48	624
Communications (transmitter or receiver)	1	13
VOR		
- Solid State	40	520
- Tube	80	1040
ILS	20	260
Radar	48	624
Console	4	52

* Source: Maintenance staff, Washington National Airport and area labor rates. ($13 per hour).

** Based on estimated time required.

clean up specific air traffic control equipments. The results are summarized in Table 8.1. Clean-up costs for generic types of equipment, such as computers and generators, may be transferrable to other settings, where similar pieces of equipment are used.

Although clean-up and repair costs appear small relative to the economic impact of a complete shut down, it may be necessary to consider these smaller costs if they occur with greater frequency. This factor, as well as vulnerability of other household equipment should be considered in further refinements of this study. Also worthy of further examination is the impact of the one-day down time assumption on the variance. The use of the Gross Domestic Product in the calculation of impacts of carbon fiber on business and industry does provide some sensitivity to secondary economic effects. A more detailed analysis of these effects should be considered.

IX. DETAILED RESULTS FOR NATIONAL AIRPORT, WASHINGTON, D.C.

SELECTION OF AIRPORT

National Airport was ORI's choice for the pilot analysis of its graphite-fiber risk assessment model. We had several reasons for selecting this airport for the initial study. ORI's Silver Spring, Maryland location is less than 20 miles from National. The airport is also close to densely populated areas in Northern Virginia, the District of Columbia, and the Baltimore-Washington corridor including the "new town" of Columbia. Of course, National is among the nation's busiest airports thereby giving it a greater potential for commercial aviation accidents than other, less heavily trafficked airports; National Airport's traffic load makes it about the tenth busiest airport in the country.

National Airport and the surrounding area do not represent a great at-risk combination, however, because there is less industrial development in this region than in the metropolitan areas served by other major airports with similar traffic levels. This effect will become apparent in the comparative results presented in Chapter X. A map of the airport and surrounding areas was shown previously in Figure 8.2. The technique representing counties by inscribed circles, described earlier, was applied to Washington, D.C. and to the areas of Maryland and Virginia within about 50 miles of National Airport. The methods described in Chapters VII and

VIII were used to prepare all model inputs for the transfer and business and residential impact calculations.

The Washington National Airport calculations were carried out for the two periods of specific interest to NASA, 1985 and 1993, as is the case for all results presented in this report; the basic aircraft - carbon fiber inputs for these calculations were shown in Table 3.2. These values were essentially developed collectively by NASA and its contractors. The table shows that the amount of fiber per aircraft is expected to increase by approximately a factor of five during the 1985-1993 period, while the fraction of aircraft expected to have graphite composite in their structures increases by approximately a factor of two to three. Projected operations at Washington National Airport are shown in Table 9.1.

Using the results presented in Section III for fraction of aircraft involved in a fire for accidents in different operational phases, and the estimated factor of 20 percent for the fraction of fiber released, we obtain the results shown in Table 9.2 for amount of fiber released in an aircraft accident with fire. These are tabulated for accidents involving different aircraft (by size) in different operational phases.

As an example of the calculation of the number of accidents, consider the 1993 scenario for Washington National Airport. The expected annual accident rate is obtained by using Equation (3.2) and the data presented in Tables 3.2 and 9.1. The annual fire-fiber accident rate for large aircraft is given by (1993):

$$\frac{29{,}621}{13{,}800{,}000} \times .50 \times 6 = .00644 \text{ accidents/year}$$

This is the mean (λ) used in the Poisson distribution that is sampled to determine the number of accidents for large jets in each replication of the stochastic model. As expected, the rate is quite small.

In 50,000 replications (samples) of the 1993 scenario for Washington National Airport, the results for large aircraft were:

- 49678 samples with no accident
- 321 samples with one accident
- 1 sample with two accidents.

TABLE 9.1

PROJECTED WASHINGTON NATIONAL AIRPORT OPERATIONS*

Aircraft Category	1985	1993**
Large	18,850	29,621
Medium	124,766	143,669
Small	60,284	24,710
Total U.S.	11,700,000†	13,800,000†

* EPA-FAA aircraft emission data base maintained by ORI.

** Projections are for 1995 - the closest to 1993 for which data unavailable.

† FAA Aviation Forecasts, Fiscal Years 1978-1989, U.S. Department of Transportation, FAA, September 1977, Washington, D.C. and FAA Office of Aviation Policy (AVP-120).

TABLE 9.2.

AMOUNT OF FIBER RELEASED (KILOGRAMS)
PER FIRE-ACCIDENT

Scenario Year	Aircraft Size	Operational Phase		
		Takeoff	Landing	In-Flight
1985	Large	18.1	45.3	27.2
	Medium	5.4	13.6	8.2
	Small	3.6	9.1	5.4
1993	Large	81.6	204.1	122.5
	Medium	27.2	68.0	40.8
	Small	18.1	45.3	27.2

Corresponding estimates, based on the Poisson distribution are 49679, 320, and 1, respectively. The total number of accidents simulated is thus 323, while the rate (.00644) computed above, when multiplied by 50,000 yields 322. For all three aircraft categories, the total number of accidents generated as a result of the random sampling process was 2430, while exact mathematical computation using the closed-form expression for the Poisson distributon would have led us to expect 2464, showing a deviation of only about one percent.

For each accident that the Monte Carlo model generates, an operational phase is randomly drawn from the relative frequency distribution obtained in Section III. The amount of fiber released is obtained from Table 9.2 and converted to individual fibers using the standard planning factor of 10^9 fiber fragments in one pound (.4536 kg) of carbon fiber.

RESULTS FOR 1985 SCENARIO

Most Costly Accidents

The 1985 analysis is based on the results of 50,000 replications, using the inputs described above. An insight into the types of accidents and related damage and costs is obtained by inspecting the "ten worst accidents" shown in Table 9.3; prepared directly from outputs of the stochastic model. The highest cost accident had an estimated impact of $324,420. This accident occurred in replication number 47277. Costs of other accidents among the most costly ten fall off to a low of $95,519. Other information in Table 9.3, shows that the ten worst accidents always involve the large and medium aircraft. Operational phases at the time of the accident are all landing, except for one takeoff. The stability class is always the most stable (Pasquill-Gifford F). Wind speed is always the lowest input value, 1.7 meters per second. Plume height is always 100 meters, which is the value associated with the most stable condition . The table also shows the amount of fiber released in numbers of fibers, which is a function of aircraft category and operational phase at the time of the accident.

The result that the ten worst accidents occur under the most stable meteorological conditions and lowest wind speed is consistent with the

TABLE 9.3

CHARACTERISTICS OF
TEN HIGHEST COST ACCIDENTS SIMULATED
1985 - WASHINGTON NATIONAL AIRPORT - 50,000 REPLICATIONS

Sample Number	Aircraft Category	Op.* Phase	Stability Class**	Wind		Release (10^9 Fibers)	Cost ($ 000)		
				Speed (m/sec)	Direction		Res.	Bus/Ind.	Total
47908	Med	TO	F	2	162^0	12	15	81	96
26860	Med	L	F	2	211^0	30	16	86	102
20948	Med	L	F	2	214^0	30	9	105	114
11411	Med	L	F	2	16^0	30	2	143	145
15613	Large	L	F	2	194^0	100	26	151	177
1778	Large	L	F	2	212^0	100	40	179	219
21900	Large	L	F	2	243^0	100	65	182	247
39020	Large	L	F	2	153^0	100	46	224	270
13033	Large	L	F	2	230^0	100	62	243	305
47277	Med	L	F	2	169^0	30	7	317	324

* T.O. = Take-Off
L. - Landing

** See Figures 5.1 and 5.2.

dispersion model described in Chapter V. The most stable meteorological condition implies the smallest dispersion and therefore the greatest downwind exposure. The most stable conditions are often associated with fog and haze with reduced visibility; they are most likely to occur in early morning and at night. In every accident identified in the table, the cost associated with equipment failures at industrial sites is greater than the cost associated with equipment failures at residences.

Statistical Description of Results

The frequency distribution of annual accident costs is shown in Table 9.4. The table shows the number of replications, or samples, in each cost class interval. The class intervals were selected to facilitate subsequent preparation of the risk profile; each interval is of equal size on a logarithmic scale. The frequency is tabulated for household damage cost, business-industry impact cost, and total cost. For example, out of 50,000 samples, the last column shows that 84 were associated with costs less than $178 but equal to or greater than $100. The last entry in the table shows that one accident had associated costs greater than or equal to $316,200 but less than $562,300. We identify this particular accident with the worst-case accident having a total associated cost of $324,420 which was shown in Table 9.3. Also shown in the table is the mean cost of $110 per year and the standard deviation of $3,377.

Table 9.5 reorganizes the model's output data tabulated in Table 9.4. The data are accumulated over cost intervals and presented as a fraction of all samples for which the cost exceeds the stated limit. This is precisely the desired risk profile. Thus the fraction of samples in which household damage exceeded $100 is 0.00926; the fraction of samples in which industry damage exceeded $100 is 0.01288, and the fraction of samples in which the total damage to residences and industry combined exceeded $100 is 0.01416. The results shown in Table 9.5 are plotted in Figure 9.1, where both 1985 and 1993 results are given. The curves are for total risk, using the sum of residential and industrial impact.

TABLE 9.4

FREQUENCY DISTRIBUTION OF 50,000 SAMPLES BY COST
WASHINGTON NATIONAL AIRPORT, 1985 SCENARIO

Upper Limit of Class Interval ($)	Number of Samples		
	Household	Industry	Total Costs
100	49,537	49,356	49,292
178	76	88	84
316	85	79	78
562	72	75	85
1,000	71	85	86
1,778	50	64	84
3,162	46	77	87
5,623	25	55	62
10,000	18	41	45
17,780	12	30	39
31,620	2	20	24
56,230	4	16	14
100,000	2	6	11
177,800	0	3	4
316,200	0	4	4
562,300	0	1	1
Mean	21	89	110
Standard Deviation	641	2,863	3,377
Minimum	0	0	0
Maximum	64,922	317,267	324,420

TABLE 9.5

FRACTION OF SAMPLES IN WHICH COST EXCEEDED AMOUNT SHOWN
WASHINGTON NATIONAL AIRPORT - 1985; 50,000 REPLICATIONS

Cost ($)	Fraction of Samples		
	Household	Industry	Total
100	0.00926	0.01288	0.01416
178	0.00774	0.01112	0.01248
316	0.00604	0.00954	0.01092
562	0.00460	0.00804	0.00922
1,000	0.00318	0.00634	0.00750
1,778	0.00218	0.00506	0.00582
3,162	0.00126	0.00352	0.00408
5,623	0.00076	0.00242	0.00284
10,000	0.00040	0.00160	0.00194
17,780	0.00016	0.00100	0.00116
31,620	0.00012	0.00060	0.00068
56,230	0.00004	0.00028	0.00040
100,000	0.0	0.00016	0.00018
177,800	0.0	0.00010	0.00010
316,200	0.0	0.00002	0.00002

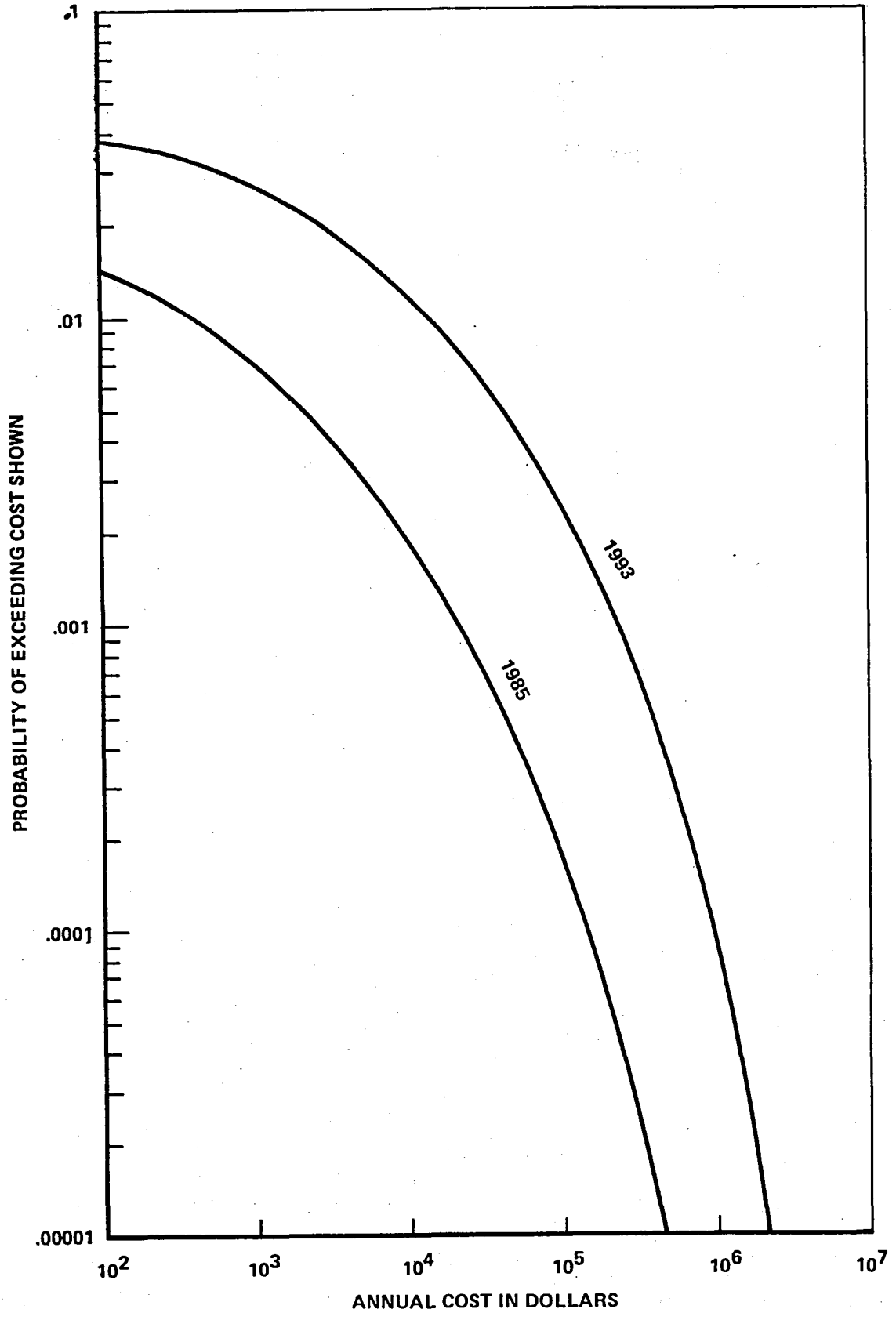

FIGURE 9.1 RISK PROFILES FOR WASHINGTON NATIONAL AIRPORT, BASE CASE, 1985 AND 1993

RESULTS FOR 1993 SCENARIO

The 1993 calculations for Washington National Airport were carried out in the same fashion as the 1985 calculations. The differences between the 1993 and 1985 scenarios consist of increased use of graphite composite per aircraft, and increased use of aircraft with graphite composite in their structure, as well as projected changes in the number of aircraft operations for the different aircraft categories. The 1993 scenario inputs for graphite fiber released in the simulated aircraft fire-accidents are given in Table 9.2 as a function of aircraft category and operational phase; each aircraft with graphite fiber composite on board is expected to have about five times as much in 1993 as in 1985.

The projected fraction of the civil aircraft fleet incorporating graphite fiber in their structure for the two time periods of interest is shown in Table 3.2. The fraction of aircraft in each size category incorporating graphite fiber goes up by a factor of about two. Another factor to consider in looking at Washington National Airport is the projected change in operations, shown above in Table 9.1. Operations of jet aircraft in the largest category are projected to increase by about 50 percent (from 18,850 to 29,621), medium-sized aircraft operations increase about 15 percent, while operations of the smallest aircraft are expected to decrease by approximately 60 percent. Thus, the outlook is for considerably more flights by the largest aircraft with the largest amount of fiber per aircraft.

In summary, we project five times as much fiber per aircraft and approximately twice as many operations of aircraft with fiber on board (cf Tables 3.2 and 9.1); this suggests that we might expect about ten times the annual damage, which is what was found in the simulation results. The mean annual impact was $110 for 1985 and $1,167 for 1993. On the other hand, the average impact per accident was $4,991 for 1985 and $24,000 for 1993. This factor of about five corresponds to the five-fold increase in amount of fiber per aircraft, indicating that at least in the low-risk domain the accident cost is approximately linear in amount of fiber released.

The risk profiles in Figure 9.1 show that the chance of exceeding $100 in total damage increased from .014 in 1985 to .038 in 1993. For $100,000 the increase is from .00018 in 1985 to .0024 in 1993. This corresponds to an increase in risk by a factor of about 2.5 for the low-cost end of the curve, and more than an order of magnitude increase -13- at the high-cost end. For a fixed risk probability of .01 the associated cost in 1985 is about $400, while for 1993 it is about $10,000.

As in the 1985 calculations, all of the ten most costly 1993 accidents (Table 9.6) occurred with the lowest wind speed, 1.7 meters per second under the most stable atmospheric condition; these accidents all occurred during landing. As pointed out earlier, the number of operations at National Airport of aircraft incorporating graphite fiber is expected to increase by a factor of approximately two between 1985 and 1993. This should be reflected in the statistics for the number of accidents in 50,000 sample replications. In fact, we found that for 1985 there were 1,068 samples in which one accident occurred and 17 in which two occurred. For 1993 there were 2,312 samples in which one accident occurred and 59 in which two occurred. Thus, the simulation results reflect the projected doubling of operations by fiber-carrying aircraft.

IMPACT OF CHANGE IN AMOUNT OF COMPOSITE ON BOARD

Two additional sets of simulations were conducted for the 1993 scenario at Washington National Airport. For each set all factors were the same as defined above for the 1993 scenario, except that in one case, the amount of graphite fiber per aircraft was increased by a factor of ten, and in the other, it was increased by a factor of 100. The increase in fiber translates directly (linearly) into increased exposure. The increased exposure appears to produce a less-than-linear corresponding increase in the resulting costs.

The worst accident results were:

- $4.1 million - 1993 scenario
- $16.8 million - ten times the 1993 fiber
- $31.4 million - 100 times the 1993 fiber.

TABLE 9.6

CHARACTERISTICS OF
TEN HIGHEST COST ACCIDENTS SIMULATED
1993 - WASHINGTON NATIONAL AIRPORT - 50,000 REPLICATIONS

Sample Number	Aircraft Category	Op. * Phase	Stability Class **	Wind		Release (10^9 Fibers)	Cost ($ 000)		
				Speed (m/sec)	Direction		Res.	Bus/Ind.	Total
6954	Med	L	F	2	181^o	150	17	593	610
15294	Large	L	F	2	194^o	450	93	564	657
21462	Large	L	F	2	244^o	450	241	698	939
1746	Large	L	F	2	212^o	450	174	782	956
2744	Med	L	F	2	161^o	150	70	903	973
16280	Med	L	F	2	183^o	150	9	1021	1031
11977	Med	L	F	2	171^o	150	100	1003	1103
12756	Large	L	F	2	230^o	450	206	984	1190
32749	Med	L	F	2	165^o	150	142	1214	1355
46354	Large	L	F	2	169^o	450	101	4023	4124

* L = Landing

** See Figures 5.1 and 5.2.

The average total annual cost went from $1,167 (1993 scenario) to $9,296 (10 x 1993 fiber) to $48,602 (100 x 1993 fiber). These increases are roughly factors of 8 and 5 for each successive 10-fold increase in fiber liberated.

Figure 9.2 presents the test case risk profiles with the 1993 scenario risk profile repeated for comparison. Where the annual costs are low and the associated level of risk is relatively high, the risk is relatively insensitive to the amount of fiber. For example, at the $100 cost level the risk goes from just under .04 to just under .05. On the other hand, the .0001 risk of producing $1 million damage for the basic 1993 scenario rises to .002 with ten times the fibers and to .01 with 100 times the fibers.

The principal term influencing the final cost impact is of the form:

$$\frac{E}{\bar{E}} V$$

where $\bar{E}$ is the mean exposure to failure of a specific type of equipment and V is the fraction of exterior exposure E that is experienced inside, where vulnerable equipment is located. The exterior exposure E is directly proportional to the amount of fiber released in the accident. Therefore, the ten-fold increase in fiber released can be considered a proxy for a ten-fold increase in V, or a decrease of $\bar{E}$ by a factor of ten, or an appropriate combination of these.

EXAMINATION OF DETAILED OUTPUT

To this point the presentation has dealt almost entirely with aggregate statistics from the Washington National Airport computer runs. In order to give the reader a better understanding of the calculations that lead to the aggregate statistics, we will devote some space to a discussion of sample detailed results from the 100 times - 1993 scenario fiber release impact set. This set of runs was selected for illustrative purposes because it is somewhat more dramatic than the base scenario simulations.

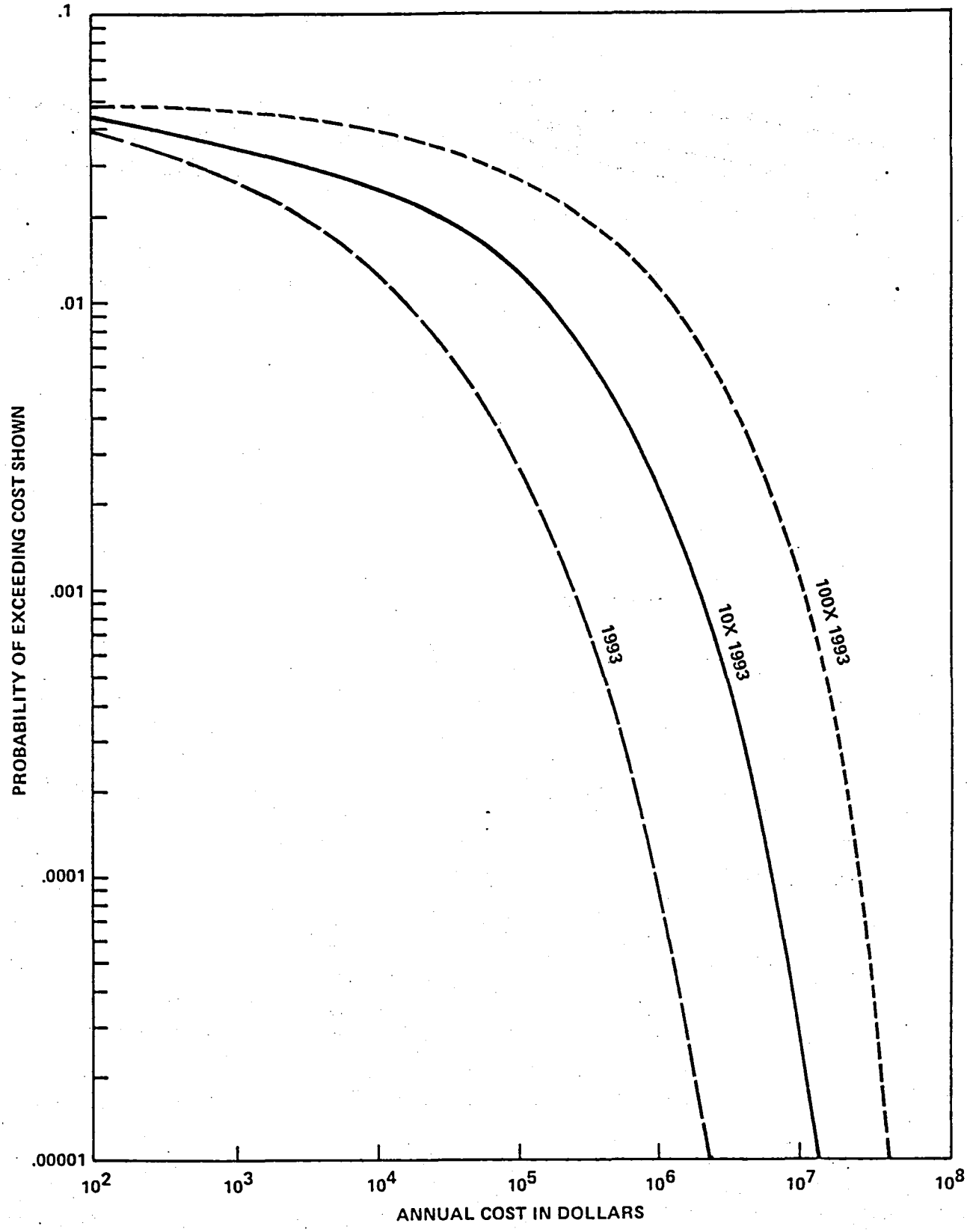

FIGURE 9.2. RISK PROFILES FOR WASHINGTON NATIONAL AIRPORT
1993 SCENARIO INPUTS, 10 x 1993 FIBERS,
100 x 1993 FIBERS

The worst accident identified for the 100 x 1993 fiber release simulations occurred in sample number 1,746 with a 1.7 meter per second-212° wind, 4.5 x 10^{13} fibers released, stability class F; the cost of residential repairs was $4,467,600, the industrial impact was $26,961,000, and the total cost was $31,429,000. We exercised an option available in the computer program to produce detailed output; the result for this accident appears in Table 9.7.

The accident location coordinates are X = 400, Y = -100 meters (measured from the tower at National Airport where X is positive to the east; Y is positive to the north). Residential points that were impacted are identified as 1, 6, 7, 8, 19, 20, 25, 30, 31, and 32 with X and Y coordinates given. The industrial points impacted were 1, 3, 7, 9, 13, 23, 24, 25, 29, 31, 32, 35, and 36 with their X and Y coordinates also given. The coordinates are for the center of the circles drawn to represent specific clusters of residences or businesses; the table also shows the radius for each circle (cf. Figure 2.4). Also shown in the table are values of the exterior exposure in fiber-seconds per cubic meter, the Gross Domestic Product per day for each business-industry location, and the cost associated with the failures at each location. The model provides an output for each exposure value greater than 0.5 fiber-second per cubic meter; for completeness we have tabulated all computer model-generated output results, even when the exposure and/or impact is essentially zero. The exposure values are for the center (X,Y) of each circle, while the dollar impact is the sum over all points within the circle of radius R about the center.

The impacted points and the accident location are plotted in Figure 9.3. Round dots represent residential sites; triangles, industrial sites. Site-identifying numbers appear to the left of the plotted points. The dashed line is in the downwind direction from the accident site.

The largest exterior dosage 106 x 10^{6} fiber-sec m^{-3}, was received at industrial site 13, which experienced only $34,000 damage. This was an almost complete shutdown (92%) at that site, which has a local daily Gross

TABLE 9.7

DETAILS OF MOST COSTLY ACCIDENT
WASHINGTON NATIONAL AIRPORT - 100 X 1993 FIBERS
(Sample 1746, Large Aircraft, Landing Accident at X=400, Y=-100 meters, Stability Class F, Wind 1.7 meters per second, 212°)

Location			Exterior Exposure (Fiber-sec/M^3)	R(Km)	GDP/Day* ($ 000)	Cost ($ 000)
No.	X(Km)	Y(Km)				
1	4	7	6.2×10^6	3		536
6	35	59	27.9×10^6	4		1078
7	25	57	0	2		0
8	30	69	0	10		3
19	15	37	0	3		0
20	21	44	71.4	2		0.05
25	70	12	38.2×10^6	4		251
30	30	45	37.6×10^6	2		1392
31	35	50	4.9×10^6	3		732
32	38	55	7.4×10^6	1		475
1	4	7	6.2×10^6	2	853	496
3	2	3	9.5×10^6	2	4021	979
7	25	55	0	2	458	0
9	36	60	35.2×10^6	1	18976	16,940
13	20	32	106.6×10^6	2	37	34
23	9	17	$.46 \times 10^6$	5	43	26
24	13	23	12×10^6	5	58	33
25	10	8	0	4	1774	0
29	38	44	0	4	356	0
31	32	47	18.5×10^6	5	890	438
32	30	50	41.8×10^6	2	890	667
35	35	47	$.11 \times 10^6$	6	24574	7348
36	33	43	$.011 \times 10^6$	1	593	1

* Shown only for business-industry locations.

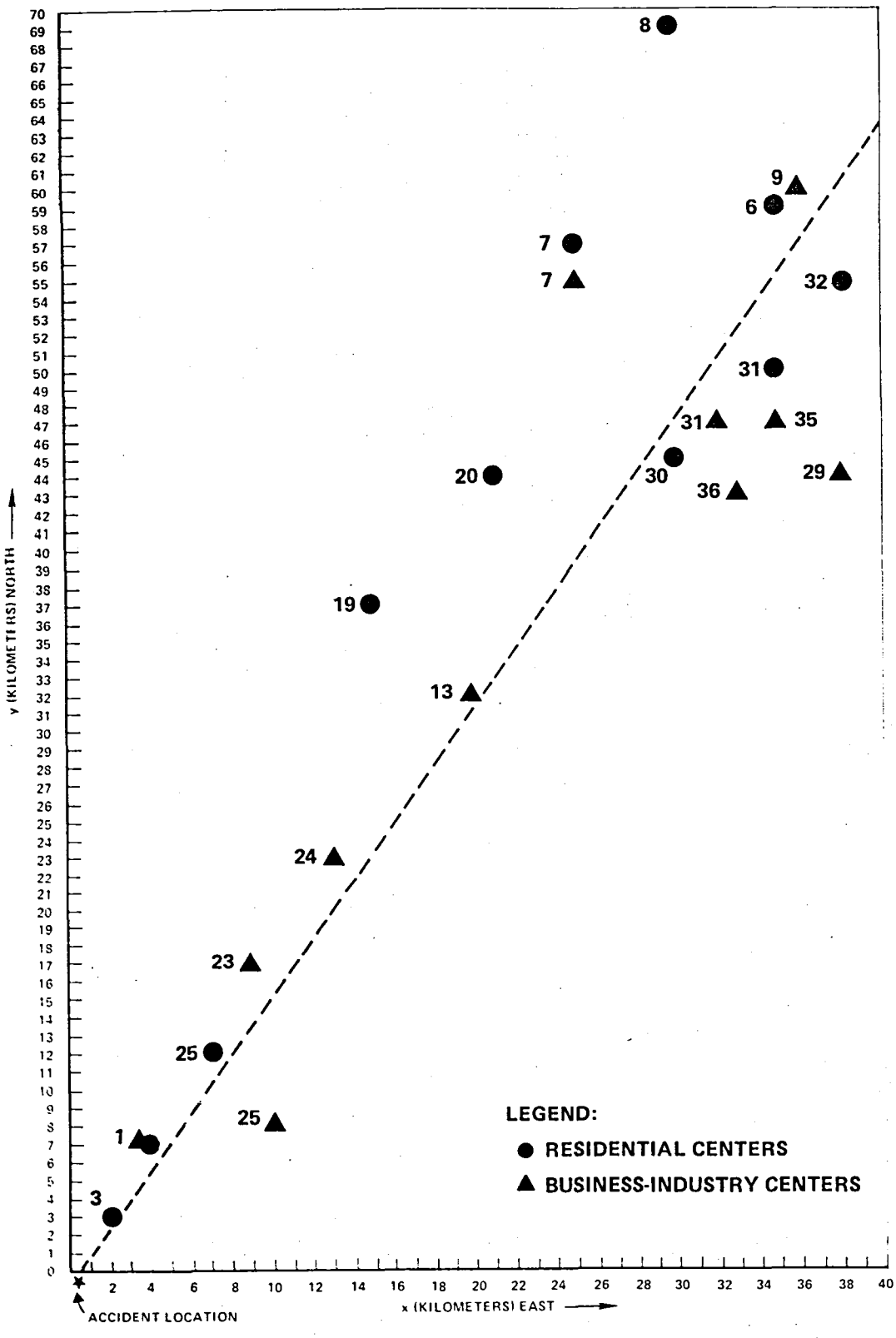

FIGURE 9.3. LOCATIONS OF RESIDENTIAL AND BUSINESS-INDUSTRY CENTERS FOR 100x1993 FIBER CASE - WASHINGTON NATIONAL AIRPORT

domestic Product of only $37,000. The largest loss was a result of an exposure of 35 x 10^6 fiber-sec m^{-3} at industrial site 9. The loss was $16,940,000, more than half (54%) of all costs resulting from this accident. Industrial site 9 had an associated value (GDP) of $18,976,000, experiencing an 89 percent over-all impact. This site is the center of wholesale, retail, and financial services in Baltimore. The Baltimore residential area represented by site 6 and the suburban area represented by site 30 account for $1,078,000 and $1,392,000 costs respectively. The heavy financial impact of this particular accident is the consequence of a wind blowing directly from Washington National Airport to Baltimore.

As a check on the manner in which aircraft accidents are seen to cause residential and industrial damage in this model, we also examined the 1993 base scenario for Washington National Airport. The most costly accident occurred under the same meteorological conditions. The residential cost for this accident was $174,410; the industrial impact was $781,590; and the total cost was $956,000. Thus the cost associated with this accident changed by a factor of about 35 when the amount of fibers released changed by a factor of 100.

As a matter of consistency, since all factors other than the amount of fiber is the same in the two calculations, we expect exposure in the base case to be related to exposure in the 100 x fiber case by a factor of 100. Comparison of the results showed that this did indeed occur. For instance, in Table 9.7, industrial sites 24 and 13 have exposures of 12 x 10^6 and 107 x 10^6 fiber-seconds per cubic meter respectively. The corresponding sites in the 1993 scenario had exposures of 12 x 10^4 and 100 x 10^4. The costs do not decrease linearly with the decrease in exposure. This non-linearity is related to the fact that, in some cases, the overall failure probability is near 100 percent, indicating a saturation effect. The single largest impact cost for the base case appears at industrial site 9 just as it did in the 100 x 1993 fiber case. Again damage in the Baltimore area was the major contributor.

X. FURTHER ANALYSIS OF SINGLE AIRPORT RESULTS

COMPARISON OF DIFFERENT AIRPORTS

In this section we present the findings for three of the major airports treated in the risk analysis. These results supplement the detailed information on Washington National Airport that was presented in the preceding chapter. The three airport-city complexes discussed here are O'Hare/Chicago, Lambert/St. Louis and Hartsfield/Atlanta. O'Hare is a busy airport (the nation's busiest commercial airport) serving a major metropolitan statistical area (SMSA). St. Louis has half the number of aircraft operations and serves an SMSA with a considerably lower population. Atlanta has two-thirds the number of annual aircraft operations and serves a smaller SMSA.

Population and aircraft operations data are shown in Table 10.1, with the average annual impact results, for these airport-city complexes, as well as Washington National Airport. As we might have expected, Chicago has the highest values for both household and business-industry costs, and therefore, in total costs. St. Louis shows by far the smallest costs. The ranking in terms of costs, whether residential or industrial impact or the sum of the two is:

1 - Chicago
2 - Washington
3 - Atlanta
4 - St. Louis

TABLE 10.1

COMPARISON OF AVERAGE ANNUAL IMPACTS AT FOUR AIRPORTS, 1993 SCENARIO

AIRPORT	ADJACENT SMSA POPULATION (Millions, 1970)	NO. OF A/C OPERATIONS (Thousands, 1976)	AVERAGE ANNUAL COSTS		
			RESI-DENTIAL	BUS/ IND.	TOTAL
National/ Washington	2.9	203	$207	$ 961	$1,168
O'Hare/ Chicago	7.0	577	647	2,093	2,740
Lambert/ St. Louis	2.4	178	93	194	287
Hartsfield/ Atlanta	1.6	417	198	574	772

In costs due to damage to residences, Washington and Atlanta are very close (within 5 percent), but otherwise, mean damage costs tend to differ by factors of one and a half or more. In every case costs due to damage to industry are at least twice the costs associated with residential impact.

It is also of some interest to compare the extreme values as well as averages. For this comparison we list the most costly accident that occurred in the simulated history at each of the airports. The most costly accidents that occurred at each airport in the base 1993 scenario cases were:

Chicago	$6,209,800
Washington	4,123,800
Atlanta	1,317,500
St. Louis	1,135,600

This ranking by most costly accident is the same as the ordering of airports by average annual impact.

As noted for Washington, the ten worst accidents occur with the lowest wind speed and the most stable conditions. We recorded one serious (i.e., among the ten most costly) accident with a 5.7-meter per second wind at O'Hare Airport, and two such cases at St. Louis. St. Louis also differs from the other airports in having two in-flight accidents and one take-off accident among the ten worst accidents. Essentially all of the ten worst accidents at the other three airports occurred during the landing phase. The assumptions regarding the relation of fiber liberated to operational phase were set forth in Chapter VIII. It was shown there that the landing phase accidents lead to twice the amount of fiber liberated in a crash and fire that would occur during a takeoff or in-flight crash and fire. We would, therefore, expect landing accidents to predominate among the ten worst accidents.

Figure 10.1 shows the risk profiles for these three airports and Washington National, for the base 1993 scenario. It illustrates the different risk profiles that result from differing demographic and economic patterns. As expected, the busiest airport with the most wealth in terms of both residences and industry at risk, Chicago/O'Hare (ORD) always shows consistently higher risk than the other airports. St. Louis/Lambert (STL) always shows the lowest risk. We account for this by both reduced aircraft operations and smaller population (and implied lower business-industry concentration) that may be impacted. The curves for Atlanta/Hartsfield (ATL) and Washington National Airport (DCA) lie between those for Chicago/O'Hare and St. Louis/Lambert and also cross each other. At the low-cost end Atlanta shows a higher probability of damage than Washington by a factor of two. At the high-cost end, the reverse is true. There DCA shows a higher probability, and again by approximately a factor of two. There is a greater chance of impacting high-value business-industry concentrations in the Washington National Airport vicinity than there is near the Atlanta airport.

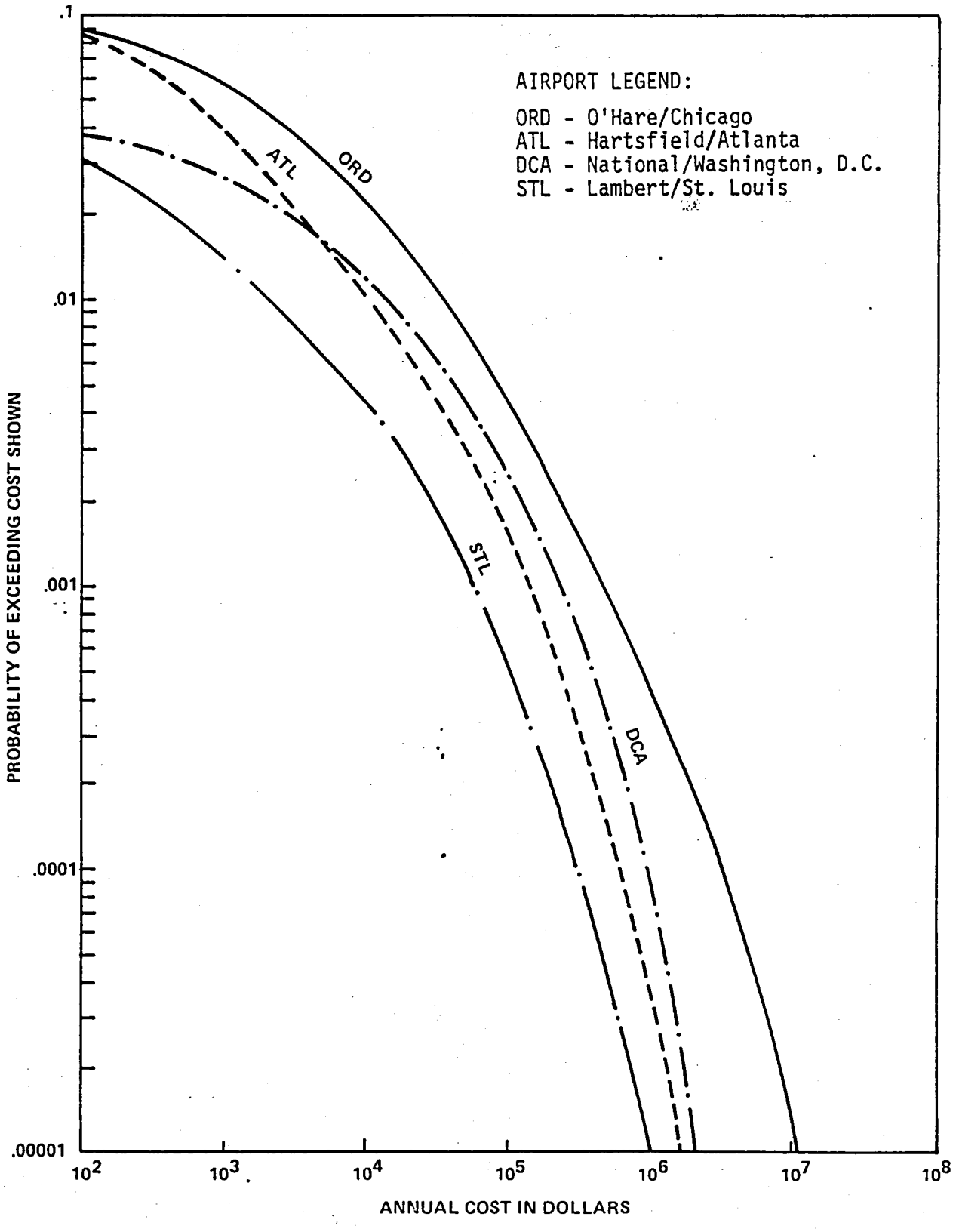

FIGURE 10.1. RISK PROFILES FOR FOUR AIRPORTS, 1993

To round out the discussion of these airports, we summarize the risk results that were obtained for the 1985 scenario. The same general comments apply to the 1985 risk profiles that applied to the 1993 risk profiles: Chicago showed the highest impact, St. Louis the lowest. The risks were considerably lower for 1985 than for 1993. Chicago has a .09 risk at the $100 annual level for 1993, it has a .03 risk at the same level for 1985. The risk for Chicago is 0.005 at the $100,000 level for 1993 while it is 0.00045 at the same level for 1985. Similarly, for 1993, St. Louis shows a .003 risk of at least $100 costs which is .007 in 1985. Where there was a .0005 risk of at least $100,000 cost at St. Louis in 1993 the risk is .00002 for 1985.

EFFECT OF INDUSTRY AT RISK

Clearly one of the important factors in the graphite fiber impact is the presence of industry or population at risk within range of the downwind zone to be hit by the diffusing cloud of fibers. In order to demonstrate this effect dramatically we ran the ORI risk assessment model for Philadelphia International Airport, for the 1993 scenario, for a special sensitivity test case -- for which Philadelphia County was omitted from the input data set. All of the counties that lie at least partly within a 50-mile circle centered on the Philadelphia International Airport have a total business and industry payroll of approximately 18 billion dollars a year (1976). Philadelphia County, which contains the City of Philadelphia has an annual business and industry payroll of 5.5 billion dollars or more than 30 percent of the total within the 50-mile circle. The results for this special run are shown in Figure 10.2 where we have plotted the resulting risk profile as well as the risk profile for the Philadelphia International Airport with all data entered. We note that the removal of the industry and business in downtown Philadelphia from the risk calculation has its most significant impact on the high-cost portion of the risk profile. The mean and extreme values also show a considerable change as a result of dropping Philadelphia County out of the calculation. These results are summarized in Table 10.2. The impact is greatest for the high cost accidents; the average annual cost is decreased by a factor of 2.5 while the average of the ten most costly accidents is decreased by a factor of about 3.5 when Philadelphia County's data is removed from the input set.

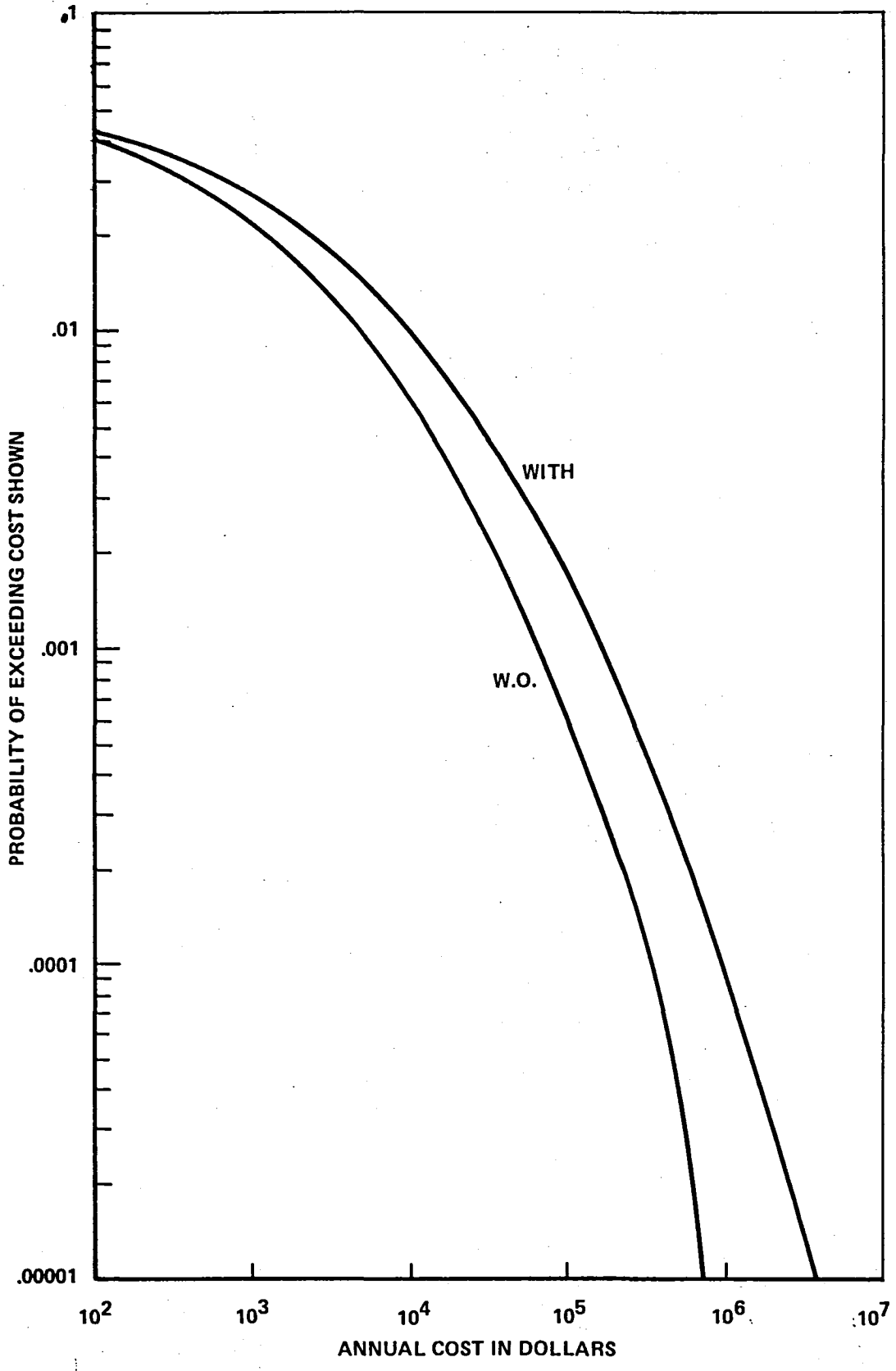

FIGURE 10.2. RISK PROFILES FOR PHILADELPHIA INTERNATIONAL AIRPORT, 1993 SCENARIO PHILADELPHIA COUNTY OMITTED FOR THE "W.O." CURVE

TABLE 10.2

SELECTED RESULTS FOR
PHILADELPHIA INTERNATIONAL AIRPORT
1993 SCENARIO

MEASURE	PHILADELPHIA COUNTY	
	With	Without
Average Cost/Year	$ 890	$ 352
Average Cost/Accident	$ 17,396	$ 6,880
Average Cost/10 Most Costly Accidents	$1,299,000	$376,000
Maximum Cost/Year	$3,500,500	$631,600

STATISTICAL CONFIDENCE LIMITS

One of the important questions to be addressed in this risk assessment is the confidence with which our results can be viewed. One part of this question is addressed to the statistical confidence limits associated with the Monte Carlo model used to generate our risk profiles. This is the confidence with which the results can be accepted on the assumption that all input values are valid.

To develop an expression for the statistical confidence limits, let P_a be the (unknown) probability of exceeding a damage level a at one airport - urban area complex in one year. Suppose that we have examined a sample of n years and that, of the n, we found r that had damage in excess of a. This is clearly one way of viewing the simulation model runs. In each replication our goal is to determine whether the cost due to graphite fiber related events is above or below the value c. This leads to our estimation of the probability of the cost being greater than x - the risk profile. Now we estimate the probability P_a by:

$$\hat{P}_a = \frac{r}{n}$$

and our statistical model is exactly that of Bernoulli trials. Each trial leads to a success, say, in which the annual accident-related cost is greater than or equal to $x or a failure, in which case the cost is below $x.

Then, r is a random variable, the number of successes in n trials, and the probability that r = i is given by:

$$\text{Prob } (r = i) = \binom{n}{i} P_a^i (1 - P_a)^{n-i}$$

and the expected value of r is

$$E(r) = nP_a$$

and the variance of r is

$$\text{Var } (r) = nP_a (1-P_a)$$

For the sample statistics, we can use the expression for $\hat{P}_a$ and write, for the expected value:

$$E(\hat{P}_a) = \frac{1}{n} E(r) = P_a$$

Similarly, the variance of $\hat{P}_a$ is given by:

$$\text{Var}(\hat{P}_a) = \frac{1}{n^2} \text{Var}(r) = \frac{1}{n} P_a (1-P_a).$$

In the absence of the complete population we only have the sample of runs that we have examined. In standard statistical fashion we estimate the sample moments from the sample statistics:

$$\text{Var}(\hat{P}_a) = \frac{\hat{P}_a (1-\hat{P}_a)}{n}$$

for a greater than zero. In many cases of interest $\hat{P}_a$ is very small and we can write:

$$\text{Var}(\hat{P}_a) \simeq \frac{\hat{P}_a}{n}$$

with negligible error. It has been demonstrated that, for the number of replications of the order of magnitude used in our analysis the distribution of sample results about the population results is approximately normal. Therefore, we can use the variance just derived to define confidence limits in the sense that 95 percent of the results obtained from additional sets of n replications will be within:

$$\hat{P}_a \pm 2\sqrt{\frac{\hat{P}a\ (1-\hat{P}a)}{n}}$$

Stated another way, the probability is 0.95 that the actual value of the probability P_a is within these limits.

To illustrate this result we have shown the 95 percent confidence limits in the risk profile for the Washington National Airport 1993 scenario in Figure 10.3. In that case 50,000 replications were run. The statistical confidence limits shown at different points along the curve clearly demonstrate one feature of the problem that has been noted earlier: our relatively large uncertainty at the high-cost, low-probability end of the risk profile. This suggests that in future work the sampling plan be structured so that the tail of the distribution is oversampled. It is relatively uneconomical to simply increase the number of runs in order to get more data for the tail of the distribution. The square root of n appears in the denominator of our expression for the confidence limits - implying that we must do four times as many replications in order to reduce the confidence limits by one-half.

STABILITY OF THE SIMULATION MODEL

One of the questions to be considered in running a model such as the ORI risk assessment model is the number of replications required and the related question of reproducibility. We have seen the number of runs required approached from the statistical confidence-limit point of view above. We now take a more pragmatic view of the problem. On a heuristic basis only we settled during early "production" runs on choosing a number of replications guaranteed to yield at least an expected 2,500 accidents. Computer time is essentially a linear function of the number of accidents simulated once a relatively small number of accidents is exceeded. Typical central processing unit time is 10-15 minutes to simulate 2,500 accidents and handle all associated input and output operations on an ITEL AS/5 computer. In order to further investigate the question of the appropriate number of replications we now use the simulation model results themselves.

Impact of Number of Replications

To examine the matter of the appropriate number of runs we ran the LaGuardia Airport risk assessment calculation for the standard number. In this case 35,000 replications was selected to yield an expected number of approximataly 2,500 accidents; as a test we also ran 18,000 replications. The results indicate a difference in mean annual cost of less than 20 percent

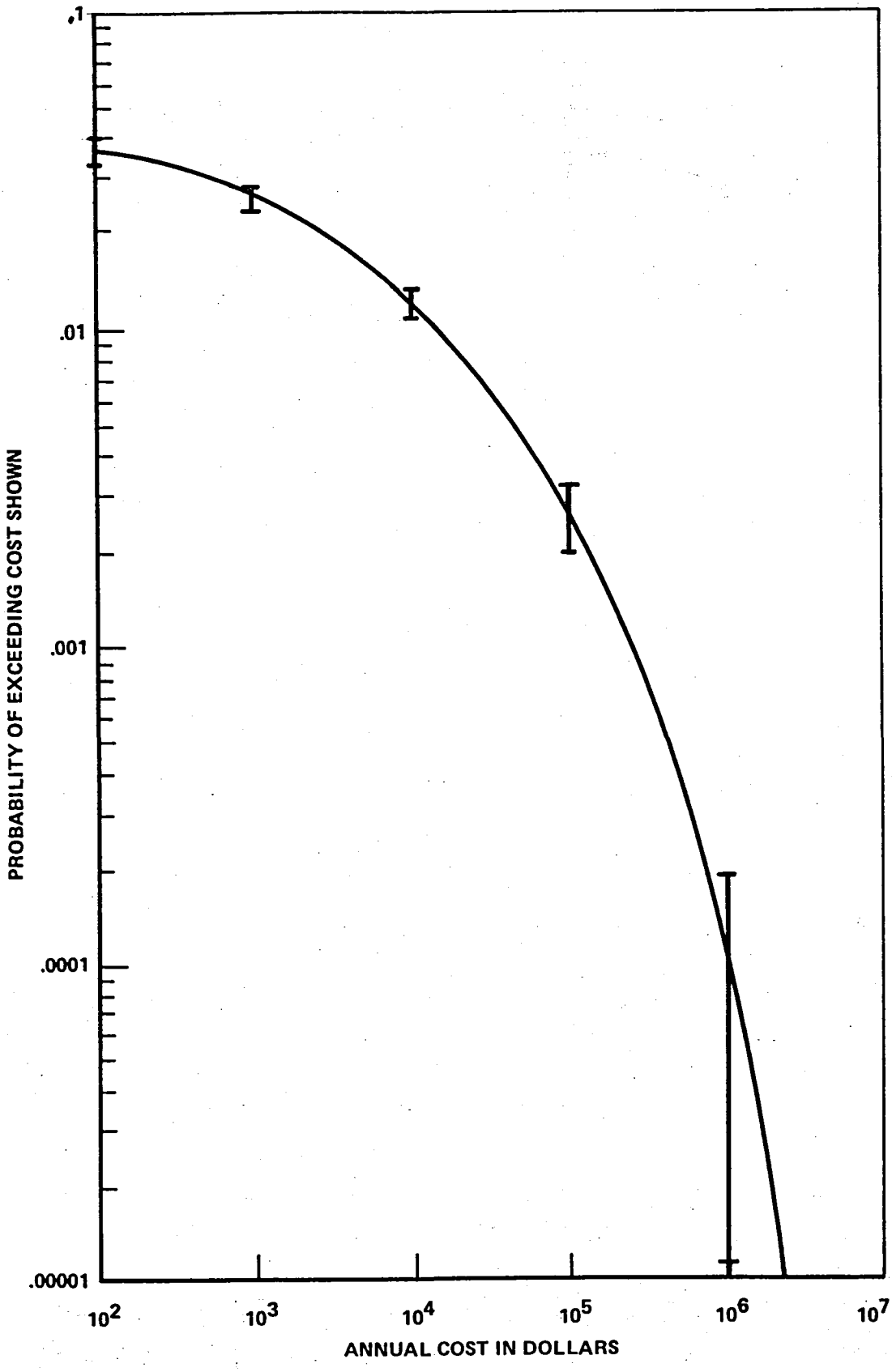

FIGURE 10.3. 1993 WASHINGTON NATIONAL AIRPORT RISK PROFILE SHOWING 95% STATISTICAL CONFIDENCE LIMITS* ASSOCIATED WITH MONTE CARLO PROCESS

*Non-Simultaneous

between the two sets of simulations, as shown in Table 10.3. The difference in the mean of the ten most costly accidents is greater than a factor of two, suggesting that the occurrence of the more costly accidents in the 35,000 - replication case has a strong impact on the mean annual costs. In Table 10.4 we have tabulated the probability of the annual cost exceeding the values shown - the risk probabilities. The results are essentially identical until we get to the million-dollar end of the curve. This result reinforces the earlier conclusion that we must be less confident about the results at the low-probability tail of the risk profile than about other portions of the risk profile. With this caveat we conclude that the shape of the risk profile over most of its length would not be significantly influenced by more replications.

Change in Accident Rate

In another test of the sensitivity to parametric change we repeated the 1993 Washington National Airport calculations for twice the standard input accident rate. Using our basic rule of generating approximately 2,500 accidents, we conducted 50,000 replications resulting in 2,430 accidents for the standard accident rate (6 fire-accidents in the U.S. per year) and 25,000 replications resulting in 2,480 accidents for the double-accident rate. It can be shown that, if the probability of exceeding a given cost in a year is the product of the probability of having an accident and the conditional probability of exceeding the given cost, given an accident, the two sets of calculations have essentially the same statistical confidence limits.

Our intuitive expectation in comparing the different accident rate results is that the annual risk should be doubled, but that the accident characteristics should be essentially unchanged. The risk probabilities are tabulated in Table 10.5. The 12 accident-per-year exceedance probabilities are double those for the 6 accident-per-year case except for the probability of exceeding $1 million a year. The mean cost per year is $1,167 for the 6-accident case and $2,067 for the 12 accident case. These results were influenced by one high-cost accident at $4 million. This accident occurred in replication 46354 of the 6-accident runs and exceeded by about a factor of three the most costly accident in the 12-accident simulations, $1.4 million. Otherwise the most costly accident characteristics were quite similar.

TABLE 10.3

COMPARISON OF RESULTS FOR DIFFERENT NUMBERS OF REPLICATIONS
LA GUARDIA AIRPORT, 1993 SCENARIO

NUMBER OF REPLICATIONS	NUMBER OF ACCIDENTS GENERATED	MEAN ANNUAL IMPACT	MEAN OF TEN MOST COSTLY ACCIDENTS
18,000	1449	$1390	$613,000
35,000	2856	$1660	$1,400,000

TABLE 10.4

EXCEEDANCE PROBABILITY FOR DIFFERENT NUMBER OF REPLICATIONS
LAGUARDIA AIRPORT, 1993

ANNUAL COST	NO. OF REPLICATIONS	
	18,000	35,000
$ 100	.064	.066
$ 1,000	.045	.046
$ 10,000	.014	.015
$ 100,000	.0038	.0037
$1,000,000	.00006*	.00017**

* 1 Case

** 6 Cases

TABLE 10.5

RISK PROFILE FOR DIFFERENT NATIONAL ACCIDENT RATES
WASHINGTON NATIONAL AIRPORT/1993

ANNUAL COST	PROBABILITY OF EXCEEDING COSTS	
	6 ACCIDENTS/YR.	12 ACCIDENTS/YR.
$ 100	.038	.075
$ 1,000	.026	.052
$ 10,000	.012	.024
$ 100,000	.0024	.0048
$1,000,000	.0001	.00016

XI. NATIONAL RISK

METHOD

In order to compute the national risk profiles we performed convolutions of various combinations of the probability density functions from which the individual airport risk profiles were obtained. The convolutions were run using the individual risk profiles which were generated for both the 1985 and 1993 scenarios for the following nine airports:

O'Hare/Chicago
John F. Kennedy/New York City
Washington National Airport/Washington, D.C.
Lambert/St. Louis
La Guardia/New York City
Logan/Boston
Hartsfield/Atlanta
Miami International/Miami
Philadelphia International/Philadelphia.

In order to develop expressions for the probability of a given risk for the nation, or more specifically, for a group of airports, we first adopt the convention of replacing the continuous probability distribution for accident-related costs at each airport by a discrete distribution. Since the class interval used for the discrete distribution can be made arbitrarily small, this implies very little loss in generality of the results. The cost

due to the impact of carbon fiber accidents on a national basis is a random variable that is the sum of random variables, the costs of accidents at individual airports. For ease of development, we first treat the case of only two airports. Let the probability of the cost at airport-city A due to aircraft-CF accidents being equal to $r\Delta\$$ be $P(X=r\Delta\$) = a_r$. For the second city B define the corresponding expression $P(Y=r\Delta\$) = b_r$. The sum of the costs incurred at both cities is a new random variable S=X+Y. The event S is the union of events:

$$(X=0,Y=r\Delta\$),\ (X=\Delta\$,Y=(r-1)\Delta\$),\ (X=2\Delta\$,Y=(r-2)\Delta\$)\ldots(X=r\Delta\$,Y=0).$$

If we let $P(S=r\Delta\$) = c_r$, then

$$c_r = a_0b_r + a_1b_r + \ldots a_rb_0 \qquad (11.1)$$

and the sequence $\{c_r\}$ is by definition the convolution of the sequence $\{a_r\}$ and the sequence $\{b_r\}$.

Now, define a generating function for the sequence $\{a_k\}$:

$$A(s) = \Sigma a_k s^k$$

and for the sequence $\{b_k\}$:

$$B(s) = \Sigma b_k s^k\ .$$

Feller[1] shows that the generating function

$$C(s) = \Sigma c_k s^k$$

is the product

$$C(s) = A(s)\ B(s)$$

or the random variable S=X+Y has the generating function A(s) B(s). The random variable X can represent the costs at a total of n city-airport combinations, in which case the variable X+Y is the total cost for n+1 cities.

In applying this result to the problem at hand, the probability distribution for the costs at each city derived from the Monte Carlo simulations is fitted by a discrete distribution with a uniform class interval. The interval was

---

[1] William Feller, An Introduction to Probability Theory and Its Applications, Volume 1, Third Edition. Wiley & Sons, 1968. pp 266-267.

conveniently set at $50,000; comparisons were made to indicate that the final results were essentially unchanged for smaller class intervals. The probability at the center of each interval is considered the coefficient of a term in a polynomial expansion, the generating function, with the power corresponding to the number of the class interval. This polynomial is then multiplied by the polynomial previously obtained for n cities (n = 1 the first time through the procedure). The coefficients in the product polynomial, which is the generating function for the sum variable, are the probabilities for the costs in each class interval due to accidents at the n+1 cities. This result can be converted to a cumulative probability distribution, to provide the risk profile for the n+1 airports.

APPLICATION

The computer program which implemented this method is written so that it can accept an essentially unlimited number of input risk profiles. Each is first converted to a probability distribution - density function - prior to the convolution operation described above. The algorithm can also repeat the convolution operation using each distribution more than once if necessary; this is controlled by a set of inputs for each risk profile. The program also provides the mean value and standard deviation after each successive convolution is performed.

In order to prepare an estimate for the national risk that we would expect to be on the high side, i.e. to bound the true value from above, we first note that the nine airports that were treated individually account for approximately 25 percent of all commercial air operations in the United States. Our concept is to allow the nine airports for which the risk profiles were available to represent all of the air carrier operations in the U.S. We, therefore, generated a risk profile from the convolution of these nine airport risk profiles, with each airport's probability distribution convoluted with itself four times. This is essentially equivalent to assuming that the national risk is associated with 36 airports, of which 4 are identical to Philadelphia International, 4 to La Guardia, etc. Here the word "like" means with regard to graphite fiber risk. The resulting national risk profiles for the 1985 and 1993 basic scenarios are shown in Figure 11.1.

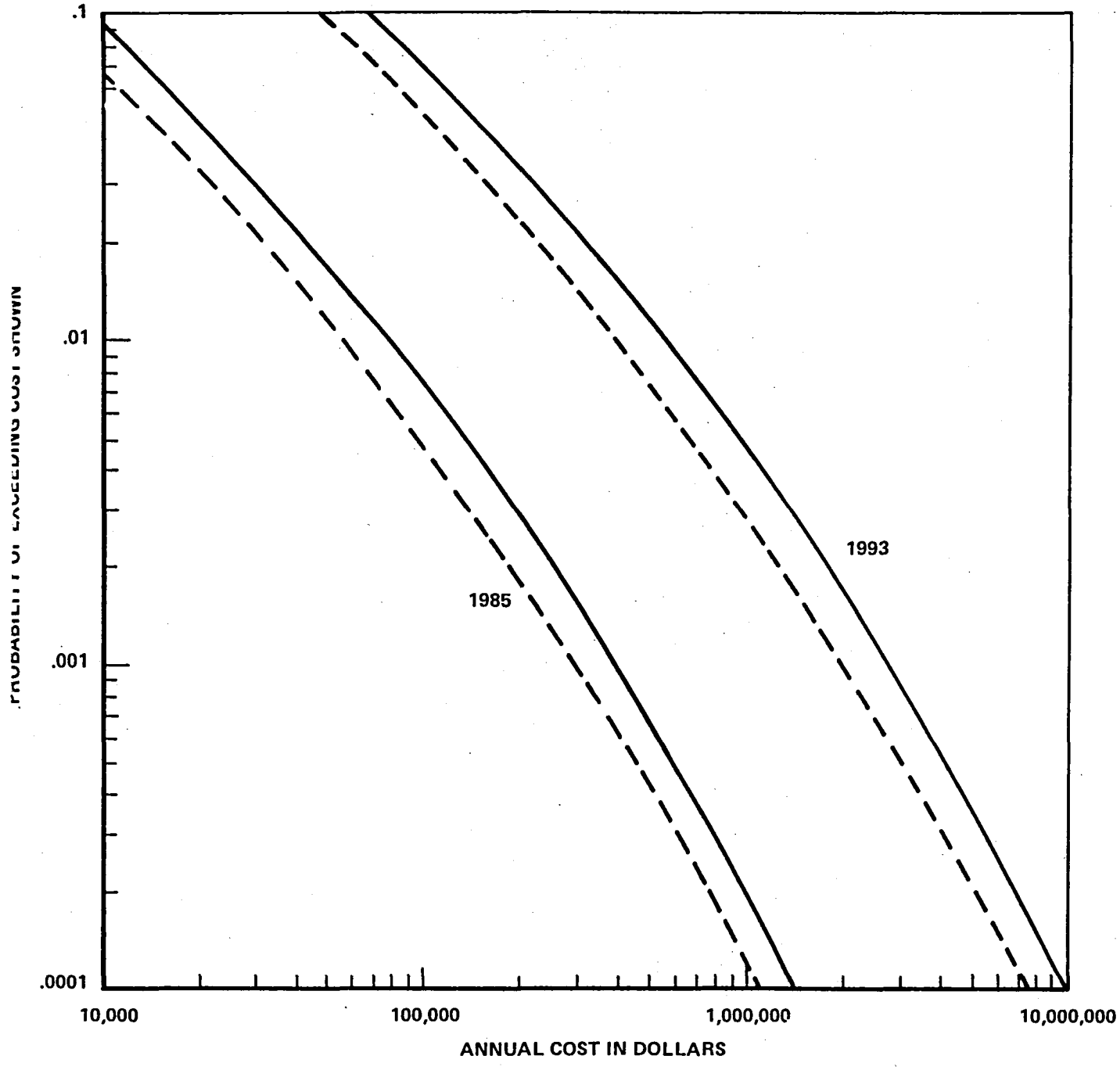

FIGURE 11.1. NATIONAL RISK PROFILES PREPARED BY CONVOLUTION OF NINE INDIVIDUAL AIRPORT ACCIDENT-COST PROBABILITY DISTRIBUTIONS ADJUSTED TO ACCOUNT FOR ALL U.S. AIR CARRIER OPERATIONS

-----Number of convolutions adjusted for population and traffic
_____Each distribution convoluted four times

The convolution described above does not take account of the differences in risk that might be related to size of airport and surrounding industrialization. We, therefore, used the nine airport-urban complex combinations in a more structured approach. With the exclusion of Atlanta, Philadelphia, and Miami, all of the airports are characterized as large, both in number of operations and in adjacent population. Each is in a Standard Metropolitan Statistical Area with more than 2,000,000 population. Each had more than 150,000 operations in 1976. This group, because of the obvious concentration of risk, received most of our attention in the conduct of the individual airport risk assessments. In performing the second national risk convolution several of the airports were used twice (all except O'Hare/ Chicago and Lambert/St. Louis) in order to account for all operations in this number of operations - population group.

The remaining airports represent different population concentrations and/or number-of-operations categories. Atlanta and Miami are both busy airports, with more than 150,000 operations a year but are adjacent to metropolitan areas with populations only between one and two million. Philadelphia is in a metropolitan area with a population greater than two million but has less than 150,000 operations a year. The probability distributions for the risk at these three airports were used nine times in order to simulate the impact on the national risk of the remainder of the national air carrier traffic. The resulting number of air carrier operations is equal to all operations not previously accounted for by the busier airports serving larger population centers treated in the preceding paragraph. These airports are thus proxies for smaller airport-population center combinations. The resulting risk profiles for 1985 and 1993 are also shown in Figure 11.1. The expected annual financial impact due to graphite fiber incidents associated with aircraft accidents in the United States are tabulated in Table 11.1 for the different cases described here.

For purposes of comparison with other results in the risk assessment field we have superimposed the ORI 1993 national risk profile (9 airports convoluted four times) on the results published by the U.S. Nuclear Regulatory

TABLE 11.1

ESTIMATED U.S. ANNUAL IMPACT AIRCRAFT-
ACCIDENT RELATED GRAPHITE FIBER INCIDENTS

CONVOLUTION RESULTS USING NINE AIRPORT RISK PROFILES
TO ACCOUNT FOR ALL U.S. AIR CARRIER OPERATIONS

CONVOLUTION DESCRIPTION		1985	1993
Each airport convoluted four times	Mean	$ 3,499	$ 38,541
	Standard deviation	$ 32,423	$ 242,946
Number of convolutions adjusted by airport-city size category	Mean	$ 2,556	$ 27,709
	Standard deviation	$ 26,070	$ 173,560

Commission[2] (The Reactor Safety Study, sponsored by the U.S. Atomic Energy Commission, performed under the independent direction of Professor Norman C. Rasmussen of the Massachusetts Institute of Technology) in Figure 11.2. The results indicate that the national graphite fiber risk appears to be somewhat below that which the nuclear reactor safety study group estimated for 100 nuclear power plants, at least over the damage range for which the results are plotted. Apparently the graphite fiber risk is somewhat higher for lower values of property damage, which in the ORI case is the sum of business dislocation and household impact. Among the approximations made by the ORI team, we note that our 1993 calculations were carried out in 1976 dollars, using 1976 Gross Domestic Product data. The use of constant dollars is reasonable in order to make results interpretable in the current time frame. The Gross Domestic Product was not adjusted in order to facilitate the 1985-1993 comparisons. Once we consider comparisons with other investigators, however, it would probably be desirable to adjust these inputs for the time frame of interest.

STATISTICAL CONFIDENCE LIMITS

The calculation of statistical confidence limits for the convoluted probability distributions, given those for the individual risk profiles, is by no means a trivial problem. In this section we present a brief derivation of an approximate form for the calculation which we have used. It depends on standard methods used in similar problems, as well as particular insights unique to the problem at hand.

As in the derivation of the expression for the convolution, first assume that the probability distribution is a discrete function. This does not affect the generality of the result but does simplify the notation; it is equivalent to allowing the dollar value of the annual impact to take on only discrete values, rather than considering it a continuous variable. The probability that the sum of the costs at two cities is equal to $r\Delta\$$ dollars

---

[2] U.S. Nuclear Regulatory Commission, Reactor Safety Study: An Assessment of Accident Risks in U.S. Commercial Nuclear Power Plants, Wash-1400 (NUREG-75/014) October 1975.

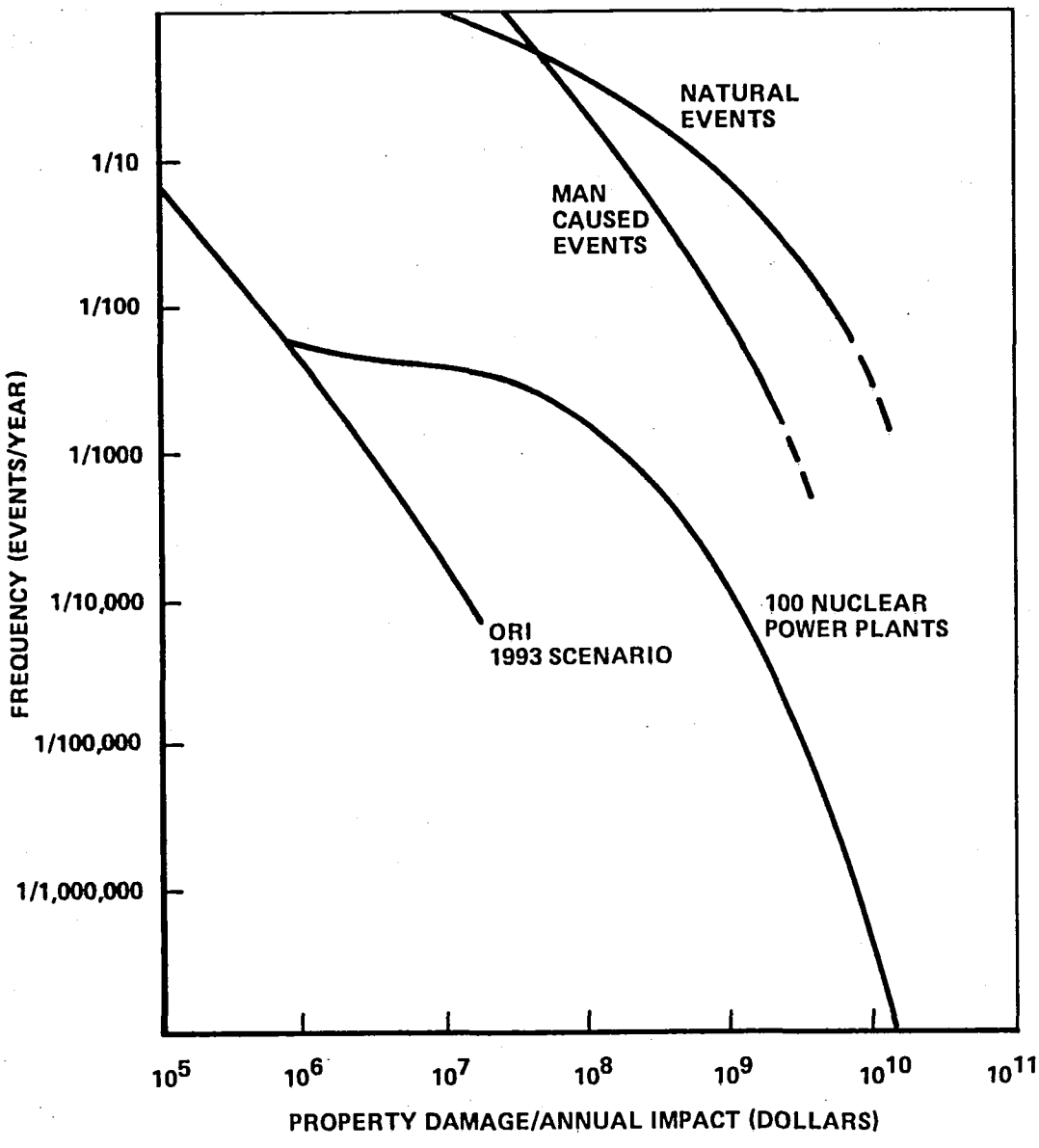

FIGURE 11.2. COMPARISON OF RISK PROFILES -
NATIONAL RISK PROFILE ("ORI") vs.
RESULTS PUBLISHED BY U.S. NUCLEAR REGULATORY COMMISSION*

*U.S. Nuclear Regulatory Commission, op. cit.

is given by Equation (11.1) which represents the result of the convolution of the probability distributions for the two airports. Now invoke several features of the problem at hand. The dominant factor in the analysis of the airports reported earlier in this document is that the probability of the cost being zero in any year is very large compared to the probability associated with any other cost. This is due, as noted earlier, to the fact that an aircraft accident accompanied by fire is a relatively rare event at any one airport. This can be expressed as:

$$a_0 >> a_i \quad \text{for } i>0$$

and

$$b_0 >> b_j \quad \text{for } j>0.$$

As long as the number of terms in Equation (11.1) is finite, the sum of terms of the form $a_n b_{k-n}$ for $n>0$ is small compared to the sum of $a_0 b_k$ and $a_k b_0$. This leads to the following approximation for c_r:

$$c_r \approx a_0 b_r + a_r b_0 \tag{11.2}$$

Since the cost probabilities at each city fill the entire sample space:

$$a_0 = 1 - \sum_{i=1} a_i$$

and

$$b_0 = 1 - \sum_{j=1} b_j.$$

Each sum is equivalent to the probability of having at least one accident in a year at each airport, typically of the order of magnitude of 1/100. Taking advantage of this fact, the estimate of the probability that the total cost at the two airports is equal to $r\Delta\$$ dollars may then be written:

$$c_r \approx a_r + b_r \tag{11.3}$$

The risk profile shows the probability that the cost equals or exceeds a given value in a year. Define the probability of this event as:

$$C_r = P\ (S \geq r\Delta\$) = A_r + B_r.$$

Define the estimate of C_r by the symbol $\hat{C}_r$. In Chapter X it was shown that the variance of $\hat{A}_r$ and $\hat{B}_r$ may be estimated by:

$$\text{var } \hat{A}_r = [\hat{A}_r\ (1-\hat{A}_r)]\ /\ n$$

$$\text{var } \hat{B}_r = [\hat{B}_r\ (1-\hat{B}_r)]\ /\ m$$

where n and m are the number of trials (replications) used to estimate A_r and B_r, respectively. Since the accidents at two or more airports are assumed to be independent events, that is, uncorrelated, we may write the variance of $\hat{C}_r$ as:

$$\text{var } \hat{C}_r = \text{var } \hat{A}_r + \text{var } \hat{B}_r$$

If M is defined as the smaller of n and m, then

$$\text{var } C_r \leq (1/M)\ [\hat{A}_r\ (1-\hat{A}_r) + \hat{B}_r\ (1-\hat{B}_r)]$$

and introducing an approximation of the same order as previously employed,

$$\text{var } C_r \approx (1/M)\ \ [\hat{A}_r + \hat{B}_r]$$

$$\text{var } \hat{C}_r \approx \hat{C}_r\ /\ M \qquad (11.5)$$

Equation (11.5) applies to two airports. To extend the result to the more general case of n airports consider the expression for three airports. Let

$$D(s) = \Sigma d_k s^k$$

be the generating function for the sequence $\{d_k\}$ representing the probabilities at the third airport, in exact analogy to the relations presented earlier. The convolution operation is associative and commutative. The probability

that the sum of the costs of accidents at all three airports is equal to r can be written:

$$e_r = d_0c_r + d_1c_{r-1} + d_2c_{r-2} + \ldots. d_{r-1}c_1 + d_rc_0$$

as in Equation (11.1). Substituting for the c's from Equation (11.2) this expression can be written:

$$e_r = d_0 (a_0b_r + a_rb_0) + d_1 (a_0b_{r-1} + a_{r-1}b_0) + \ldots. d_{r-1} (a_0b_1 + a_1b_0) +$$

$$d_ra_0b_0$$

Introducing the same approximation used previously in deriving Equation (11.3) provides the following approximate results:

$$e_r \approx d_0a_0b_r + d_0b_0a_r + a_0b_0d_r$$

and

$$e_r \approx a_r + b_r + d_r \qquad (11.6)$$

Equation (11.6) implies, by induction, that the expression (11.5) can be used to estimate the statistical confidence limits for the convolution used to generate the national risk profile. It is relatively conservative to assume further that the distribution of estimates about the true population values of the probabilities are normally distributed. It can then be stated that 95 percent of the values resulting from the simulation runs lie within $\pm 2\sqrt{\hat{C}_r/M}$ of the actual computed value, as shown in Figure 11.3 for M = 50,000. These results are statistical confidence limits for different values of the risk probability, and are related only to the confidence associated with the Monte Carlo sampling errors. They do not reflect uncertainty in the input parameter values; some insight into input error effects can be gained by examining the sensitivity analyses reported in Chapter X.

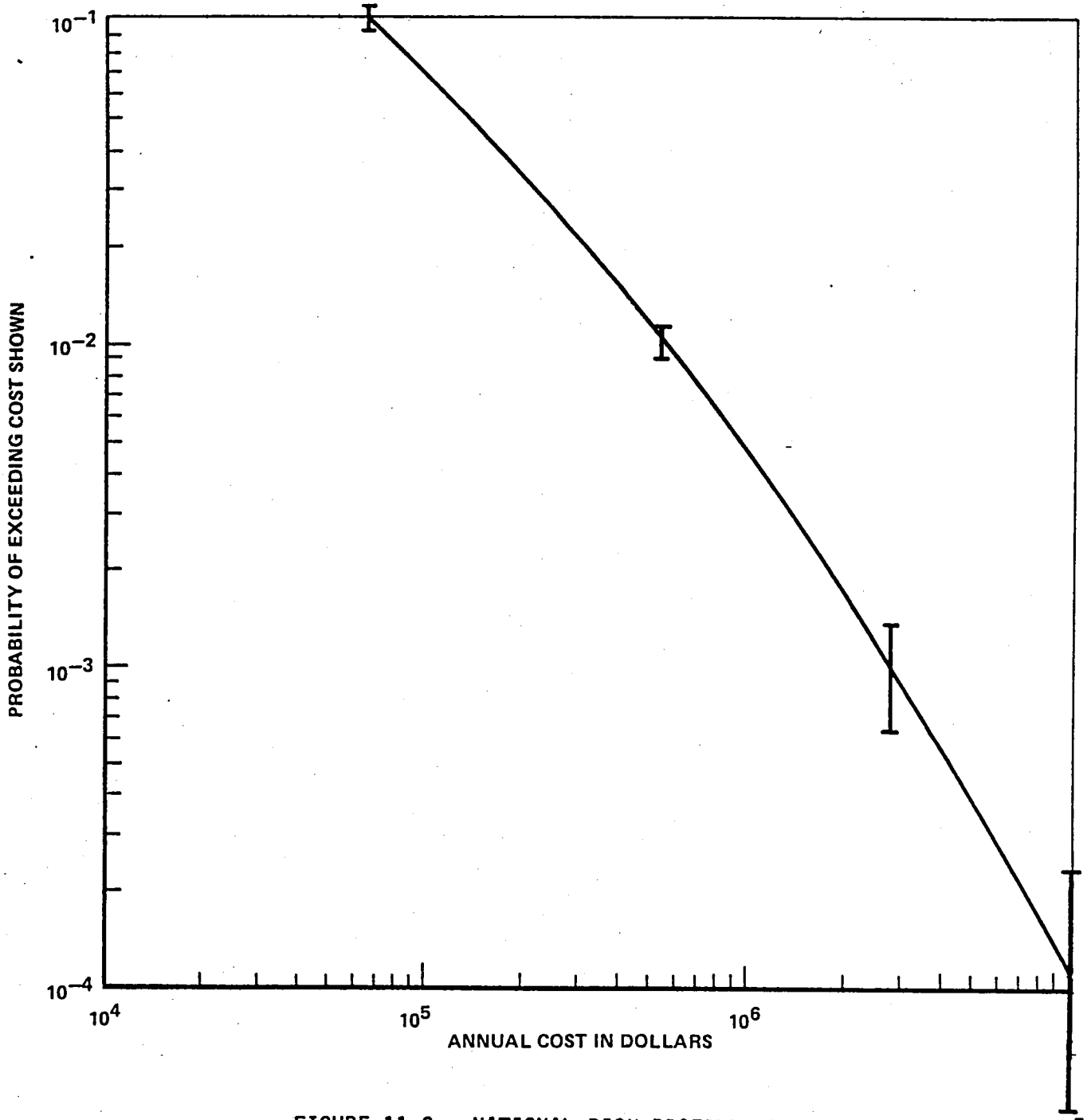

FIGURE 11.3. NATIONAL RISK PROFILE: 9 AIRPORTS CONVOLUTED 4 TIMES; 1993 SCENARIO SHOWING 95% STATISTICAL CONFIDENCE LIMITS*

*Non-Simultaneous

APPENDIX A

COMPUTER PROGRAM DOCUMENTATION

(Bound Separately)

APPENDIX B
BASELINE FACILITY DESCRIPTIONS

INTRODUCTION

This appendix summarizes the facility descriptions used as a baseline for developing the penetration values, failure constants, and failure models described in Sections VI and VII of this report.

Methods

Facility definitions for this study are based on the U.S. Census Standard Industrial Classification (SIC) Code numbers. These SIC codes provide a standardized basis for defining facilities in a manner that is directly relatable to demographic areas for which Census data are readily available.

The types and configurations of equipments which most generally typify a facility identified by a specific SIC number were obtained through a broad literature search supported by a limited number of site visits, augmented by discussions with representatives of various industries. The equipment types and their specific components identified by the SIC number with each SIC facility are then compared against the equipment types and designs contained in failure threshold data from the Ballistics Research Laboratory (BRL). Exposure threshold values which appear to best fit the situation are assigned.

Buildings and enclosures are specified for typical facilities and equipments; these were compared with air conditioning and ventilation standards published in several handbooks. Note that the actual building size is not

particularly important as long as design is in accordance with standard practice, since the standards are aimed at maintaining ventilation constant in terms of air changes per hour regardless of the building size.

Facility descriptions were obtained from the sources listed in Section VII. Air conditioning and ventilation standards and practices were obtained from the Handbook of Air Conditioning System Design[1] and the Standard Handbook of Mechanical Engineers[2].

Problems and Assumptions

There are, of course, a wide range of facilities, in terms of size and type, of interest to us in this risk assessment investigation. There is also a wide range of types of equipment from facility to facility, and even within facilities of the same type. In some instances there may be greater differences between equipments and designs within facilities characterized by the same SIC code number than between those with different SIC code numbers. For example, the circuits used for relay-type telephone switching are very similar to those used for supervisory controls in transportation and utilities, and not at all similar to the electronic switching used in newer telephone central offices.

The only approach considered practical in this study was to define as "typical" facilities believed to best represent the facilities identified by each SIC code number during the time frame of interest, and to base penetration values and facility failure computations on these "typical" facilities.

A facility is defined on the basis of those equipments or components which appear to dominate the facility's vulnerability to carbon fiber penetration and subsequent equipment failure. A modular approach was used, synthesizing facilities from a few generic types of equipment for which mean exposure-to-failure values are reasonably well established. The relationship between

---

[1] Carrier Air Conditioning 6. Handbook of Air Conditioning System Design, McGraw-Hill Book Co., 1965.

[2] Baumeister and Marks, Standard Handbook for Mechanical Engineers, McGraw-Hill Book Co., 1967.

facilities of interest and the equipments for which generic failure data are available is very loose. The published value for the equipment which most closely represents the equipment of interest was used. In many instances the equipment of interest is assumed equivalent to a multiple of the generic components (e.g., a process control station might be assumed equivalent to 10 of the TTL-PC boards for which test data are available, and would then be assumed to be 10 times more vulnerable).

The published failure exposure values are often based on fiber types and sizes, air flow rates, etc., not representative of conditions expected in this analysis. Care was taken to select the most appropriate value possible. Specific assumptions are defined below as they relate to particular facilities.

ELECTRIC UTILITIES

Conventional electric utility stations are considered in this study. It was agreed early in this project that NASA Langley Research Center would investigate the potential vulnerability of nuclear power stations. Electric utilities can be described in terms of the following functions:

- Generation
- Transmission
- Distribution

These functions are performed by the following basic types of subsystems:

- High voltage
- Control
- Communications

Electric utility facilities consist of a network of generating stations, transmission (switching) stations, and distribution stations. Often these three functions are combined in a single station.

System Configurations

Figure B.1 illustrates a typical configuration of generators (circles), circuit breakers (boxes), transformers and buses, and transmission lines in a power system. Secondary stations are discussed under industries, hospitals, etc. Generators are usually arranged in the generator--step up transformer--breaker--high voltage bus segment module as shown so that loss of a single

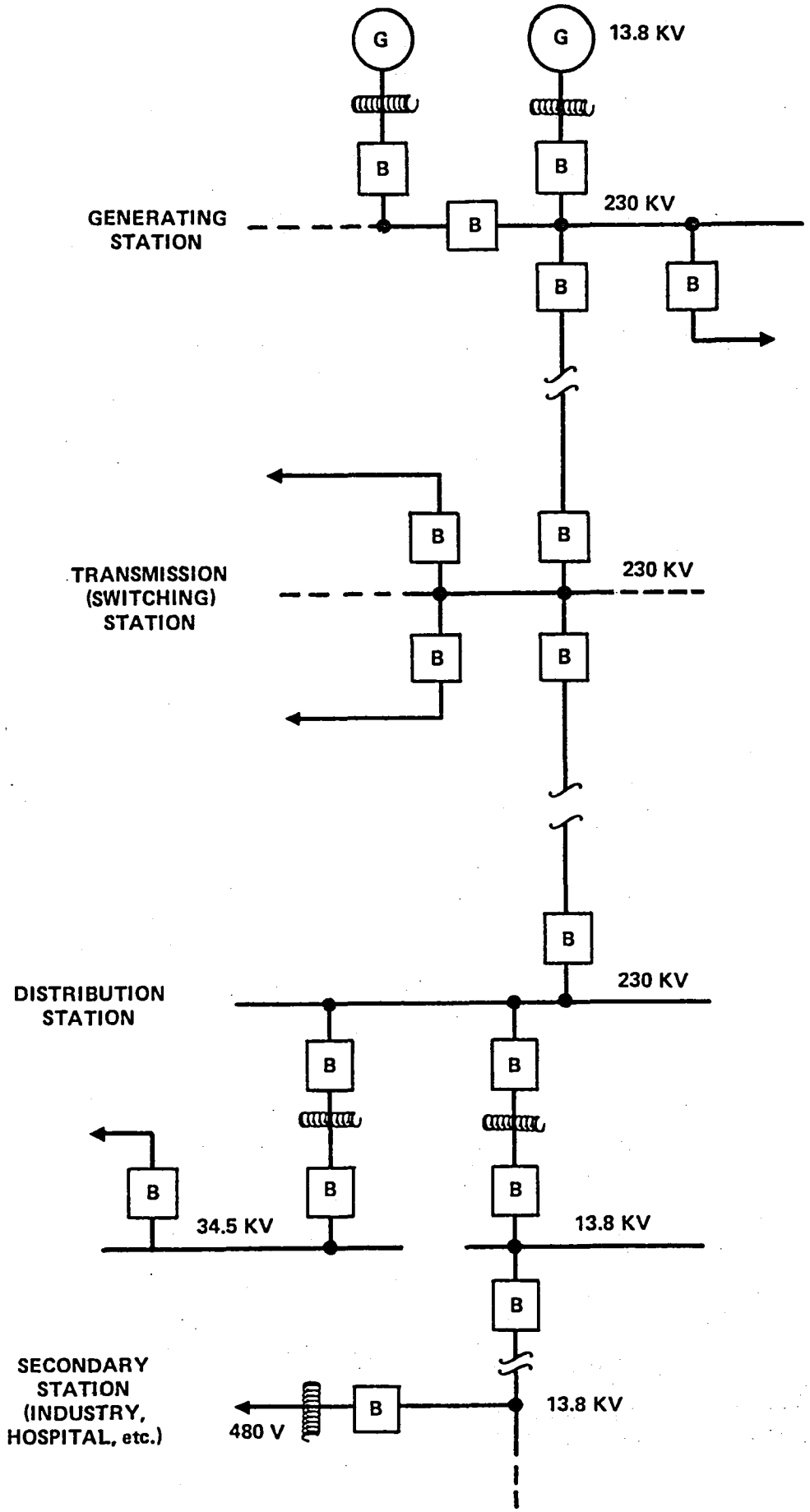

FIGURE B.1 ILLUSTRATION OF A POWER SYSTEM

generator unit does not result in the loss of a multi-generator station. Breakers are arranged to control, protect, and isolate each bus segment, each transmission line and each major transformer, as indicated.

Station Configurations

Figure B.2 illustrates a typical utility station or substation configuration. Communications and common control equipment are common to all station functions. High voltage bus structures and their associated transformers and breakers are usually located outside the station building. Each bus section, each generator, etc. has its own associated controls in a section of the switchgear panel inside the station building (or in a special enclosure when located outside in a unit type of substation).

The high voltage subsystem at each station consists of high voltage buses, breakers, transformers, and high voltage transmission lines together with their associated disconnect switches, fuses, insulators and bushings. Insulators and bushings are the most vulnerable equipment from the standpoint of carbon fibers.

Generators, as well as transformers and breakers and other high voltage equipment such as rotary converters, are well sealed and often pressurized so that they can be neglected as far as their vulnerability to carbon fibers is concerned.

Switchgear Controls. Generators and breakers are controlled and protected by means of switchgear consisting of switches, electromagnetic and solid-state relays, terminal boards and associated wiring. Most breaker tripping circuits are 125 Volts DC although some stations use 250 Volts DC. Switchgear panels at generating stations may also contain field exciters (e.g., thyratrons) operating at 125, 250, or 375 Volts DC. Specific switchgear panels or panel sections are usually assigned to each generator, each transmission line, and each bus and associated transformers so that switchgear failures tend to affect only their associated portions of the station. Switchgear is highly standardized so that panels are quite similar whether for use with generators, transmission lines, or buses and associated transformers.

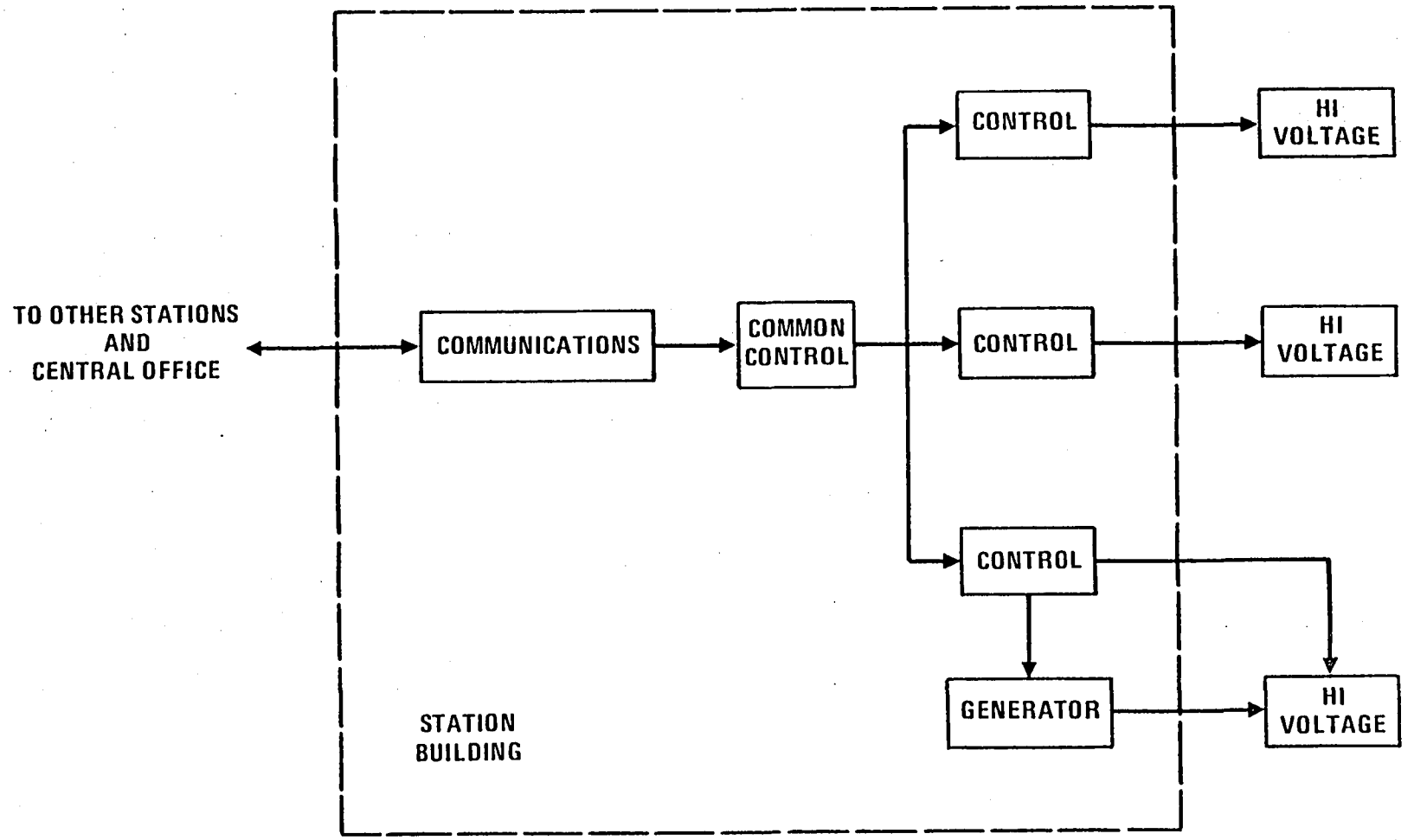

FIGURE B.2. ILLUSTRATION OF A UTILITY STATION CONFIGURATION

Common controls consist of interface units used to input supervisory controls to the switchgear panels and to monitor output signals from the panels to produce alarms etc. for transmission via the communications system.

Communications are used for remote control of unmanned stations, to obtain load management and to obtain better system coordination in the event of system faults. The communications subsystem is particularly important in restoring a system after a major outage. Communications systems may use older telephone (relay) type or newer solid-state supervisory controls. Newer stations may have solid-state minicomputers for A/D conversion, interface with station controls, etc. TTL logic is typically used. Communication links may be via telephone lines, microwave, or via carrier on HV transmission lines.

Failure Parameters

The methods used to estimate mean exposure-to-failure values are described in this section. Each generator unit, each transmission line, and each bus segment/transformer is assumed to consist of a high voltage module, a switchgear panel, and associated communication interface. The communications/common control subsystem is assumed to be associated with the entire station. No attempt is made to account for the length of exposed transmission or distribution lines.

- All high voltage modules (or bays) are assumed to be similar. The vulnerability of each high voltage module, including transformer bushings, is assumed equal to the average values obtained by BRL at 25 KV. Vulnerability is assumed constant with voltage since the design factors of insulators, gaps, etc., are intended to compensate for voltage: $\overline{E} \cong 1.6 \times 10^7$ [3]
- All switchgear panels are assumed to be similar. The vulnerability of each switchgear panel is assumed equal to the generic value for relay and control logic from BRL: $\overline{E} \cong 7 \times 10^5$
- The vulnerability of each control interface assumes use of a single TTL printed IC board: $\overline{E} \cong 7 \times 10^8$
- The station communication system is assumed to consist of a processor equivalent to the PDP-8 ($\overline{E} \cong 1 \times 10^7$) together with

[3] All values are expressed in fiber-seconds/meter^3 unless otherwise noted.

a microwave transmitter-receiver ($\overline{E} \gtrsim 1 \times 10^7$), for an overall vulnerability $\overline{E} \gtrsim 5 \times 10^6$.

Buildings and Enclosures

Typical substation buildings are small sheet metal buildings with industrial type doors and windows with weatherstripping. They are typically air conditioned with window units to provide 2 or 3 air changes per hour. Switchgear panels are housed in standard metal switchgear panels without forced ventilation (see, for example, Westinghouse Construction Specifications Cat. 55-000, 57H Edition, 1978-1979). Enclosures for common controls and communications can be neglected because they are already accounted for in failure testing.

INDUSTRIAL PLANTS

From the standpoint of vulnerability, an industrial plant can be defined in terms of:

- Process controls
- Power
- Communications (will not be critical in many types of industries).

Although there is a large variety of types and sizes of industrial plants, modularization of process controls has been developed to the degree that similar equipment modules may be added together to handle nearly any kind and size of application. In the paragraphs below, generalized configurations and equipment modules are first described, followed by pertinent detailed applications.

Typical Configuration (and Notes on its Application)

Figure B.3 shows a typical arrangement of power inputs, communications, central computer, controllers, and machine stations in a highly automated industrial plant. This type of configuration is found in industrial systems of all types ranging from steel mills to bakeries, printing plants, and test facilities. Each of the major elements in this typical configuration is discussed in turn here:

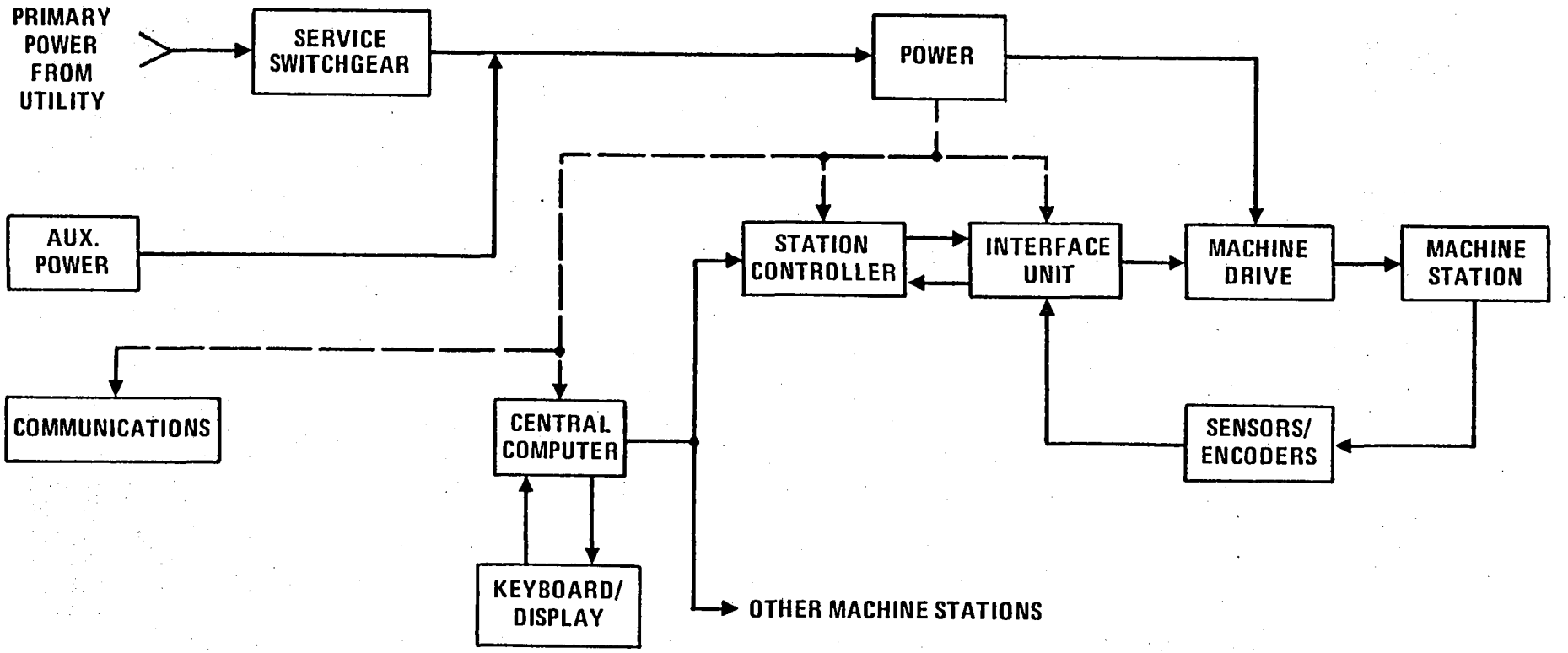

FIGURE B.3. TYPICAL INDUSTRIAL PLANT CONFIGURATION

Power for a large industry may include a substation equivalent to a major utility distribution substation with primary voltage in the major transmission (e.g., 230 KV) range. Smaller industries may have a secondary unit-type substation with primary voltages in the 13.8 KV to 34.5 KV range. Heavy industries may require secondary voltages as high as 13.8 KV. Typical process industries require secondary voltages of 120 V, 208 V, and 480 V AC.

The outside (high voltage portion of an industrial power substation) is treated as part of the public utility system even though it may be owned by either the utility or by the industrial plant. The failure of that high voltage part of the power system is included in the failure calculation for the primary power system (SIC 49). Primary power enters the larger industrial plants through service switchgear located inside the plant.

Service Switchgear includes step-down transformers, enclosed breakers, contactors, relays and manual switches. Service switchgear receives the primary power and delivers 120 V, 208 V, 408 V, and sometimes 480 V and 600 V to the plant or installation.

Distribution Panels. For small, low energy-consuming industries, primary power may be received directly at 120/240 V and enters the industry through a distribution panel consisting of breaker-switches and fused feeders.

Auxiliary Power. Most industrial plants are assumed to have engine-driven generators to provide power in the event of failure to the primary power. Small light industries are assumed to have no auxiliary power.

Central Computers. These are used in highly automated industries to provide overall (executive) control of the process. Redundant computers and keyboard/display terminals are often used to minimize outage time in the event of failures.

Station Controllers. Minicomputers or microprocessors are used to provide local processing at each machine station. These may be used in conjunction with a Central Computer or may stand alone.

Interface Units. In 1975 the IEEE adopted a standard module for the interface unit and station controller called CAMAC. (IEEE Spectrum, April 1976). These modules provide a flexible interface between nearly any type of industrial

process and any type of central computer. Future systems can be expected to have this type of modularity. The CAMAC interface unit can accommodate a large variety of available connectors, buffers, clocks, registers, readers, displays, etc. while the controller module can accommodate numerous minicomputers such as the PDP-8. Examples of plants using this concept are an aluminum plant in which 23 CAMAC modules control 45 preheat furnaces, a computerized steel slab casting mill, and a General Motors test facility.

A typical variation on the above scheme is the use of a low-cost programmable controller at each machine station without a central computer. Originally developed for control of machine tools and assembly operations, programmable controllers are currently in use in chemical, petrochemical, food processing, pharmaceutical, paper, and other industries.

Processing Components. These make heavy use of solid state TTL but these are being replaced with CMOS because of better noise immunity and lower power requirements. Programmable controllers and interface units often use microprocessor chips.

Machine Drives and Sensor/Encoders. These cannot be easily typified since they are designed to fit the particular type of machine station. Machine drives will include components such as motor controls, servos, injectors, solenoids, etc. Sensor/encoders will include components such as pressure or temperature transducers, motion encoders, etc.

When machine stations perform low energy precision operations for material handling, milling machines, etc., it is assumed that machine drive functions will be performed by servo systems. When machine stations consist of heavy duty motors (as in rolling mills) it is assumed that machine drive functions will require high voltage motor contactors and controls. High voltage switchgear is required for this.

Small Industrial Plants

Small industrial plants are characterized by machine stations with small or medium-duty motors and/or servo units. These facilities are assumed to have no auxiliary power, and no central computer or displays. The SIC codes listed below are assumed to fall into this category even though these

SIC codes are sometimes characterized by large highly automated facilities. Specific plants (identified by SIC number) typically have the following characteristics:

- SIC 20 - Food processing plants are assumed to have machine stations consisting of station controllers, interface units, and servos together with small motors. Power enters through service switchgear.
- SIC 23 - Apparel plants are assumed to have machine stations consisting of small motors run directly from station controllers. Primary power is assumed to be received at 115/230 V and goes directly into low voltage distribution panels without use of service switchgear.
- SIC 24 - Lumber and wood products plants are assumed to have machine stations consisting of medium duty motors and high voltage control switches (used to drive saws, planers, and shapers), without use of station controllers. Power entrance is through service switchgear.
- SIC 27 - Printing and publishing plants are assumed to have machine stations consisting of small motors run directly from station controllers.
- SIC 38 - Instruments Plants are assumed to have machine stations consisting of controllers, interface units, and servos. Primary power is assumed to be received directly at 115/230 V and to go directly to power distribution panels without use of service switchgear.

Large Light Industries

Large light industries are similar to small light industries except that they are assumed to have auxiliary power available. All are assumed to receive primary power through service switchgear. Machine stations are as follows:

- SIC 22 - Textile mill products plants are assumed to have work stations consisting of station controllers, interface units, and servo units, together with small motors which are neglected for failure calculation purposes.
- SIC 25 - Furniture plants are assumed to have work stations consisting of high voltage controllers and motors driving dimension saws, planers, shapers/routers, and sanders, without the use of station controllers (non-automatic).
- SIC 34 - Fabricated metal plants are assumed to have work stations with line controllers, high voltage motor control and motors driving machine tools, presses, etc.
- SIC 35 - Machinery plants are assumed to have work stations similar to those of SIC 34.
- SIC 36 - Electric and electronic equipment plants are assumed to have work stations consisting of line controllers, interface units and servos together with small motors.

Heavily Automated Industries are assumed always to receive primary power through service switchgear and to have central computers together with keyboard/displays exercising executive control over all lines. Machine stations are as follows:

- SIC 26 - Paper and allied products plants are assumed to have work stations consisting of a station controller, high voltage motor controls and heavy duty motors.
- SIC 28 - Chemicals and allied products factories are assumed to have work stations dominated by servo systems (consisting of station controller, interface unit, and servo circuits).
- SIC 29 - Petroleum and Coal product plants are assumed to be similar to those of SIC 28.
- SIC 30 - Rubber and plastic product plants are assumed to be similar to those of SIC 28.
- SIC 33 - Primary metal products are assumed to have work stations dominated by high voltage motor/control (consisting of station

controller, motor control, and heavy duty motors), driving rolling mills, etc.

- SIC 37 - Transportation equipment factories are assumed to have work stations similar to SIC 28. (Highly automated milling machines, etc.)

Failure Parameters

Mean exposure-to-failure values (fiber-seconds/meter^3) for the equipment identified in this section are:

- Power service switchgear, based on generic values for relay and control logic: $\overline{E} = 7 \times 10^5$
- Power distribution circuits, based on generic AC power distribution values: $\overline{E} = 1.5 \times 10^6$
- Auxiliary power, based on 220-440 V engine-generator tests: $\overline{E} = 2.2 \times 10^6$
- Central computers, based on LSI-11 average over various tests: $\overline{E} = 5 \times 10^5$
- Keyboard/displays, based on TTL and CMOS oscilloscope: $\overline{E} = 4.5 \times 10^5$
- Station controllers, based on PDP-8 minicomputer tests: $\overline{E} = 1 \times 10^7$
- Interface units, based on use of power supply modules[4] which is probably the worst case: $\overline{E} = 1.4 \times 10^7$
- Servo Units, based on generic servo motor circuits (including enclosure): $\overline{E} = 1 \times 10^8$
- High-Voltage motor control, assumed to be dominated by H.V. power supply: $\overline{E} = 1.4 \times 10^7$
- Motors are assumed to have negligible vulnerability to carbon fibers: $\overline{E}$ = Infinity

---

[4] Used when H.V. is required for X-ray measurements, etc.

Buildings and Enclosures

Industries are assumed to be in factory-type buildings with weather-stripped doors and windows. Small light industries are assumed to be located in medium-sized equipment buildings ventilated to provide 3 or 4 air changes per hour. Large industries are assumed to be located in large factory buildings, with 1 or 2 air changes per hour. Central computers are assumed to be located in a separate equipment room inside the factory building (but with an exterior wall). Service switchgear is located in standard metal clad enclosures without forced air. High voltage controls and interface power supplies are assumed to be located in standard metal clad switchgear cabinets with forced air cooling. Enclosures for all other equipment are accounted for in the failure threshold values. Power and auxiliary power are assumed to be located in unfiltered utility rooms.

BUSINESS SERVICES

Typical Configurations

System Architecture for business service facilities is very similar to that found in industrial process controls. Like industrial process controls, business service systems are found in a variety of sizes and configurations, although they are built up from the same general types of modules.

Typical retail or banking systems consist of a small computer, with or without external storage, interconnected through data interface units (such as multiplexers) to distributed keyboard/display stations.

Typical data processing centers comprise one or more large computers with external core storage and program/control consoles together with peripheral units such as disks, tapes, line printers, and card readers. The central computers are often connected through input/output processors to remote minicomputers and keyboard/displays, to teletype lines, and sometimes to microwave data links. Data processing functions are sometimes distributed to several minicomputers, for example, using a minicomputer together with a keyboard/display console at data input stations. With this arrangement, a computer failure will affect only a portion of the data system.

Power for data processing systems is usually directly from the building distribution circuits. A battery operated inverter is often used to provide uninterrupted power during power outages of less than about 8 hours. Large central computer facilities will usually have auxiliary power; however, local systems in banks, brokerages, insurance offices, may not have auxiliary power.

Failure Parameters

Mean exposure-to-failure value thresholds are estimated to be:

- Converters, based on discrete PC rotary inverter: $\overline{E} = 1 \times 10^6$
- Central Computer, based on LSI-11 test data: $\overline{E} = 5 \times 10^5$
- Keyboard/Display, based on TTL + CMOS scope: $\overline{E} = 4.5 \times 10^5$
- Processor, based on PDP-8 tests: $\overline{E} = 1 \times 10^7$
- I/O Interface, based on use of TTL PC boards: $\overline{E} = 1 \times 10^7$
- Communications, based on RF trans/receiver test data: $\overline{E} = 1 \times 10^7$ per channel.

Buildings and Enclosures

All computing equipment is assumed to be housed in an equipment room with one exterior wall. Power and auxiliary power equipment are assumed to be located in air conditioned and filtered utility rooms.

AIR TRANSPORTATION

Air traffic control systems are of prime interest to this study and are used to represent the failure probability of air transportation.

Air traffic controls are divided into:

- Enroute controls
- Terminal/airport controls.

Enroute controls consist of enroute centers (ARTCC's) at Albuquerque, Anchorage, Atlanta, Boston, Chicago, Cleveland, Denver, Fort Worth, Great Falls, Houston, Indianapolis, Jacksonville, Kansas City, Los Angeles, Memphis, Miami, Minneapolis, New York, Oakland, Salt Lake City, Seattle, and Washington, D.C. (Leesburg, Va.). Each enroute center is divided into about 15-20 sectors. The ARTCC has a central computer with redundant backup. Each sector has a

radar console/display and a data terminal. The ARTCC's are supplied with radar data from 97 long range (200 mile) L-band radars distributed so as to cover the continental U.S. (actual locations and ARTCC assignments are listed in the ATS Fact Book). Radar-ARTCC data is via C-band microwave links. VHF and UHF voice communications coverage is via about 450 remote transmitter/receiver stations (RCAGS) connected to ARTCC's by telephone voice lines. (Actual locations and ARTCC assignments are listed in the ATS Fact Book).

Enroute Nav-aid includes about 1000 VOR stations and 850 RF beacons (low and medium frequency) distributed along the airways (actual locations shown on aeronautical charts). There are also about 320 flight service stations with about 600 remote communications sites and 170 direction finding facilities (locations are shown in the ATS Fact Book). There are about 500 airports with towers, about 200 of these having radar approach control facilities (including about 25 military facilities). There are about 580 Instrument Landing Systems (ILS).

A typical airport approach control is divided into 4 or 5 sectors to cover various feeders, final approaches, and departures. Each sector has radar console/display and a data terminal located in separate RAPCON room and connected to the terminal control (e.g., ARTS-III) computer located in the tower equipment room. Sector positions are often combined during light traffic periods. Radar data is provided by an airport surveillance radar (ASR) which operates at S-band and is located at the airport. Air-ground communications is via VHF and UHF with transmitters located in remote vans on the airport and with receivers in the tower equipment room.

The tower room has several communications consoles, each of which can handle several VHF and UHF frequencies. A high degree of redundancy is available in the event of a failure to a single console. Major runways have ILS localizer (VHF) and glideslope (UHF) located in vans near the associated runways. Some of the VOR facilities mentioned under enroute Nav-aid are located at major airports.

Other ATC facilities of possible interest at airports include the approach light controls which are currently electro-magnetic.

Typical ATC Configurations

Figure B.4 shows a simplified reliability diagram for terminal ATC.

Power. The terminal building, as well as each facility, such as ILS, has a commercial power source, and each is backed up by an auxiliary engine-generator set. The airport terminal building typically will receive a distribution voltage (e.g., 13.8 KV) from the power company through disconnect switches to a transformer, where it is stepped down to 120/208/408 V and distributed through a switchgear cabinet. The 480 V is distributed to various remote sites where an enclosed self-contained transformer/breaker/controls unit steps this down to voltage required at that site. Automatic transfer switches and automatic engine start are used to restore power during an outage at each site.

Computers. Although no redundancy is shown in Figure B.4, there are various functional redundancies and several levels of degraded modes designed into the computing systems.

Communications. The air-ground transmitters and receivers and voice consoles in the tower and RAPCON were mentioned previously under enroute and terminal controls. There is also vital voice and data communications between the tower and RAPCON and also between the airport and its associated ARTCC. Voice and data communication interfaces are through coordination consoles, switches, and numerous terminal boards in the equipment room. Communications consoles, transmitters, and receivers all have dual redundancy with cross-strapping capability.

Radar. Radar transmitters and receivers have dual redundancy and can be cross-strapped. There is at least dual redundancy with PPI displays with additional displays available during sector sharing operations.

ILS has redundant glide-slope transmitters and redundant localizers.

VORTAC has redundant DME transporters and VOR transmitters.

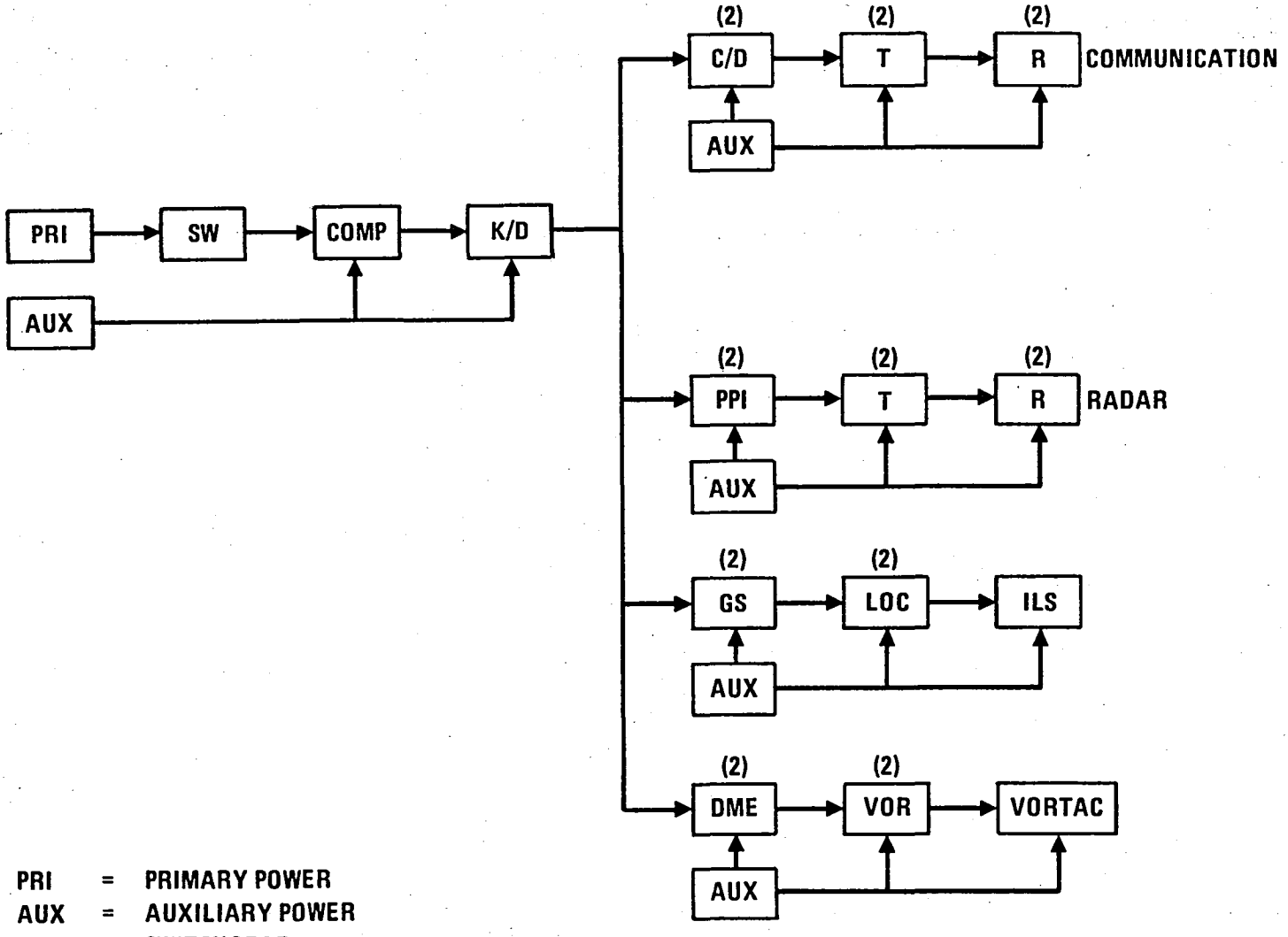

PRI = PRIMARY POWER
AUX = AUXILIARY POWER
SW = SWITCHGEAR
COMP = COMPUTER
K/D = KEYBOARD/DISPLAY
C/D = COMMUNICATIONS CONSOLE/DISPLAY
T = TRANSMITTER
R = RECEIVER
GS = GLIDE SLOPE
LOC = LOCALIZER
PPI = PLAN POSITION INDICATOR
DME = DISTANCE MEASURING EQUIPMENT
VOR = VHF OMNIRANGE
(2) = REDUNDANT UNITS

FIGURE B.4. SIMPLIFIED RELIABILITY DIAGRAM FOR TERMINAL ATC

and terminal controls. There is also vital voice and data communications between the tower and RAPCON and also between the airport and its associated ARTCC. Voice and data communication interfaces are through coordination consoles, switches, and numerous terminal boards in the equipment room. Communications consoles, transmitters, and receivers all have dual redundancy with cross-strapping capability.

Radar. Radar transmitters and receivers have dual redundancy and can be cross-strapped. There is at least dual redundancy with PPI displays with additional displays available during sector sharing operations.

ILS has redundant glide-slope transmitters and redundant localizers.

VORTAC has redundant glide-slope transmitters and redundant localizers.

Failure Parameters

Mean exposure-to-failure values are estimated to be:

- Service Switchgear (listed previously): $\overline{E} = 7 \times 10^5$
- Auxiliary Power (listed previously): $\overline{E} = 2.2 \times 10^6$
- Central computer (listed previously): $\overline{E} = 5 \times 10^5$
- Keyboard/Displays (listed previously): $\overline{E} = 4.5 \times 10^5$
- Transmitters/receivers (listed previously): $\overline{E} = 1 \times 10^7$
- Radar transmitter (no filter), based on test data: $\overline{E} = 3 \times 10^6$
- Radar receiver (no filter), based on test data $\overline{E} = 1 \times 10^6$
- ILS (no filter), based on ASR-3 receiver tests: $\overline{E} = 1 \times 10^6$
- VOR (no filter), based on ASR-3 receiver tests: $\overline{E} = 1 \times 10^6$
- Communications consoles, based on relay and control circuits: $\overline{E} = 7 \times 10^5$

Failure Parameters

Mean exposure-to-failure values are estimated to be:

- Service Switchgear (listed previously): $\overline{E} = 7 \times 10^5$
- Auxiliary Power (listed previously): $\overline{E} = 2.2 \times 10^6$
- Central computer (listed previously): $\overline{E} = 5 \times 10^5$
- Keyboard/Displays (listed previously): $\overline{E} = 4.5 \times 10^5$
- Transmitters/receivers (listed previously): $\overline{E} = 1 \times 10^7$
- Radar transmitter (no filter), based on test data: $\overline{E} = 3 \times 10^6$
- Radar receiver (no filter), based on test data $\overline{E} = 1 \times 10^6$
- ILS (no filter), based on ASR-3 receiver tests: $\overline{E} = 1 \times 10^6$
- VOR (no filter), based on ASR-3 receiver tests: $\overline{E} = 1 \times 10^6$
- Communications consoles, based on relay and control circuits: $\overline{E} = 7 \times 10^5$

Buildings and Enclosures

The terminal power equipment is assumed to be in an unfiltered utility room. Computers, keyboard/displays, PPI scopes, and communications consoles as well as communications receivers are assumed to be located in an equipment room with one exterior wall. Communications transmitters, radar transmitters and receivers, ILS, VOR, and all site located auxiliary power are assumed to be located in equipment vans.

HEALTH SERVICES

Hospitals can be described in terms of the following functions or systems:

- Life support
- Power
- Communications.

Typical Configurations

Hospital configurations can be synthesized from one or more operating rooms, recovery rooms, and intensive care areas where life support equipment might be used, together with primary and auxiliary power facilities and emergency communications facilities. The following equipments are assumed on the basis of that found at a typical suburban or small city hospital:

- Each operating room contains 5-10 medical devices (monitors, defibrillators, etc., similar in construction to GE Series 3000 equipments).
- Each nurse's station has a console/display and small processor.
- Power includes a coordinated secondary substation together with an auxiliary motor-generator set.
- Emergency communication includes a telephone terminal and PBX and a radio transmitter/receiver tied into the municipal emergency communications network (VHF or UHF).

Power. The coordinated secondary substation includes a 13.8 KV primary fused disconnect switch, 13.8 KV to 480/208/120 Volt transformer and 480/208/120 Volt distribution switchgear panels. Auxiliary power is via a 480/208/120 Volt engine-generator with its own control panel.

Life Support equipment typically use TTL and CMOS IC boards for processors together with solid state displays. Those devices vital to life support are sealed for safe use in an oxygen-rich environment.

Failure Parameters

The following exposure-to-failure values are estimated:

- Service switchgear (listed previously): $\overline{E} = 7 \times 10^5$
- Auxiliary power (listed previously): $\overline{E} = 2.2 \times 10^6$
- Processors, based on 10 TTL IC boards: $\overline{E} = 1 \times 10^7$
- Medical monitors, based on TTL + CMOS scopes: $\overline{E} = 4.5 \times 10^5$

Buildings and Enclosures

Service switchgear and auxiliary power units are assumed to be located in an unfiltered utility room. All other equipment is assumed to be located in double-filtered operating rooms or intensive care areas.

TELEPHONE CENTRAL OFFICE

Telephone central offices can be described in terms of the following functions:

- Switching
- Control
- Communications/interface.

Central office equipment ranges from all-relay to all-electronic using one or more combinations of: strowager switches in old stations, crossbar switches, reed relays, discreet semiconductors, minicomputers, and microprocessors.

Crossbar systems are now the most prevalent with a trend toward replacement by electronic switching. Current state-of-art is represented by the No. 4 ESS which can handle about 550,000 long distance calls per hour and has a capacity of 107,000 terminations. ESS systems use ferrite core memories, integrated circuits for logic and switching, TDM switching, etc. Recently developed systems are replacing the conventional 24 V and 48 V switching with 140 Volt D.C. (IEEE Spectrum, Feb. 1976).

Station Configuration

Figure B.5 shows a greatly simplified schematic diagram of a No. 5 crossbar office. Such an office might consist of 10,000 or more line pairs terminating on a line frame. Crossbar switches interconnect these lines to junctors at the rate of 1 junctor for every 5 lines (i.e., 20% of all lines can be served at one time). Other crossbar switches then connect the junctors to trunk lines terminating on a trunk frame. Trunks include operator trunks, outgoing and incoming trunks to other Central Offices, and intra-office trunks to other subscribers in the same office. The crossbar switches also connect their respective lines and trunks through time-shared connectors to time-shared markers and time-shared registers and senders. Markers (about 7 per 10,000

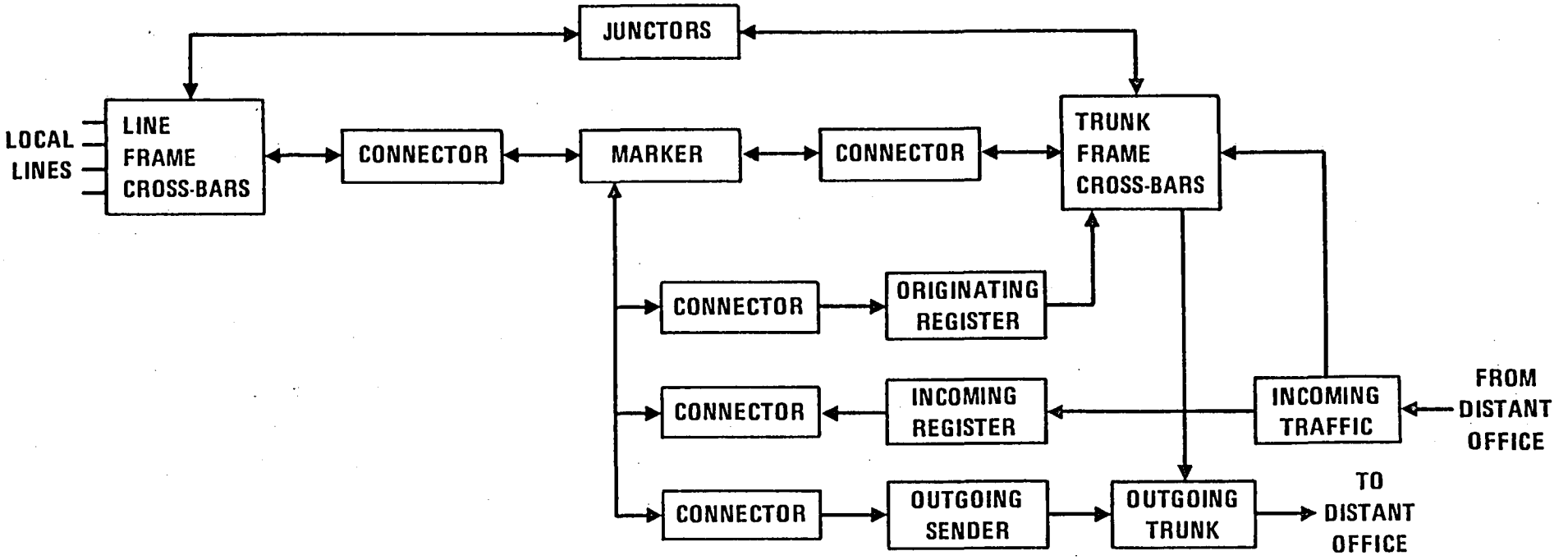

FIGURE B.5. SIMPLIFIED SCHEMATIC OF CROSS-BAR TELEPHONE SWITCHING

Source: Control System Engineering, Goode and Machol, McGraw-Hill Book Co., 1957.

lines) control all selection and switching through the time-shared connectors. Registers and senders provide dialing, ringing, and call termination functions.

A simplified reliability model can be defined by assuming that marker and register circuits are time-shared by a number of lines and that lines are served by a number of parallel crossbar modules (e.g., one 10 x 10 Crossbar module serving 100 lines). Failure effects may be approximately defined as:

- Failure of crossbar switches might put 10 lines or 10 trunks and/or 10 junctors out of service.
- Failure of a marker or its associated connectors would cause about a 15% reduction in capacity (calls/hour). A marker is used about 1/2 sec. for each call.
- Registers are used for about 12 seconds per call. If markers were continually busy at a rate of about 1 second per call it would take 12 registers/markers. Loss of one register would reduce capacity by about 2%.

An even simpler assumption is that all telephone service can be defined by a large number of parallel modules, each consisting of markers + registers + switch modules in series.

Failure Parameters

Mean exposure-to-failure values are estimated as follows:

- Service Switchgear (listed previously): $\overline{E} = 7 \times 10^5$
- Auxiliary power (listed previously): $\overline{E} = 2.2 \times 10^6$
- Marker circuits, based on discrete solid state circuit data: $\overline{E} = 1 \times 10^7$
- Register circuits, based on discrete solid state circuit data: $\overline{E} = 1 \times 10^7$
- Crossbar switches, based on relay and control circuit results: $\overline{E} = 7 \times 10^5$

Buildings and Enclosures

All equipment, including power equipment, is assumed to be in an equipment room located within a building, and having one exterior wall (see category 4 type enclosure in Table 6.1). Markers and registers are assumed to be in a louvered equipment cabinet without forced air circulation (see Type 9b in Table 6.1).

RADIO STATIONS

Radio stations of interest include Commercial AM and FM stations as well as municipal/emergency communications.

Municipal/emergency communications include police and fire communications in the 25-50 MHz, 148-162 MHz and 450-470 MHz bands. A typical system will include a central office connected to police stations, fire stations, and hospitals via microwave and telephone links, and to mobile units via radio. Remote radio transmitters are often used to obtain sufficient coverage.

Typical Configurations

Commercial and municipal radio communications systems typically consist of a central office (dispatcher's office, broadcast house) connected to remote transmitter sites via RF microwave links.

A typical central office will include consoles and displays, a computer, a communications controller to interface the computer and consoles to RF and telephone communication links, telephone terminal equipment, and RF transmitter-receiver units. The system is often arranged so that the communications controller will still interconnect the console/display stations to the communication links if the computer fails.

Remote transmitter sites typically consist of dual RF microwave receivers, dual modulators, dual transmitter power supplies, and dual transmitters together with local/remote control cabinets and consoles and remote monitoring via return RF microwave. Auxiliary engine generators provide backup power. Manual and automatic switching of redundant units and automatic start-up and power transfer are used to provide very high transmission reliability.

Failure Parameters

Mean exposure-to-failure values are estimated as follows:

- Service Switchgear (listed previously): $\bar{E} = 7 \times 10^5$
- Auxiliary Power (listed previously): $\bar{E} = 2.2 \times 10^6$
- Console/displays (listed previously): $\bar{E} = 4.5 \times 10^5$
- Communications Controller, PDP-8: $\bar{E} = 1 \times 10^7$
- Central Computer, LSI-11: $\bar{E} = 5 \times 10^5$
- RF transmitters/receivers (listed previously): $\bar{E} = 1 \times 10^7$ (per unit)
- Power supply, based on data on high voltage power supplies: $\bar{E} = 1.4 \times 10^5$

Buildings and Enclosures

The radio station visited during this project had all equipment located in an air conditioned and filtered building with all transmitting units additionally air cooled and filtered by a central air conditioning system.

MUNICIPAL WATER PLANTS

Water treatment plants include both water supply and sewage treatment plants. These plants consist of motor driven pumps and valves, motor controls, power supply, and supervisory controls in case of remotely operated stations. Modular construction is usually used and companies such as GE, Westinghouse, and Square D provide modules which are applicable to small utility stations, pipelines, and various process controls as well as for water treatment plants.

Station Configurations

Westinghouse Catalog 55-000 shows the applications of the Westinghouse Electro-Centro to a typical water treatment plant. Motor driven pumps for 600 V, 2300 V, or 5000 V, 30 AC wound-rotor motors are used. Each motor has an associated high voltage switchgear cabinet, high voltage

motor starter, high voltage manual switch, low voltage panelboard or switchboard, dry type distribution transformer, and station batteries. When connected to a primary line voltage of less than 34.5 KV, the distribution transformer can be connected directly to the utility supply through fused disconnects. Otherwise a second transformer and oil type breaker are usually required.

Failure Parameters

Mean exposure-to-failure values are estimated as follows:

- Service Switchgear (listed previously): $\bar{E} = 7 \times 10^5$
- Auxiliary Power (listed previously): $\bar{E} = 2.2 \times 10^6$
- High voltage controls (listed previously): $\bar{E} = 1.4 \times 10^5$
- High voltage motors: vulnerability assumed negligible.

RAIL/RAPID TRANSIT SYSTEMS

From the standpoint of vulnerability, the rail/transit systems can be described in terms of:

- Motive Power
- Control/communications
- Power supply.

Motive Power for both railways and rapid transit is provided by electric motors in the 600-750 volt DC range. These motors are open and air cooled without filters. Control panels with contactors, braking switches, and terminal boards are located in compartments with louvers without air filters.

Control/Communications for both railroad systems and rapid transit systems are composed of control centers, field circuits, and communication links which connect the field circuits to the control centers. Control centers for rapid transit and for railroad centralized traffic control, control of interlockings, and yard controls are similar. Older office facilities consist of telephone type relay control panels with panel-mounted push buttons, switches, and indicator lights. New office facilities consist of computers plus keyboards with solid-state CRT displays and solid-state logic.

Communication links in older systems use telephone type relay line coding units to transmit and receive low rate PCM for controls and indications over line wires. In new systems these relay units have been replaced by higher data rate solid-state modulators and demodulators (communication terminals).

Power Supply for control/communications typically consists of small substations to transform commercial power (e.g., 13.8 KV) to a system distribution voltage (e.g., 550 Volts). This distribution voltage is transformed to 110 V AC and rectified to required DC control voltages at each station and remote site. Twenty-four hour standby batteries are used at each station and remote site. Propulsion requires substations every 10 to 20 miles for railroads and every 1 to 2 miles for rapid transit. Auxiliary propulsion power is not provided; however, systems are often sectionalized so that power can be fed from more than one substation. Failure of a single substation then results in degraded operation (e.g., more spacing between trains) rather than a total system outage.

Field ciruits for newer rapid transit systems consist of discrete solid-state logic and relay circuits located at stations and on-board trains to enforce train protection and to improve train operation. Train-to-station communication is typically via audio frequency track circuits.

System Configurations for Washington METRO and for San Francisco BART are described briefly below. These represent the current state-of-art in rapid transit controls.

Washington METRO consists of:

- A control center with a normal and back-up Sigma-5 Computer and solid-state keyboard/display consoles assigned by route-segments. Solid-state voice-band digital transmitter/receivers connect the central office to stations via cable.
- Stations contain discrete solid-state and relay logic circuits for automatic train control, voice-band transmitters/receivers for cable communications with the

central office, and audio frequency FSK encoders and decoders connected to each individual track circuit.

- Trains contain discrete solid-state and relay logic circuits together with tachometer generators for automatic train control and audio frequency FSK encoders and decoders inductively coupled to the track.

San Francisco BART consists of:

- A control center with normal and back-up PRODAC-250 computers and solid-state consoles for programming, train control, electrification control, and support facilities control. Communication to stations is via 45, 1200 bps digital transmission lines. The control center also contains an HP minicomputer system for sequential occupancy release of track sections to correct problems with track circuits.
- Stations contain discrete solid-state and relay logic circuits for automatic train control; an added oscillator and transposed cable system are included to provide precise train location and speed information at stations. Track circuits use time division multiplexing of audio frequency FSK so that several track circuits use a single channel.
- Trains contain discrete solid-state and relay logic together with tachometer generators for automatic train control with audio frequency FSK encoders and decoders inductively coupled to the track. An additional receiver and control system are included for precision stopping at a station.

Failure Parameters

Mean exposure-to-failure values are estimated as follows for the different equipment groups defined here:

Control Centers

- Central computer — $\bar{E} \simeq 5 \times 10^5$ each (LSI-11)
- Consoles/displays — $\bar{E} \simeq 4.5 \times 10^5$ each (TTL + CMOS)
- Communications terminals — $\bar{E} \simeq 1 \times 10^7$/line (line drivers, amplifiers)
- Power - switchgear — $\bar{E} \simeq 7 \times 10^5$ (relay & control logic)
- Power - aux. MG Set — $\bar{E} \simeq 2.2 \times 10^6$

Stations or remote sites (about 1 per mile)

- Control circuits — $\bar{E} \simeq 1 \times 10^7$/station (discrete)
- Communications terminals — $\bar{E} \simeq 1 \times 10^7$/station (line drivers, amps)
- (10) track circuits — $\bar{E} \simeq 1 \times 10^7$/station (TTL PC)
- Primary power — $\bar{E} \simeq 1.5 \times 10^6$ (AC power distribution)
- Auxiliary power — $\bar{E} \simeq 1 \times 10^8$ (battery/terminals)

Propulsion substation (similar to industrial power)

- High voltage power — $\bar{E} \simeq 1.6 \times 10^7$ per station
- Low voltage power — $\bar{E} \simeq 7 \times 10^5$ per station

Trains/motive power (per unit)

- Control system — $\bar{E} \simeq 1 \times 10^7$ (discrete circuits)
- Motor controls — $\bar{E} \simeq 7 \times 10^5$ (relay & control logic)
- HV. propulsion motors — neglected.

HOUSEHOLDS

A typical household is assumed to include a color TV set; a stereo Hi Fi system; 4 or 5 larger applicances such as freezers, refrigerators, washers, dryers, and hotplates. Small appliances consisting only of 110 V motors (such as sewing machines, mixers, etc.) are assumed to have negligible vulnerability. The vulnerability of large appliances will reside in the electronic controls which are prevalent in the current state-of-art.

Failure Parameters

Mean exposure-to-failure value thresholds are as follows:

- Color TV — $\overline{E} \simeq 1.7 \times 10^7$
- Stereo amp — $\overline{E} \simeq 6.6 \times 10^5$
- Large appliance — $\overline{E} \simeq 1 \times 10^7$ each (discrete electronics)
- Ranges/toasters/hotplates — $\overline{E} \simeq$? each.

OFFICE BUILDINGS

A typical office building has a small power substation, a telephone PBX, intercom equipment, and office machinery including electric typewriters and reproduction facilities. One or more small computers may also be used in the building. A typical office building has 3 or 4 elevators.

Failure Parameters

Mean exposure-to-failure values are estimated to be:

- High voltage power — $\overline{E} \simeq 1.6 \times 10^7$ per building
- Low voltage switchgear — $\overline{E} \simeq 7 \times 10^5$ per building
- Telephone PBX — $\overline{E} \simeq$?
- Electric typewriters — $\overline{E} \simeq$?
- Reproduction facilities — $\overline{E} \simeq$?
- Elevators — $\overline{E} \simeq 7 \times 10^5$ each (relay & central logic)

Rail/Transit Systems

From the standpoint of vulnerability, the rail/transit systems can be described in terms of:

- Motive Power
- Control/communications
- Power supply.

Motive Power for both railways and rapid transit use electric motors in the 600-750 volt DC range. These motors are open and air cooled without filters. Control panels with contactors, braking switches, and terminal boards are located in compartments with louver without air filters.

Control Communications for both railroad systems and rapid transit systems are composed of control centers, field circuits, and communication links which connect the field circuits to the control centers. Control centers for rapid transit and for railroad centralized traffic control, control of interlockings, and yard controls are similar. Older office facilities consist of telephone type relay control panels with panel-mounted push buttons, switches, and indicator lights. New office facilities consist of computers plus keyboards with solid-state CRT displays and solid-state logic.

Communication links in older systems use telephone type relay line coding units to transmit and receive low rate PCM for controls and indications over line wires. In new systems these relay units have been replaced by higher data rate solid-state modulators and demodulators (communication terminals).